

**The effects of Rooibos (*Aspalathus linearis*) supplementation on the
pancreas, liver, and kidney of male Wistar rats
following antiretroviral treatment**

by

Daniella Lagoa Pereira

Thesis presented in fulfilment of the requirements for the degree of
Master of Science in the Faculty of Medicine and Health Sciences at
Stellenbosch University



Supervisor: Prof S.H. Kotzé

Co-supervisor: Dr N. Chellan

December 2017

The financial assistance of the National Research Foundation (NRF) towards this research is hereby acknowledged. Opinions expressed and conclusions arrived at, are those of the author and not necessarily to be attributed to the NRF.

DECLARATION

By submitting this thesis electronically, I declare that the entirety of the work contained therein is my own, original work, that I am the sole author thereof (save to the extent otherwise stated), that reproduction and publication thereof by Stellenbosch University will not infringe any third-party rights that I have not previously in its entirety or in part submitted it for obtaining any qualification.

December 2017

Copyright © 2017 Stellenbosch University

All rights reserved

ABSTRACT

The health burden of human immunodeficiency virus (HIV) has improved with the introduction of antiretroviral therapy (ART). Near perfect adherence to ART is needed to ensure the maximum benefits of the drugs. Adherence is compromised by side effects and adverse drug reactions (ADRs) which may, in part, be due to drug induced oxidative stress. Rooibos (*Aspalathus linearis*) is a shrub-like bush native to South Africa and is cultivated primarily as an herbal tea. Rooibos contains various polyphenols that add to its overall antioxidant capabilities. Aspalathin, the most abundant polyphenol present in rooibos, has shown potent antioxidant capabilities *in vitro*, providing an attractive model for therapy. The following study questions whether the histological observable effects of ART can be attenuated with the introduction of rooibos tea *in vivo*. The study aimed to assess the effects of combination ART, and rooibos tea on the histology of the pancreas, liver, and kidney in a HIV-negative rat model.

Rats (n=40) were subcategorized into four groups namely: control (C), control ART (C-ART), control rooibos (C-R), and experimental (ART+R) groups. The C-ART and ART+R groups were administered a dose of combination ART consisting of 200 mg Emtricitabine (EMT), 600 mg Efavirenz (FTC) and 300 mg Tenofovir (TDF). A 2% (w/v) rooibos tea solution was administered *ad libitum* to C+R and ART+R groups. Samples of rooibos tea were analysed using liquid chromatography-mass spectrometry techniques to determine whether rats received the same concentrations of polyphenols throughout the investigation. Samples from the pancreas, liver, and kidney underwent standard histological processing. Routine haematoxylin and eosin stains and appropriate immunohistochemical and tinctorial techniques were conducted. Detailed morphometric measurements on pancreatic islet size, number and percentage of α and β -cells were performed. Serum alanine aminotransferase (ALT) and aspartate aminotransferase (AST) levels were evaluated to test liver function. Changes in size of the glomerular corpuscle, glomeruli and proximal convoluted tubules (PCT) in the kidney were measured. Organ architecture, cellular structure and associated pathology were analysed in each organ, scored, and confirmed by a histopathologist.

The size and number of pancreatic islets and the percentage of α and β -cells did not vary significantly from the control group. Serum AST and ALT levels did not vary significantly from controls indicating normal liver function. Glomerular corpuscle, glomeruli and PCT size remained constant compared to controls. No overt histopathology was present indicative of ART induced pancreatic toxicity, hepatotoxicity or nephrotoxicity. The results indicated no major changes between the various tea solutions indicating that the rats received similar concentrations of rooibos polyphenols throughout

the week. The study maintains that ART, when given to rats, does not cause significant changes to organ histomorphometry. While rooibos tea administration did not worsen, or improve organ histomorphometry.

OPSOMMING

Die bekendstelling van antiretrovirale terapie (ART), het die gesondheidslas van die menslike immuuniteitsgebreksvirus (MIV) verbeter. Om optimale voordeel uit die terapie te verkry, moet ART nakoming optimaal gehandhaaf word. Nakoming word egter belemmer deur newe-effekte en ongunstige geneesmiddelreaksies, wat gedeeltlik aan geneesmiddel geïnduseerde oksidatiewe stress toegeskryf kan word. Rooibos (*Aspalathus linearis*) is 'n struikagtige gewas wat inheems aan Suid Afrika is en word hoofsaaklik as 'n kruietee gekweek. Rooibos bevat verskeie polifenole wat tot die algehele antioksidatiewe effek van die tee bydra. Aspalathin, die hoof polifenol wat in rooibos teenwoordig is, het sterk antioksidantiewe eienskappe wat *in vitro* waargeneem is, en wat dit dus 'n aanloklike model vir terapie maak. Die studie poog om te bepaal of die waarneembare histologiese effekte wat deur ART veroorsaak word, met die toediening van rooibostee *in vivo* verminder kan word. Die doel van hierdie studie was om die effek van 'n kombinasie van ART en rooibostee op die histologie van die pankreas, lewer, en nier in 'n MIV-negatiewe rotmodel waar te neem.

Rotte (n=40) was in vier groepe verdeel, naamlik 'n kontrole groep (K), kontrole ART groep (K-ART), kontrole rooibos groep (K-R) en eksperimentele (ART+R) groep. Die K-ART en ART+R groepe het 'n kombinasie ART middel ontvang, wat bestaan het uit 200 mg Emtricitabine (EMT), 600 mg Efavirenz (FTC) en 300 mg Tenofovir (TDF) ingesluit het. 'n Twee persent (w/v) rooibostee oplossing is *ad libitum* aan die K+R en ART+R groepe toegedien. Monsters van die rooibos tee was met behulp van 'n vloeibare chromatografie-massaspektrometrie tegniek geanaliseer om te bepaal of die rotte dieselfde polifenol konsentrasie gedurende die eksperiment ontvang het. Monsters van die pankreas, lewer, en nier het standaard histologiese prosesering ondergaan, waartydens roetine Hematoksilien en Eosin-kleuring in kombinasie met toepaslike immunohistochemiese -en spesiale kleuring gedoen is. Gedetailleerde morfometriese afmetings is van die eilandgroottes van die pankreas gedoen, en die aantal en persentasie van α -en β -selle, is bepaal. Om lewerfunksie te bepaal, is serum alanien aminotransferase (ALT) en aspartaat aminotransferase (AST) vlakke geëvalueer. Veranderinge in die grootte van die glomerulêreliggaampie, glomeruli en proksimale kronkelbuise (PKB) in die nier is gemeet. 'n In-diepte analise van die orgaan argitektuur, sellulêre struktuur, en gepaardgaande patologie is in elke orgaan gedoen. Die analise is deur 'n histopatoloog bevestig.

Die grootte en aantal pankreaseilande en die persentasie van α en β -selle in die eksperimentele groep het nie aansienlik van die kontrole groep verskil nie. Serum AST en ALT vlakke wat aanduidend van normale lewerfunksie is, het nie beduidend verskil van die kontrole groep nie, wat aanduidend van normale lewerfunksie is. In vergelyking met die kontroles, het die grootte van die glomerulêre

liggaampie, glomeruli en PKB konstant gebly. Geen duidelike histopatologie was teenwoordig, wat ART geïnduseerde pankreas-toksiteit, hepatotoksiteit of nefrotoksiteit kon aandui nie. Die resultate het geen groot veranderinge tussen die verskeie tee oplossings getoon nie, wat bevestig dat die rotte soortgelyke polifenol konsentrasies gedurende die week ontvang het. Die studie bevind dat wanneer ART aan rotte toegedien word, dit nie betekenisvolle veranderinge aan die orgaan histomorfometrie veroorsaak nie. Verder, toediening van rooibos-tee versleg of verbeter nie die orgaanhistomorfometrie nie.

ACKNOWLEDGEMENTS

The completion of this Masters thesis would not have been possible without the support, guidance, assistance and contributions of the following individuals and institutions:

- To my supervisor, Prof S.H. Kotzé for her supervision, encouragement, support, assistance and expertise. Thank you, Prof, for always challenging me.
- To my co-supervisor, Dr N. Chellan for her encouragement, guidance, and support throughout this whole thesis. Thank you.
- To the Medical Physiology Department of Stellenbosch University specifically Dr I. Webster.
- To the Medical Research Council of South Africa, for the use of their equipment and laboratories.
- To Prof I. Wiid for assistance with the freeze drying of samples.
- To my wonderful colleagues and friends; Lauren Sahd, Karen Cilliers, Jodi Layman and Hilde du Plooy for the constant support and encouragement.
- To Karen Cilliers for thorough editing.
- To everyone at the Division of Anatomy and Histology of Stellenbosch University.
- To Reggie Williams and Rochelle van Wijk for help with the histology and their continual assistance and support throughout this thesis. Thank you.
- To Professor Martin Kidd for assistance with the statistical analysis.
- To the Harry Crossly foundation for the financial support.
- To the National Research Foundation (NRF) for financial support.
- Finally, to my wonderful sister Jennavive Pereira and parents, Rosa Pereira and José Pereira. For your unwavering support, love, words of encouragement, and prayers.

This thesis is dedicated to my parents

Rosa & José Pereira

Thank you for all that you have done and sacrificed for me.

CONTENTS

DECLARATION	ii
ABSTRACT	iii
OPSOMMING	v
ACKNOWLEDGEMENTS	vii
TABLES	xi
FIGURES	xiii
EQUATIONS	xv
APPENDICES	xvi
ABBREVIATIONS	xvii
CHAPTER ONE: INTRODUCTION	1
CHAPTER TWO: LITERATURE REVIEW	4
2.1 DEFINITIONS AND MECHANISM OF ACTION OF ANTIRETROVIRAL DRUGS	5
2.1.1 Efavirenz	6
2.1.2 Emitricitabine	7
2.1.3 Tenofovir	8
2.2 ANTIRETROVIRAL TREATMENT AND ADVERSE DRUG REACTIONS	9
2.2.1 Pancreatic adverse drug reactions	9
2.2.2 Liver adverse drug reactions	12
2.2.3 Kidney adverse drug reactions	14
2.3 OXIDATIVE STRESS, REACTIVE OXYGEN SPECIES AND ANTIRETROVIRAL THERAPY	16
2.4 OVERVIEW OF ROOIBOS	17
2.4.1 Composition of rooibos	19
2.4.2 Protective effects of rooibos	20
2.4.3 Bioavailability of rooibos	23
2.5 ORGAN SYSTEMS: HISTOLOGY AND PATHOLOGY	24
2.5.1 Pancreas histology	24
2.5.2 Pancreas pathology	26
2.5.3 Liver histology	27
2.5.4 Liver pathology	29
2.5.5 Kidney histology	30
2.5.6 Kidney pathology	32
CHAPTER THREE: RESEARCH DESIGN	34

3.1	RESEARCH QUESTIONS	35
3.2	AIM	35
3.3	OBJECTIVES	35
3.4	HYPOTHESES	35
CHAPTER FOUR: MATERIALS AND METHODS		36
4.1	ETHICAL APPROVAL	37
4.2	STUDY GROUPS AND ANIMAL CARE	37
4.3	ANTIRETROVIRAL ADMINISTRATION	37
4.4	SUPPLEMENTATION OF ROOIBOS	38
4.5	PROCEDURES	38
4.5.1	Anaesthesia and euthanasia	38
4.5.2	Tissue harvesting	38
4.5.3	Blood sampling	39
4.6	HISTOLOGICAL PROCEDURES	39
4.6.1	Sectioning and staining of the pancreas	39
4.6.2	Sectioning and staining of the liver	40
4.6.3	Sectioning and staining of the kidney	41
4.7	STEREOLOGY AND MORPHOMETRY	43
4.7.1	Pancreas	43
4.7.2	Liver	44
4.7.3	Kidney	45
4.8	PATHOLOGICAL SCORING OF THE PANCREAS, LIVER, AND KIDNEY	46
4.9	POLYPHENOL CHARACTERISATION	48
4.10	STATISTICAL ANALYSIS	50
CHAPTER FIVE: RESULTS		51
5.1	DESCRIPTIVE AND STATISTICAL ANALYSIS ON BODY MASS	52
5.2	THE EFFECTS OF TREATMENT ON PANCREATIC ISLETS	52
5.3	THE EFFECTS OF TREATMENT ON THE LIVER	53
5.4	THE EFFECTS OF TREATMENT ON THE KIDNEY	54
5.5	PATHOLOGY	56
5.5.1	Scoring of the pancreas	56
5.5.2	Scoring of the liver	58
5.5.3	Scoring of the kidney	64
5.6	ROOIBOS TEA STANDARDS	65
CHAPTER SIX: DISCUSSION		66

CHAPTER SEVEN: CONCLUSION.....	75
REFERENCES	78
APPENDICES	94
Appendix A: Outputs and awards arising from this study	94
Appendix B: List of materials.....	95
Appendix C: Odimmune dose calculations.....	97
Appendix D: Blood transaminase methods (NHLS)	99
Appendix E: Tissue processing.....	107
Appendix F: Haematoxylin and eosin automatic staining protocol.....	108
Appendix G: Immunolabelling for anti-glucagon and anti-insulin.....	109
Appendix H: Gordan and Sweet staining protocol	111
Appendix I: Periodic acid schiff staining protocol	113
Appendix J: Masson's trichrome staining protocol.....	114
Appendix K: Randomisation techniques for the kidney	115
Appendix L: Freeze drying techniques	116
Appendix M: Supplementary data	117

TABLES

Table 2.1: Current antiretroviral drugs approved by the United States Food and Drug Administration.	6
Table 2.2: Summary of the short-and long-term antiretroviral therapy associated adverse drug reactions	11
Table 2.3: Summary of studies on tenofovir induced adverse drugs reactions.	15
Table 2.4: Main polyphenols found in rooibos	19
Table 2.5: Polyphenol changes and total antioxidant capacity between fermented and unfermented samples of rooibos	20
Table 2.6: Summary of <i>in vitro</i> studies conducted on fermented and unfermented samples of rooibos.	22
Table 4.1: Definitions and scoring of liver pathology.	45
Table 4.2: The semi-quantitative methods of grading and scoring including identifying pathological features.	48
Table 5.1: Number of samples, and mean body mass between the different groups.....	52
Table 5.2: The space and width of the renal space	56
Table 5.3: The average surface area and diameter of the proximal convoluted tubules of antiretroviral therapy and rooibos treated rats	56

Appendices:

Table 1: List of materials	95
Table 2: Active ingredients in one Odimune [®] tablet.	97
Table 3: Tissue processing steps	107
Table 4: Haematoxylin and eosin staining protocol.	108
Table 5: Results of immunolabelling	109
Table 6: Reagents and quantities of immunolabelling kits.	109
Table 7: Immunolabelling protocol.	110
Table 8: Results of Gordan and Sweet's silver impregnation	111
Table: 9: Gordan and Sweet's staining solutions.	111
Table 10: Period acid Schiff stain results.	113
Table 11: Periodic acid Schiff staining solutions.	113
Table 12: Staining procedure for periodic acid Schiff.	113
Table 13: Results of Masons trichrome stain.	114

Table 14: Masson's Trichrome staining solutions.	114
Table 15: Masson's trichrome staining procedure.....	114
Table 16: Freeze drying procedures.....	116
Table 17: Post hoc tests for body weight.	117
Table 18: Pancreas tissue, islet and α -and β -cell areas.	118
Table 19: Post hoc tests for the pancreas.	119
Table 20: Descriptive statistics and standard deviations (\pm) of serum analysis.	121
Table 21: Post hoc tests of serum tests.	121
Table 22: Descriptive statistics and standard deviations (\pm) of kidney measurements.	122
Table 23: Post hoc tests of glomerular corpuscle and glomerulus.....	123
Table 24: Post hoc tests of the proximal convoluted tubules.....	124
Table 25: Pathology overview: Pancreas.	128
Table 26: Pathology overview: Liver.	130
Table 27: Pathology overview: Kidney.	132

FIGURES

Figure 2.1: The chemical structures of the antiretroviral drugs.....	7
Figure 2.2: The human immunodeficiency virus life cycle and antiretroviral therapy drug targets ...	8
Figure 2.3: Demonstration of the cellular mechanism involved in drug induced liver toxicity leading to histological visible changes.	13
Figure 2.4: Types of reactive oxygen species and electron pairs.	16
Figure 2.5: Exogenous and endogenous sources leading to reactive oxygen species.	17
Figure 2.6: Aspalathus linearis bush and the chemical structure of Aspalathin.	18
Figure 2.7: Graphical representation of the islets of Langerhans	26
Figure 2.8: Graphical representation of the functional units of the liver.....	29
Figure 2.9: Described are the various kidney diseases and their pathological features.....	33
Figure 4.1: Summary of methodology	42
Figure 4.2: Morphometric analysis of the islets of pancreatic islets using immunohistochemical labelling.....	44
Figure 4.3: Morphometric measurement of the glomerular corpuscle and proximal convoluted tubules.....	46
Figure 4.4: Rooibos tea allocation	49
Figure 5.1: Effects of treatment on pancreatic islet size and number	53
Figure 5.2: Effects of treatment on the percentage of α - and β -cells areas.....	53
Figure 5.3: Effects of treatment on liver function biomarkers.....	54
Figure 5.4: Effects of treatment on the size of the glomerular corpuscle and glomeruli.....	55
Figure 5.5: Pancreatic islet micrographs showing islet histomorphology in the various groups	57
Figure 5.6: Haematoxylin and eosin stained pancreatic lymph node	58
Figure 5.7: Occurrence of granular cytoplasm in the treatment groups	59
Figure 5.8: Occurrence of vacuolation in the treatment groups.....	60
Figure 5.9: Occurrence of inflammatory foci in the treatment groups	61
Figure 5.10: Photomicrographs depicting liver histology in a control animal.	62
Figure 5.11: Photomicrographs of subtle tissue changes in the liver.	63
Figure 5.12: Photomicrographs (200 x magnification) of the rat kidney.	64
Figure 5.13: Rooibos chromatograms showing the amount of rooibos polyphenols.	65

Appendices:

Figure 1: Bench work of the reticulin stain and photomicrograph of positive skin control.	112
Figure 2: Periodic acid Schiff positive control.	113
Figure 3: Randomisation of the kidney images to be measured.	115
Figure 4: Tea preparation for freeze drying	116
Figure 5: Final tea product in powdered form.	116
Figure 6: Body mass and Post hoc values of the various treatment groups.....	117
Figure 7: Bar graphs showing the size of the PCTs.....	125
Figure 8: Single rooibos chromatograms of Day 1 samples, with retention times and molecular weights of the compounds	126
Figure 9: Single rooibos chromatograms of Day 7 samples, with retention times and molecular weights of the compounds	127

EQUATIONS

Equation 4.1: Equation demonstrating the surface area in (μm^2) of the Bowman's space	46
Equation 4.2: Quantifying tubular wall area (μm^2).	46

APPENDICES

Appendix A: Outputs and awards arising from this study	94
Appendix B: List of materials	95
Appendix C: Odimmune dose calculations	97
Appendix D: Blood transaminase methods (NHLS)	99
Appendix E: Tissue processing	107
Appendix F: Haematoxylin and eosin automatic staining protocol	108
Appendix G: Immunolabelling for anti-glucagon and anti-insulin	109
Appendix H: Gordan and Sweet staining protocol	111
Appendix I: Periodic acid schiff staining protocol	113
Appendix J: Masson's trichrome staining protocol	114
Appendix K: Randomisation techniques for the kidney	115
Appendix L: Freeze drying techniques	116
Appendix M: Supplementary data	117

ABBREVIATIONS

3TC:	Lamivudine
ABC:	Abacavir
ADR:	Adverse drug reactions
AIDS:	Acquired immunodeficiency syndrome
ALT:	Alanine aminotransferase
ART:	Antiretroviral treatment
ART+R:	Experimental group
AST:	Aspartate aminotransferase
BCSA:	Bowman's capsule surface area
C:	Control group
CAF:	Central analytical facility
cART:	Combination antiretroviral therapy
C-ART:	Control antiretroviral treated group
CCl ₄ :	Carbon tetrachloride
CNS:	Central nervous system,
C-R:	Control rooibos group
D1:	Day 1
D2:	Day 2
d4T:	Stavudine
DCT:	Distal convoluted tubule
ddI:	Didanosine
DILI:	Drug induced liver injury
DM:	Diabetes mellitus
DNA:	Deoxyribonucleic acid
DSS:	Dextran sodium sulphate
EFV:	Efavirenz
EI:	Entry inhibitors
EM:	Electron microscopy
FCE 26184:	Fibroblast growth factor
FDA:	United States Food and Drug administration
FI:	Fusion inhibitors
FTC:	Emtricitabine

GA:	Glomerular area
GAE:	Gaelic acid equivalent
GMB:	Glomerular basement membrane
GSA:	Glomerular surface area
GSGG:	Reduced Glutathione
GSH:	Glutathione
H&E:	Haematoxylin and Eosin
HAART:	Highly active antiretroviral treatment
HBV:	Hepatitis B virus
HIV:	Human immunodeficiency virus
HPLC:	High performance liquid chromatography
IHC:	Immunohistochemical
LC-MS:	Liquid chromatography mass spectrometry
LSA:	Luminal surface area
LSD:	Fischer's least significant difference
MT:	Masson's Trichrome
NGS:	Normal goat serum
NHLS:	National health laboratory services
NHS:	Normal horse serum
NNRTI:	Non-nucleoside reverse transcriptase inhibitor
NRTI:	Nucleoside reverse transcriptase inhibitor
NVP:	Nevirapine
OAT:	Organic anion transporters
ORAC:	Oxygen radical absorbance capacity
OSA:	Outer surface area
PAS:	Periodic Acid-Schiff
PCT:	Proximal convoluted tubule
PI:	Protein inhibitor
PP-cell:	Pancreatic polypeptide cell
REC: ACU:	Research Ethics Committee: Animal care and use
REDOX:	Reduction and oxidation reaction
RNA:	Ribonucleic acid
ROS:	Reactive oxygen species
RS:	Renal space

S1-Fresh:	Sample one fresh tea
S2-Fridge:	Sample two refrigerated tea
S3-Frozen:	Sample three frozen tea
SANS:	South African national standards
SARC:	South African Rooibos Council
SAVC:	South African veterinary council
SEM:	Standard error or mean
SOD:	Superoxide dismutase
Std. Dev:	Standard deviation
STZ:	Streptozotocin
TBARS:	Thiobarbituric acid reactive substances
t-BHP:	Tert-butyl hydroperoxide
TDF:	Tenofovir disoproxil fumarate
TNF:	Tumour Necrosis factor
USFDA:	United States food and drug administration
α -cell:	Alpha cell
β -cell:	Beta cell
δ -cell:	Gamma cell

UNITS OF MEASUREMENTS

°C:	Degrees Celsius
μL:	Microliter
μm:	Micrometres
kg:	Kilogram
L:	Litre
m/z:	Mass to charge ratio
mg:	Milligrams
Min:	minute
mL:	Millilitre
nm:	Nanometre
V:	Volts
w/v:	Weight to volume ratio
±:	Standard deviation

CHAPTER ONE: INTRODUCTION

Infectious diseases, such as human immunodeficiency virus (HIV), are a global concern (World Health Organisation, 2016). Morbidity and mortality rates in HIV-infected individuals have been successfully reduced with the introduction of antiretroviral therapy (ART) (Pallela *et al.*, 1998; El-Sadre *et al.*, 2003). Adherence plays a critical role in ensuring the success of treatment (Carr, 2013). Success is defined by the reduction in the human immunodeficiency pathogen and associated co-morbid effects (Meintjes *et al.*, 2017). However, increasing reports of adverse drug reactions (ADRs) in individuals receiving ART, has reduced adherence, thereby compromising the efficacy of treatment (Carr, 2003; Meintjes *et al.*, 2017). The introduction of combination therapy in a single tablet design has increased adherence, however, ADRs are still reported (DeJesus *et al.*, 2009; Meintjes *et al.*, 2017). Although it is important to understand the drugs individually, emphasis should be placed on ADRs of combination therapy, due to its emerging success. Little is known on the histological effect of the ART combination of Efavirenz (EFV), Emtricitabine (FTC) and Tenofovir disoproxil fumarate (TDF).

There is sufficient evidence demonstrating drug associated pathology due to oxidative stress in the pancreas, liver and kidney following various ARTs (Puoti *et al.*, 2003; Carr, 2003; Rudolf & Krikorian, 2005; Schmid *et al.*, 2007; Deavall *et al.*, 2012; Soriano *et al.*, 2012, Meintjes *et al.*, 2017). However, these changes are difficult to assess histologically due to the lack of tissue samples, as these effects are often observed in a clinical environment on patients with HIV. It is therefore important that these changes be studied in a HIV-negative rodent model, to assess the histological observable effects of ART at a tissue level. This is to ascertain whether ART is the sole cause of reported ADRs or is influenced by external variables. Thus, it is imperative to introduce alternative, safe and effective therapies that will improve adherence by preventing ADRs.

There has been a notable interest on the health promoting benefits of “functional foods” that have both nutritional and added health benefits (Joubert *et al.*, 2005). Rooibos (*Aspalathus linearis*) can be described as a functional food with known *in vitro* (Ku *et al.*, 2014, Gelderblom *et al.*, 2016) and *in vivo* (Marnewick *et al.*, 2003; Ulicina *et al.*, 2005; Ayeleso *et al.*, 2014, Canda *et al.*, 2014; Ku *et al.*, 2014) antioxidant capabilities, which have been well assessed. Rooibos is a readily available, low tannin, non-caffeinated, and popular beverage in South Africa (Morton, 1983). Due to its impressive antioxidant capabilities, *in vitro* (Viliano *et al.*, 2010; Adjuwon *et al.*, 2013; Chen *et al.*, 2013) rooibos tea has been posited as a therapy for the prevention or reversal of adverse reactions caused by oxidative stress. Therefore, it is necessary to describe the effects of ART and rooibos tea consumption on the histomorphology of the pancreas, liver, and kidney. It is hypothesised, that the administration

of rooibos tea to rats receiving combination antiretroviral therapy (cART), may reduce the effects of ADRs at a tissue level.

This study makes use of histomorphometry and semi-quantitative analyses by considering organ architecture and associated pathology. This was conducted to describe the histological observable effects of cART and rooibos on various organs. Additionally, an assessment of the polyphenol content of a standardised rooibos tea solution is reported, with notes on the effects of different storage scenarios on the polyphenolic content. This study will add to the academic body of work regarding the histological effects of cART and rooibos in a rat model, potentially contributing to the wellbeing of HIV-positive individuals receiving cART.

CHAPTER TWO: LITERATURE REVIEW

It is estimated that more than 30 million individuals are globally affected by the human immunodeficiency virus (HIV) with South Africa at the epicentre of the epidemic (World Health Organisation., 2007). The advent of highly active antiretroviral therapy (HAART) has significantly reduced morbidity and mortality rates (Jao & Wyatt, 2010). Highly active antiretroviral treatment typically makes use of three or more antiretroviral drugs from one or more classes, in a single tablet design (Rudorf & Krikorian, 2005). This design is a convenient method of providing the benefits of multiple drugs in a single dose, taken daily (Meintjes *et al.*, 2017). The Southern African HIV Clinicians Society guidelines (2017) state that the main goal of antiretroviral therapy (ART) is to provide maximum suppression of HIV, restore immune function, decrease the risk of co-opportunistic infections, increase life-expectancy, and prevent HIV transmission while minimising adverse drug reactions (ADRs) (Meintjes *et al.*, 2017). Although these drugs are highly successful, reports on ART associated ADRs hinder the efficacy of treatment by compromising adherence (Brinkman *et al.*, 1998; Carr & Cooper, 2000; Ammassari *et al.*, 2001; Fellay *et al.*, 2001; Carr, 2003; Rudorf & Krikorian, 2005; Jao & Wyatt, 2010).

There are various classes of ART including non-nucleoside reverse transcriptase inhibitors (NNRTI), nucleoside reverse transcriptase inhibitors (NRTI), protein inhibitors (PI), fusion inhibitors (FI) (Carr & Cooper, 2000), and entry inhibitors (EI) (US Food and Drug Administration, 2015). Adherence to these drugs is critical to maximise the long-term benefits, while minimising the risk of opportunistic infections and lowering infection rates (Monforte *et al.*, 2001).

Rudorf and Krikorian (2005) reviewed the short-and long-term effects of ARTs, and reported that severe adverse events were associated with long term exposure. These ADRs may be due to combination treatment or individual drug interactions (Carr & Cooper, 2000). As a result, long term exposure has resulted in oxidative stress, compromising organ systems and cellular components (Brinkman *et al.*, 1998; Rudorf & Krikorian, 2005). Although, clinical studies have been conducted on the efficacy of the ART in clinical settings, the long term and short term exposure has been under reported and poorly studied, specifically in HIV-negative animal models (Styrt *et al.*, 1996; Saag, 2007; Carr & Cooper, 2000; Jao & Wyatt, 2010).

2.1 DEFINITIONS AND MECHANISM OF ACTION OF ANTIRETROVIRAL DRUGS

Antiretroviral drugs are orally administered to treat the actions of retro-viruses, such as HIV (Carr & Cooper, 2010). Six classes of the drug have been approved by the United States Food and Drug administration (US FDA) (2015), however only the three most used classes in South Africa are described (Table 2.1). The following section will focus on the actions of the antiretroviral drugs,

Efavirenz (EFV), Emetricitabine (FTC) and Tenofovir (TDF), alone and in combination. These drugs are currently used in first line combination treatment, particularly, in South Africa (Meintjes *et al.*, 2017) and are prescribed in combination as either Odimune[®] or Atripla[®]. Odimune[®] is used in South Africa as a cost-effective alternative to monotherapy (Meintjes *et al.*, 2017). It is imperative to study the adverse events of ARTs, as this could potentially lead to safer more effective long term treatment options (Carr, 2003). The scope of the research is limited to the ADRs in the pancreas, liver, and kidney.

Table 2.1: Current antiretroviral drugs approved by the United States Food and Drug Administration. Dates indicate year of release (Adapted from: US Food and Drug Administration: FDA-Approved HIV Medicines, 2016).

Nucleoside reverse transcriptase inhibitors (NRTIs)	Non-nucleoside reverse transcriptase inhibitors (NNRTIs)	Protease Inhibitors (PIs)
Zidovudine, 1987	Nevirapine, 1996	Saquinavir, 1995
Stavudine, 1994	Efavirenz, 1998*	Indinavir, 1996
Lamivudine, 1995	Etravirine, 2008	Ritonavir, 1996
Abacavir, 1998	Rilpivirine, 2011	Fosamprenavir, 2003
Didanosine, 2000		Atazanavir, 2003
Tenofovir disoproxil fumarate, 2001*		Tipranavir, 2005
Emtricitabine, 2003*		Duranavir, 2006

* Drugs used in combination in the current study.

2.1.1 Efavirenz

Efavirenz was first approved in 1998 by the US FDA for the treatment of HIV in combination with other antiretroviral agents for use in adults and children over three years of age (Staszewski, 2007). Chemically, the drug is described as (S)-6-chloro-4-(cylopropylethynyl)-1, 4-dihydro-4-(trifluoromethyl) – 2H-3, 1-benzoxazin-2-one (Atripla[®] product information, 2017) (Figure 2.1 A). The drug is a NNRTI, functioning as a non-competitive inhibitor of HIV reverse transcriptase (Figure 2.2). The drug binds directly to the reverse transcriptase enzyme, causing the disruption of catalytic site. This inhibits the polymerase activity of HIV and reduces the formation of new viral deoxyribonucleic acid (DNA) (Young *et al.*, 1995).

In the liver, EFV is metabolised by hepatic cytochrome isoenzymes (Mutlib *et al.*, 1998; Deeks & Perry, 2010), leading to glucuronidation. Glucuronidation refers to the process where drugs and other compound are mixed with glucuronic acid, forming water soluble compounds that are easily excreted by the kidneys. Efavirenz is primarily excreted in the faeces as a metabolite and in its original form (Atripla[®] product information, 2017). Efavirenz is recommended for combination therapy

regimes, as monotherapy could lead to the selection of highly drug resistant variants (Staszewski, 2007). Due to the excellent bioavailability and potency, EFV is optimal for combination treatment (Young *et al.*, 1995).

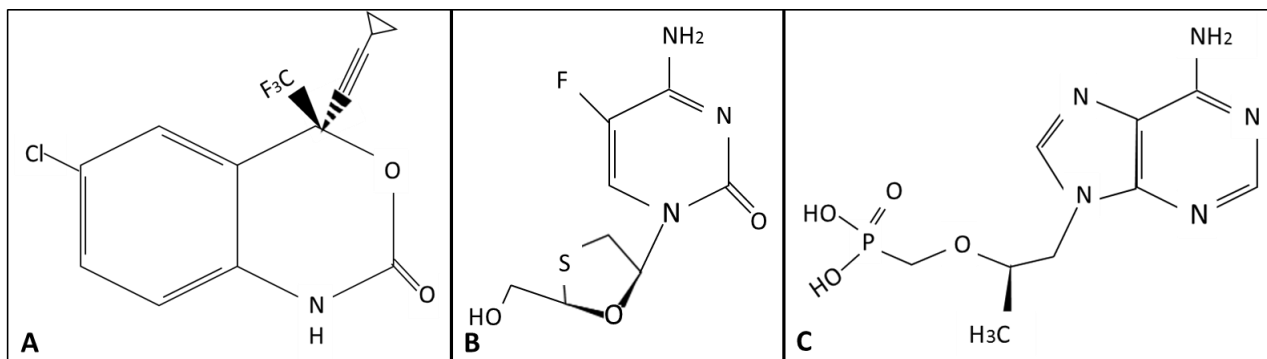


Figure 2.1: The chemical structures of the antiretroviral drugs. A) Efavirenz $C_{14}H_9C_1F_3NO_2$; B) Efavirenz $C_8H_{10}FN_3O_3S$; and C) Tenofovir $C_{19}H_{30}N_5O_{10}P$ Adapted from: (Atripla®, product information, 2017).

2.1.2 Efavirenz

First described by Schinazi and colleagues in 1992, Efavirenz (FTC) is a NRTI with antiviral activity against the actions of HIV, and in some cases, Hepatitis-B virus (HBV) (Schinazi *et al.*, 1992a). Efavirenz only received approval for the treatment of HIV by the FDA in 2003 (US FDA, 2016). The drug is in the “preferred category” for combination treatments due to its safety and low toxicology effects (Mugavero & Wellons, 2008).

Chemically, FTC is a negative or *cis* enantiomer of 2', 3'-dideoxy-5-fluoro-3'-thiacytidine (Schinazi *et al.*, 1992a; Van Roey *et al.*, 1993) (Figure 2.1 B). Like other NRTIs, the drug must be metabolised to its active form by intra-cellular kinases (Paff *et al.*, 1994). The drug inhibits the binding of HIV phosphatases to reverse transcriptase, limiting DNA synthesis of new HIV virions (Wilson *et al.*, 1993) (Figure 2.2). Efavirenz is rapidly absorbed following oral administration and is mainly excreted by the kidneys (Deeks & Perry, 2010). Administration of a single dose of FTC (200 mg) demonstrated an 85% recovery in urine and 13% in faeces (Mugavero & Wellons, 2008; Deeks & Perry, 2010). Few adverse events were recorded in animal studies, placing FTC in the “preferred category” of ART (Schinazi *et al.*, 1992b; Frick *et al.*, 1993).

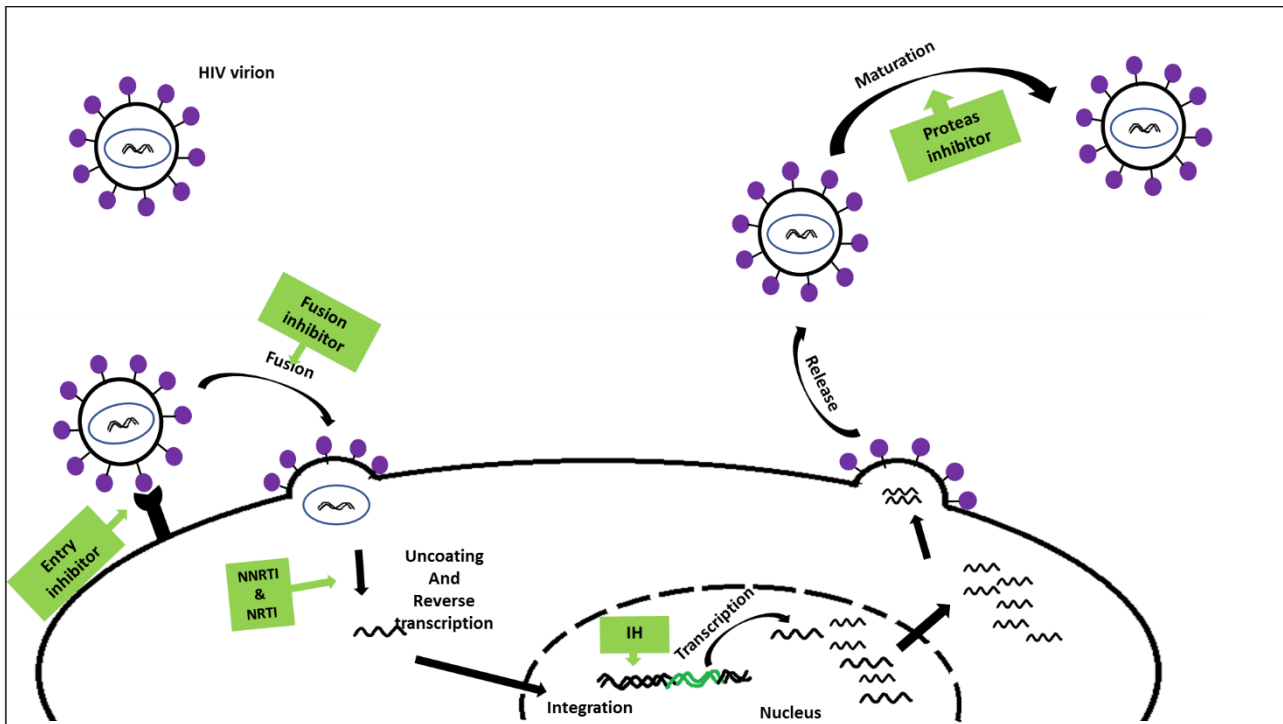


Figure 2.2: The human immunodeficiency virus life cycle and antiretroviral therapy drug targets. Illustration of the main steps in the HIV replication cycle showing recognition of the virion into the host CD4⁺ cell, fusion within the host membrane, uncoating of the capsid releasing viral RNA strands. Through reverse transcription viral RNA is transcribed to viral DNA which is then integrated into the host cell DNA. The host cell then undergoes normal replication of the new viral DNA, which is assembled and released. The image further shows the major targets of ART (green blocks) in the virus life cycle. Adapted from: (Barré-Sinoussi *et al.*, 2013).

2.1.3 Tenofovir

Tenofovir disoproxil fumarate (TDF) is an oral drug with activity against HIV and hepatitis infections (Hoesley, 2008). Chemically, the structure of TDF is a 9-[(R)-(2-phosphonylmethoxy) propyl] adenine (Figure 1.2 C). The drug is a lipophilic ester that is designed to improve oral bioavailability (Naesens *et al.*, 1997), which is enhanced by a high-fat meal (Kearney *et al.*, 2004). The drug differs from other classic nucleoside analogues as it does not depend on intracellular enzymes for activation (Naesens *et al.*, 1997). Tenofovir was approved by the US FDA in 2001 and was released for triple fixed dose combination treatment in 2006 (Hoesley, 2008).

The drug interacts with viral DNA polymerases and reverse transcriptase, acting as both a competitive inhibitor and an alternative binding site for the DNA polymerase chain reaction, subsequently terminating HIV DNA replication (Naesens *et al.*, 1997) (Figure 2.2). Due to the intracellular (≥ 60 hours) and serum (17 hours) half-life, the drug provides an ideal model for flexible once-daily administration (Kearney *et al.*, 2004). Tenofovir is primarily excreted in the kidneys, mediated by the action of glomerular filtration and secretions of the proximal convoluted tubules (PCT) (Ray *et al.*,

2006). *In vitro* metabolic studies and animal studies have found that TDF is eliminated unchanged in urine 24 hours after the initial dose (Lebrecht *et al.*, 2009). Tenofovir is a substrate for the organic anion transporters OAT-1 and OAT-3 in PCTs, it is hypothesised that these transporters are responsible for the drugs secretion in urine in its unchanged form (Ray *et al.*, 2006). It is important to understand the drugs individually as Mathias *et al* (2007) concluded that TDF/FTC/EFV drugs in combination are equivalent to their individual actions. The emerging success of combination therapy has provided an opportunity for their research in various organ systems.

2.2 ANTIRETROVIRAL TREATMENT AND ADVERSE DRUG REACTIONS

Highly active antiretroviral treatment is the combination of two or more antiretroviral drugs that act synergistically to suppress HIV replication (Deeks & Perry, 2010). Combination therapy is a first line treatment that drastically increases the life span of infected individuals (May *et al.*, 2014).

There are two main draw backs associated with combination treatment. Firstly, low compliance to medication and secondly, ADRs (Monforte *et al.*, 1998; Monforte *et al.*, 2001). Fellay and colleagues (2001) reported that out of 1160 patients receiving combination ART (cART), 74% presented with ADRs. Additionally, O'Brien *et al* (2003) found that at least 24% of 345 patients discontinued treatment as result of ADRs. Multiple organs, cells, and cellular organelles are affected by ART, possibly due to the type of drug, drug class, or the actions of HIV itself (Rudorf & Krikorian, 2005). A summary of the short and long term effects of ART is presented in Table 2.2.

2.2.1 Pancreatic adverse drug reactions

Metabolic changes (Lagathu *et al.*, 2007; Stein *et al.*, 2008; Lugassy *et al.*, 2010), acute pancreatitis (Andersen *et al.*, 2001) and an increased incidence of diabetes (Brown *et al.*, 2005) have been reported with ART. A systematic review conducted by Oliveira *et al* (2014), summarised that EFV and TDF were risk factors for acute pancreatitis, however, these were secondary to hyperlipidaemia. Acute pancreatitis refers to the activation of pancreatic enzymes, such as amylase levels, leading to pancreatic damage (Kloppel & Maillet, 1993). Histologically, this is observed in the pancreatic acinar cells where necro-inflammatory changes occur, leading to oedema in severe cases (Kloppel & Maillet, 1993). Manfredi and Calza (2008) noted that patients using NRTIs in combination had an increased risk of pancreatic enzyme elevations, which were worsened by alcohol use, occurrence of co-infections or the combination of these factors.

Post-mortem histological studies found no evidence of pancreatic lesions associated with the use of ART (Barbosa *et al.*, 2013). However, a decrease in zymogen granules, and core dysplasia-like

alterations were observed (Barbosa *et al.*, 2013). The study concluded that these changes may be due to nutritional or HIV related factors (Barbosa *et al.*, 2013). Additionally, Ferreira *et al* (2015) noted increased islet areas in ART-treated individuals compared to control groups. However, the same study found larger islets in HIV-infected individuals agreeing with observations conducted by Chehter *et al* (2000). This study further stated that pancreatic changes may have been due to nutritional or HIV related causes (Chehter *et al.*, 2000). These studies (Chehter *et al.*, 2000; Barbosa *et al.*, 2013) further reiterate the gap of knowledge on the effects of combination ART on the histomorphometry of pancreatic islets in HIV-negative rodent models.

Table 2.2: Summary of the short-and long-term antiretroviral therapy associated adverse drug reactions (adapted from Rudolf & Krikorian, 2005).

Adverse Reaction	Drug or Drug Class	Initiation After Therapy	Comments
Short Term			
Central nervous system	EFV, FTC	2-4 weeks/ long term	Exacerbated by existing CNS or psychiatric conditions and CNS drugs
Gastrointestinal	PIs, some NRTIs	Early treatment	Diarrhoea common, conditions exacerbated by pre-existing conditions
Hyperpigmentation	FTC	First few months	Noticed primarily in black individuals
Skin irritations	NRTIs	From onset	Severe reactions may lead to discontinuation
Long Term			
Pancreatitis	ddI, d4T	Weeks to months	Increased risk with history of disease, associated in combination with TDF
Hepatotoxicity serum	PIs, NNRTIs, NRTIs	Weeks to months	Increased risk with co-infections, alcohol, or hepatotoxic drug use
Hepatotoxicity necrosis	Mostly NVP	First few weeks to 18 weeks	Accompanied by ALT/AST elevation, coinfections, alcohol, or hepatotoxic drug use
Nephrotoxicity	TDF	Weeks to months	Increased risk with history of renal disease, decreased fluid intake, use of nephrotoxic drugs
Hyperglycaemia/ hyperinsulinemia	Mostly NVP	Weeks to months	Increased risk with diabetes

Protease inhibitor (PI); Nucleoside reverse transcriptase inhibitor (NRTI); Non-Nucleoside reverse transcriptase inhibitors (NNRTI); Efavirenz (EFV); Emtricitabine (FTC); Tenofovir (TDF); Didanosine (ddI); Stavudine (d4T); Nevirapine (NVP); Central Nervous system (CNS); Alanine aminotransferase (ALT); Aspartate aminotransferase (AST).

2.2.2 Liver adverse drug reactions

Liver toxicities have been reported to occur across all classes of ARTs (Carr, 2003). Efavirenz is linked to liver toxicities specifically in combination treatment (Pérez *et al.*, 2009). Although, a study by Minzi *et al* (2009) noted that these toxicities were higher in nevirapine (NVP) treated patients compared to those prescribed EFV. Schouten *et al* (2010) found severe cases of liver pathology in only 4% of patients who substituted NVP with EFV; however, these changes were reversible.

Liver toxicities present as liver enzyme elevations, specifically those of alanine aminotransferase (ALT), aspartate aminotransferase (AST), bilirubin and alkaline phosphatases (Schouten *et al.*, 2010). The study conducted by Wit *et al* (2002) noted that approximately 8% of patients receiving ART in combination had liver enzyme elevations 10 times above the average, with 35% of patients discontinuing treatment. While Wester *et al* (2010) reported that only 6.3% of the total population studied reported hepatotoxicity in the form of liver enzyme elevations.

The exact mechanism of ART associated liver toxicity is poorly understood (Sulkowski 2004). This could be due to compounding factors and/or drug-drug interactions (Dieterich *et al.*, 2004; Sulkowski, 2004). However, the mechanisms of drug induced hepatotoxicity leading to histologically observable changes has been defined (Bissell *et al.*, 2001; Bliebel *et al.*, 2007). Figure 2.3 illustrates the various ways in which the liver may be damaged by drugs. Hepatotoxicity may present as necro-inflammatory changes similar to that observed in chronic viral hepatitis (Zimmerman, 1999). Additionally, distortion to liver architecture may occur (Neuman *et al.*, 2012). Instances of necrosis and severe congestion of the portal and venous system have been reported with the use of ART (Adaramoye *et al.*, 2012). Often, these changes may be exacerbated by the presence of co-opportunistic infections such as hepatitis (Núñez, 2006).

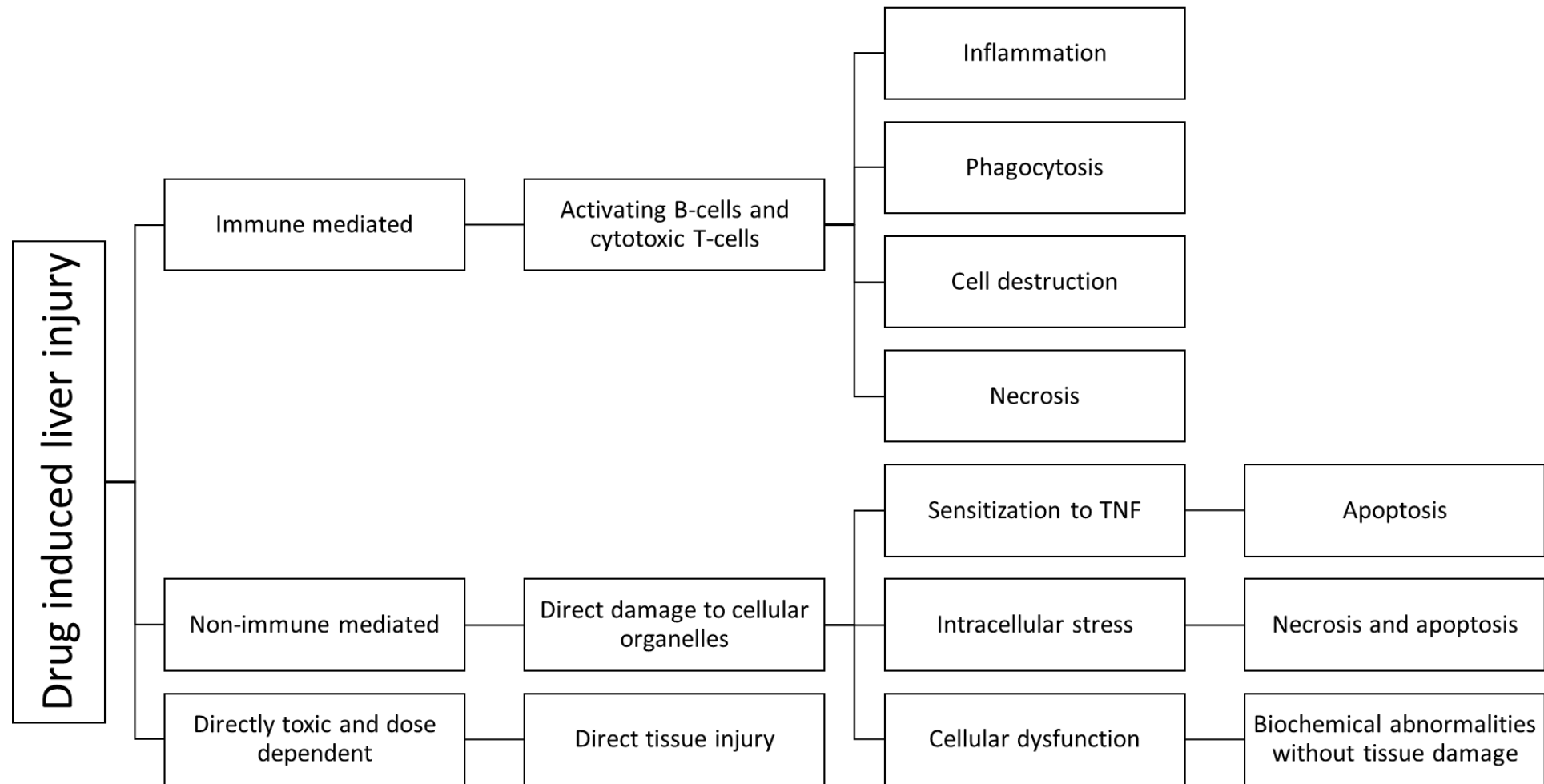


Figure 2.3: Demonstration of the cellular mechanism involved in drug induced liver toxicity leading to histological visible changes. Drug induced liver injuries (DILI) may be immune mediated, non-immune mediated, directly toxic or dose dependant. Immune mediated changes activate immune responses leading to cellular destruction, inflammation, phagocytosis or apoptosis. Non-immune mediate injuries may be directly toxic to cellular organs, leading to intracellular stress and cellular dysfunction leading to necrosis or elevations of liver enzyme. Toxic events may be dose dependent leading to direct cellular injury however these are limited to specific drugs (Adapted from: Bleibel *et al.*, 2007).

2.2.3 Kidney adverse drug reactions

Numerous studies have reported renal toxicities associated with TDF (Kohler *et al.*, 2009; Lebrecht *et al.*, 2009; Herlitz *et al.*, 2010). Tenofovir associated glomerular toxicity accounts for 20% of consultations to nephrologists (Hall, 2013), often resulting in damage to the PCTs or changes in glomerular filtration (Post *et al.*, 2010; Fabien *et al.*, 2013). However, glomerular filtration rate changes have been associated with the action of the PCTs and not to the actions of the glomerulus (Vrouenraets *et al.*, 2011). Nephrotoxicity may depend on specific patient profiles, the type of drug, and regimen which the patient is prescribed (Kalyesubula & Perazella, 2011). Diabetes mellitus (DM), kidney disease and additional nephrotoxic agents are additional factors that may account for renal changes in HIV-infected patients receiving ART (Kalyesubula & Perazella, 2011). Table 2.3 summarises adverse events associated with TDF use in the kidney.

The persistence of ADRs and subsequent withdrawal from treatment suggests the need for therapeutic agents to attenuate these reactions. These adverse effects lead to additional medical expenses which is not sustainable in low socioeconomic countries. This further illustrates the need for affordable products that can attenuate ADRs (Núñez, 2006). Although, ADRs are numerous and compounded by opportunistic infections, these should not motivate withdrawal from treatment (Schmid *et al.*, 2007). Other factors, including oxidative stress may play a significant role on the incidence of ADRs in HIV-positive individuals.

Table 2.3: Summary of studies on tenofovir induced adverse drugs reactions.

Study	Drug or Drug Combination	Subjects	Duration	Adverse Event	Comments
Gallent <i>et al.</i> , 2005	TDF	HIV-Positive Patients (n=344)	Case Reports	Increases in creatinine levels	Increased creatinine elevations were not associated with co-infections
Kohler <i>et al.</i> , 2009	TDF 100 mg/kg/day	HIV-Transgenic Mice (n=20)	5 Weeks	No histological observable changes using light microscopy	Electron microscopy showed increased mitochondria with irregular shape and fragmented cristae in PCTs
Lebrecht <i>et al.</i> , 2009	TDF or ddI 100 mg/kg/day	Male Sprague Dawley Rats (n=8)	8 Weeks	Increased diameter of PCTs with TDF	Lower body and kidney weight with TDF, lipid droplets observed in PCTs
Herlitz <i>et al.</i> , 2010	TDF	HIV-Positive Patients (n=13)	19.6±26.1 Months	Degenerative changes to PCTs and acute tubular necrosis	Nephrotoxicity was associated with intra-cytoplasmic inclusions in the PCT epithelial cells
Post <i>et al.</i> , 2010	ABC / 3TC / EFV vs TDF / FTC / EFV	HIV-Positive Patients (n=385)	96 Weeks	Increased markers of tubular dysfunction in TDF/FTC/EFT	No difference in glomerular filtration rate between regimens

Abacavir (ABC); Lamivudine (3TC); Didanosine (ddI); Tenofovir (TDF); Efavirenz (EFV); Emtricitabine (FTC); Proximal convoluted tubule (PCT).

2.3 OXIDATIVE STRESS, REACTIVE OXYGEN SPECIES AND ANTIRETROVIRAL THERAPY

Oxidative stress is a natural product of cellular metabolism and is defined as the overproduction or insufficient removal of reactive oxygen species (ROS). Reactive oxygen species are in the form of superoxide, hydroxyl, peroxy and hydroperoxy radicals (D'Autréaux & Toledano, 2007), including the non-radicals, hydrogen peroxide, and hydrochloric acid (Figure 2.4).

Oxygen	O^2
Peroxide	O_2^{-2}
Hydrogen peroxide	H_2O_2
Hydroxyl radical	OH
Hydroxyl ion	OH^-
Superoxide anion	O_2^-

Figure 2.4: Types of reactive oxygen species and electron pairs (Adapted from: Deavall *et al.*, 2012).

Chemically, ROS can be described in terms of reduction and oxidation reactions (REDOX). Oxidants, are oxygen compounds that receive electrons, while reductants refer to oxygen compounds losing electrons. Therefore, oxidation is the loss of electrons, and reduction is the subsequent gain (Kohen & Nyska, 2002). Reductants and oxidants are chemical terms for antioxidant and pro-oxidants, respectively, and will hereon be referred to as such.

A balance must be found between pro-oxidants and antioxidants for normal cellular function (Kuwabara *et al.*, 2008). Reactive oxygen species are able to initiate and mediate normal physiological processes (Kuwabara *et al.*, 2008). However, damage occurs when the accumulation of ROS exceeds cellular tolerance leading to oxidative stress (Kohen & Nyska, 2002). Long term exposure to oxidative stress leads to toxicity (Kohen & Nyska, 2002). An interest in the effects of oxidative stress has emerged in biomedical research due to the evidence that oxidative stress is a risk factor for the development of different diseases (Pitocco *et al.*, 2013). This is exacerbated by external factors such as drugs, food, and ultra-violet radiation (Figure 2.5). The over production of ROS can be attenuated by the introduction of antioxidants.

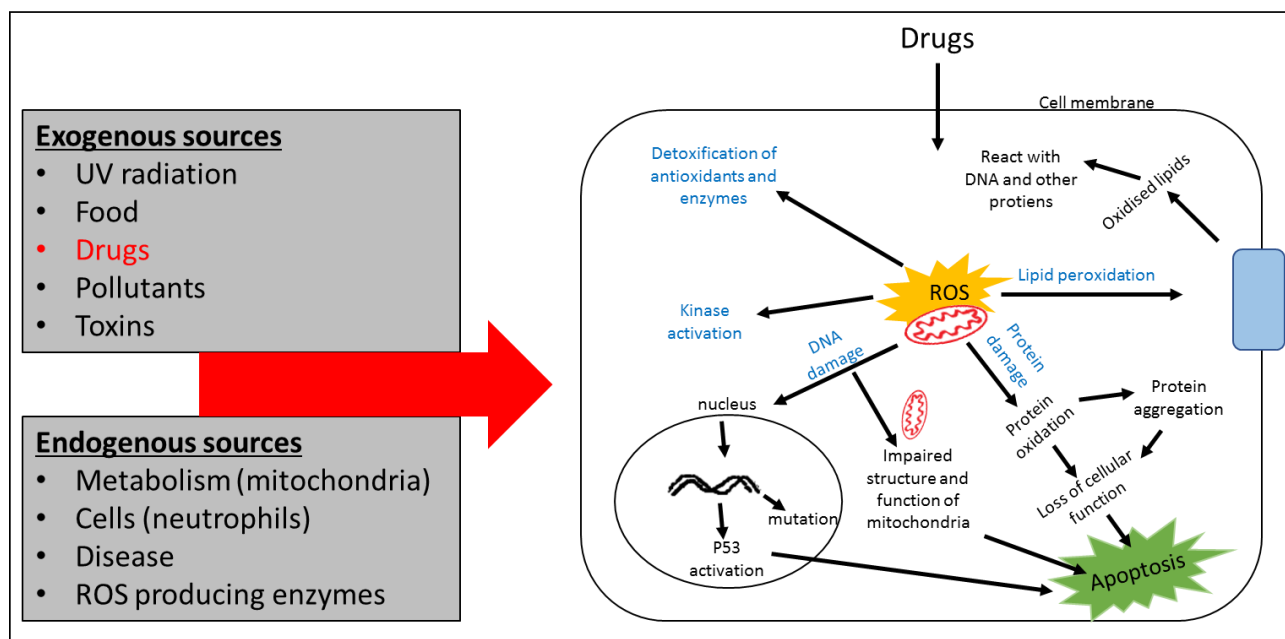


Figure 2.5: Exogenous and endogenous sources leading to reactive oxygen species. Both exogenous and endogenous sources of ROS are listed. Drugs enter the cellular membrane for normal metabolism causing an increase in reactive oxygen molecules in mitochondria. The overaccumulation of ROS leads to lipid damage, protein damage, DNA damage or the activation of kinases. These processes may eventually lead to apoptosis. Adapted from (Kohen & Nyska, 2002; Deavall *et al.*, 2012). Reactive oxygen species (ROS); Tumour protein (P53).

Cellular mitochondria are directly associated with the production of ROS (Kohen & Nyska, 2002). The occurrence of oxidative stress has been implied with the use of ART due to the emergence of mitochondrial toxicities, which have been extensively reviewed (Brinkman *et al.*, 1998; Carr & cooper, 2000; Carr, 2003). Long term exposure to ART is associated with morphological and ultrastructural changes to mitochondria (Kohler *et al.*, 2009; Deavall *et al.*, 2012). Two *in vitro* studies have directly associated the use of ART to increased ROS, resulting in mitochondrial dysfunction and oxidative stress (Jiang *et al.*, 2007; Manda *et al.*, 2011). These effects could potentially be mediated by introducing external sources of antioxidants such as rooibos.

2.4 OVERVIEW OF ROOIBOS

Rooibos or *Aspalathus linearis* (Burm.f.) Dahlgren, is native to the Cederberg mountains in the Western Cape region of South Africa (Morton, 1983). Rooibos (*Fabacea*, tribe: *Crotalariae*) is described as a shrub-like bush containing bright green, linear, sharp leaves with small clusters of yellow flowers resembling those found on pea plants (Figure 2.6) (Morton, 1983). There are two types of rooibos plants; the commonly cultivated “Nortier”-red type, and the wild “Cederberg” type (Morton, 1983; Joubert & de Beer, 2011).

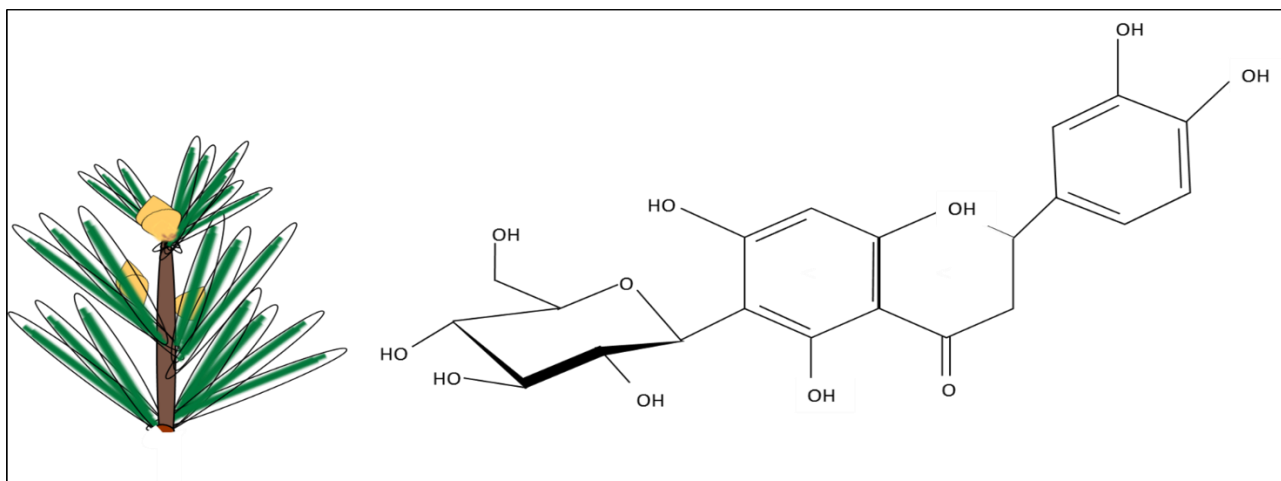


Figure 2.6: *Aspalathus linearis* bush and the chemical structure of Aspalathin. Adapted from: (Bramati *et al.*, 2002).

The South African Rooibos Council (n.d.), reported that the first account of rooibos use was in 1772 by the botanist and Dutch settler Carl Thunberg. Yet, it was only in 1904 that Benjamin Ginsberg first began the commercial sale and marketing of rooibos (Joubert & de Beer, 2011). The shortage of oriental black tea (*Camillia sinensis*) in the Second World War, and subsequent market collapse, spurred the production of alternative tea types resulting in the establishment of the Clanwilliam Tea Co-operative company in 1948 (Joubert & de Beer, 2011). However, in 1953 and 1954, rooibos became uneconomical due to market declines which lead to the founding of the Rooibos Tea Board in 1954 that aimed to establish a stable industry for rooibos (Joubert & de Beer, 2011). Now, the production, marketing and sustainable cultivation of rooibos falls under the South African Rooibos Council (SARC) (Joubert & de Beer, 2011). Currently over 14 000 tons of rooibos is produced in South Africa with approximately 6 000 tons being exported to international markets in Germany, United Kingdom and Japan (South African Rooibos Council, n.d.).

Rooibos is recognised as a herbal tisane, although marketed as “tea”. The term “tea” is only recognised for leaves from *Camillia senensis*; however, this term is used interchangeably in literature (Mckay & Blumberg, 2007). Rooibos first gained popularity as a herbal, low tannin, caffeine-free beverage that contributes to the total daily water recommendations (Joubert & de Beer, 2011). However, this shifted when a mother, Anique Theron, provided anecdotal evidence stating that the tea could be used to treat colic in infants (Morton, 1983). Now, rooibos popularity had increased due to its postulated antioxidant potential (Marnewick *et al.*, 2000).

Rooibos contains a unique array of polyphenols that contribute to the overall antioxidant capacity of the tea. The tea is the only known source of the C-C linked dihydrochalcone, aspalathin (Figure 2.6), and one of only two known sources of nothofagin (Standley *et al.*, 2001; Mckay & Blumberg, 2007).

The processing style of the tea is known to affect the chemical composition of the tea (Mckay & Blumberg, 2007).

2.4.1 Composition of rooibos

Rooibos contains approximately 25 major polyphenols (Iswaldi *et al.*, 2011) of which the 15 principle polyphenols are listed in Table 2.4. These are grouped as dihydrochalcones, flavones, flavanols, phenylpropanoid and hydroxycinnamic acid (Joubert *et al.*, 2008; Beelders *et al.*, 2012).

Table 2.4: Main polyphenols found in rooibos adapted from (Beelders *et al.*, 2012).

Group	Phenolic compound
Dihydrochalcones	Aspalathin, Nothofagin
Flavones	Orientin, Iso-orientin, Vitexin, Iso-vitexin, Luteolin, Luteolin-7-O-glucoside, Chrysoeriol
Flavanols	Quercetin, Iso-quercetin, Hyperoside, Rutin
Phenylpropanoid	Phenylpyruvic acid-2-o-glucoside
Hydroxycinnamic acid	Ferulic acid

Rooibos cultivators still employ the traditional methods of fermentation by sun drying, browning, and bruising of leaves and stems to achieve the familiar red-brown colour of the tea (Joubert & de Beer, 2011). The fermentation process causes a significant loss in the polyphenol composition of the tea, specifically, the main antioxidant, aspalathin (Koeppen & Roux, 1966; Joubert, 1996a; Canda *et al.*, 2014). During fermentation, aspalathin is replaced, due to degradation, with the high molecular weight compounds iso-orientin and orientin (Krafczyk & Glomb, 2008), allowing for the rich red colour associated with the tea (Krafczyk *et al.*, 2009). To reduce the loss of polyphenols during fermentation, the Agricultural Research Council (ARC) proposed a new processing method that contained higher concentrations of the polyphenols specifically aspalathin (Joubert & de Beer, 2011). Although, both the fermented and unfermented versions are commercially available the fermented version still remains the most commonly consumed of the two (Beelders *et al.*, 2012).

Fermented rooibos is appealing due to its taste; however, from a therapeutic stance, the loss of its antioxidant capability is concerning, since fermented samples contain less than 10% of the original phenolic content (Table 2.5) (Joubert, 1996b, Muller *et al.*, 2016). This loss is problematic as aspalathin, followed by quercetin, and nothofagin (Snijman *et al.*, 2007), have shown impressive antioxidant capabilities (Yoshikawa *et al.*, 1990; Snijman *et al.*, 2009; Villaño *et al.*, 2010). This makes rooibos an attractive therapeutic agent to attenuate the effects of oxidative stress (von Gadow *et al.*, 1996; Marnewick *et al.*, 2004; Krafczyk *et al.*, 2009).

Table 2.5: Polyphenol changes and total antioxidant capacity between fermented and unfermented samples of rooibos (Marnewick, 2014).

Rooibos type	Total polyphenol content (mg GAE) ^b	Total flavones/flavanols (mg quercetin equivalents) ^c	Total antioxidant capacity ^d
Fermented *	73.43±1.79	33.44±0.38	1537.60± 27.40
Unfermented	106.46±2.14	26.85±0.28	2093.57±50.20

^a Fermented rooibos based on one cup = 200 mL prepared by steeping one rooibos tea bag in 200 mL fresh boiled water. ^b Folin-Ciocalteu methods measured against gallic acid equivalents(GAE).^c 360 nano method.

^d Based on the oxygen radical absorbance capacity (± Std. Dev) of ten samples.

In order to preserve rooibos polyphenols, Joubert and de Beer (2011) patented a new vacuum drying technique; however, the high costs of the method hinders its commercialisation. By limiting the exposure of rooibos leaves and stems to oxygen, direct sunlight (Koeppen & Roux, 1966), pH fluctuations, and low temperatures, the preservation of the aspalathin and other phenolic compounds may be limited (Joubert & de Beer, 2011). The demand for investigations on the therapeutic actions of rooibos stresses the need for quantitative and qualitative polyphenol amounts to be reported in the literature. This allows for researchers to make convincing conclusions on the putative therapeutic actions of rooibos.

2.4.2 Protective effects of rooibos

Studies have shown the anti-inflammatory activity (Baba *et al.*, 2009, Hendricks & Pool, 2010; Schloms *et al.*, 2012), chemo-protective (Marnewick *et al.*, 2009 Joubert & de Beer, 2011), antimutagenic (Snjiman *et al.*, 2007; Canda *et al.*, 2014; Gelderblom *et al.*, 2016), anti-carcinogenic (Petrova, 2009), antidiabetic (Ulcina *et al.*, 2006; Francisco, 2010; Muller *et al.*, 2012, Mazibuko *et al.*, 2013; Kamakura *et al.*, 2015), anti-obesity (Beltran-Debon *et al.*, 2011, Son *et al.*, 2013; Sanderson *et al.*, 2014), and antioxidant effects (Bramati *et al.*, 2003; Awoniyi *et al.*, 2012; Chen *et al.*, 2013) of rooibos. Table 2.6 summarises some of the *in vitro* studies conducted.

One of the first rat studies conducted on rooibos showed reduced lipid peroxidation in the brain of aged female Wistar rats (Inanami *et al.*, 1995), concluding that the flavonoids found in rooibos acted as free radical scavengers (Inanami *et al.*, 1995). Panti *et al* (2011) showed the cardiac protective capabilities in male Wistar rats exposed to both fermented and unfermented rooibos. The study observed that rooibos extracts significantly improved aortic output with no effect on the REDOX status (Panti *et al.*, 2011). The authors further postulated, that protection exhibited by rooibos may be due to the inhibition of apoptosis. Baba *et al* (2009) demonstrated the anti-inflammatory effects using a rat colitis model in male Wistar rats. Colitis was induced using dextran sodium sulphate

(DSS), and the authors concluded that rooibos reduced inflammation by decreasing super oxide dismutase (SOD) levels in colic rats (Baba *et al.*, 2009).

Kawano *et al* (2009) demonstrated the amelioration of glucose intolerance and insulin secretion in db/db mice with aspalathin introduction. Francisco and colleagues (2010) reported that fermented rooibos reduced plasma glucose, low density lipoprotein (LDL) cholesterol, and thiobarbituric reactive substances (TBARS) levels, a measure of lipid peroxidation (Janero, 1990). These changes led to an increase in the total plasma antioxidant capacity (Francisco *et al.*, 2010). In streptozotocin-induced (STZ) diabetic rats Muller *et al* (2012) observed that aspalathin reduced blood glucose levels thereby reducing hyperglycaemia.

The protective effects of rooibos on hydroperoxide-induced hepatotoxicity (t-BHP) in male Wistar rats, decreased AST and ALT levels (Ajuwon *et al.*, 2013). This was further illustrated by Ulicna *et al* (2008) in CCl₄-induced liver damage, causing the histological regression of steatosis and cirrhosis, while reducing elevated ALT and AST levels. Marnewick and colleagues (2003) demonstrated that continual feeding of aqueous extracts of fermented and unfermented rooibos in male Fischer rats had no effects on the antioxidant capacity of the liver. However, it significantly improved glutathione (GSH) redox status, by increasing the oxidative markers glutathione (GSH), and reduced glutathione (GSSG) (Marnewick *et al.*, 2003).

Serum cholesterol, triglycerides and free fatty acid levels were reduced in rats fed a high fat diet following rooibos treatment (Beltran-Debon *et al.*, 2011). Recent studies conducted by Monsees and Opawari (2017) reported that rooibos had no effect on the liver, however, the study showed that a 5% rooibos aqueous solution caused liver hypotrophy compared to control groups. No necrotic, structural or lymphocyte infiltration was observed in the liver (Monsees & Opawari, 2017). Similar observations were seen in the kidney; however, serum creatinine levels were higher in fermented compared unfermented rooibos treated rats (Monsees & Opawari, 2017). Although rooibos has shown attenuating effects in these organs, three cases of hepatotoxicity have been reported with excessive rooibos consumption presenting as elevated AST and ALT levels (Sinsalo *et al.*, 2010; Engels *et al.*, 2013; Zacharia & Whitlatch, 2013).

Table 2.6: Summary of *in vitro* studies conducted on fermented and unfermented samples of rooibos.

Study	Rooibos type	Effect	Cell model	Result
Petrova, 2009	Fermented & Unfermented	Anti-carcinogenic	Skin carcinogenic mouse model	Reduced incidence and volume of tumours reduced oxidative stress
Beltran-Debon <i>et al.</i> , 2011	Fermented	Anti-obesity	3T3-L1 mouse adipocytes	Inhibited triglyceride accumulation
Muller <i>et al.</i> , 2012	Unfermented	Anti-diabetic	C2C12 and Chang cells	Increased glucose uptake and hyperglycaemia
Schloms <i>et al.</i> , 2012	Unfermented	Anti-inflammatory	Transiently transfected CIS-1 cells with 0.1 µg DNA (baboon, CYP17A1, CYP21, CYP11B1)	Decreased total steroid output 4-fold, reduced aldosterone, and cortisone precursors
Dludla <i>et al.</i> , 2014	Fermented	Cardio-protective	Ex vivo STZ-induced diabetic rat cardiomyocytes	Protected diabetic cardiomyocytes against exogenous and ischemic oxidative stress
Sanderson <i>et al.</i> , 2014	Fermented	Anti-obesity	3T3-L1 adipocytes	reduced adipogenesis
Kamakura <i>et al.</i> , 2015	Fermented & Unfermented	Anti-diabetic	Insulin resistant C2C12 muscle cells	Reversed palmitate induced insulin resistance

Reactive oxygen species (ROS); Streptozotocin (STZ); Deoxyribonucleic acid (DNA).

Multiple *in vivo* studies on rooibos have been conducted in humans with varying results. A study conducted by Sauter (2005) showed no changes in the antioxidant activity using rooibos extracts in 20 subjects following copper induced low density lipoprotein oxidation. Wanjiku, (2009) agreed that no significant changes in antioxidant parameters were met in eight healthy males exposed to an oral dose of 500 mL of fermented rooibos. Marnewick *et al* (2011) reported significant decreases in lipid peroxidation, decreased levels of LDL cholesterol, and triglyceride levels with a significant increase in high density lipoproteins in humans (n=41) at risk of cardiovascular disease. The discrepancy observed *in vitro* and *in vivo* studies may be attributed to the bioavailability of rooibos *in vivo* (Marnewick, 2014).

Although numerous studies have demonstrated the potent antioxidant activity of rooibos, the pro-oxidant effects have also been noted. Joubert *et al* (2005) demonstrated that pure aspalathin extracts compared to aqueous extracts had pro-oxidant activity. Therefore, caution must be taken when applying rooibos polyphenols in herbal medicines as the pro-oxidant activity may cause cytotoxicity (Marnewick, 2014).

2.4.3 Bioavailability of rooibos

The effectiveness of any natural compound as a source of antioxidants is dependent on its bioavailability (Manach *et al.*, 2005). The bioavailability of a compound refers to its absorption, distribution, metabolism and excretion (Manach *et al.*, 2005). Muller *et al* (2016) stated that the efficacy of any flavonoid is based on how it is introduced. The method of introduction could be in the form of an aqueous solution that is introduced in drinking water, mixed in feed, orally gavaged or added to another compound acting as a vehicle. Muller *et al* (2016) further stated that the method of consumption may be the cause for the discrepancy observed between the action of rooibos *in vitro* and *in vivo*.

One of the first studies evaluating the absorption of aspalathin was conducted in pigs (n=3) (Kreuz *et al.*, 2008). The study used an enriched green rooibos extract mixed in pig feed. The amount of aspalathin present in urine and plasma were measured after seven and eleven days. It was found that aspalathin was able to pass from the small intestine to the large intestine where the interaction with colonic microflora caused the formation an a-glycon and sugar moiety with the subsequent breakdown of aspalathin to its c-glucoside forms (orientin and iso-orientin) (Kreuz *et al.*, 2008). These results confirmed that aspalathin undergoes glucorondination and methylation allowing absorption (Kreuz *et al.*, 2008). No aspalathin was present in serum samples (Kreuz *et al.*, 2008). This lack of aspalathin in serum may be attributed to its affinity for plasma proteins (Muller *et al.*,

2016). Yet, when the same pigs were given a three times higher dose of aspalathin, trace amounts were found in the serum (Kreuz *et al.*, 2008).

The synergistic action of aspalathin and its flavonoids may assist in the bioavailability of aspalathin (Muller *et al.*, 2016). Using a Caco-2 monolayer cell model, Huang *et al.* (2008) demonstrated that a green rooibos extract was a better model for aspalathin absorption compared to a pure aspalathin extract. Using the same model, Courts and Williamson (2009) concluded that aspalathin uses passive diffusion in intestinal epithelium, thus, the actions of the other polyphenols in rooibos allows for greater absorption.

The poor bioavailability of aspalathin may be due to the fact that it does not follow Lipinski's Rule of Five (Lipinski *et al.*, 2012; Muller *et al.*, 2016). For any drug or therapeutic agent to be bioactive or pharmacologically active Lipinski's Rule of Five must be considered. This rule refers to the multiples of five and not the number of rules. In general, the rule states that orally active substance must not violate more than one of the following criteria: It must have no more than five hydrogen bonds (aspalathin has nine hydrogen bonds). No more than ten hydrogen bond acceptors (aspalathin has 11 hydrogen bond acceptors). Aspalathin must have a molecular mass less than 500 daltons (aspalathin is 453 daltons). Finally, aspalathin must have $\text{Log } P > 5$ (aspalathin $\text{Log } p = -0.322$). Despite aspalathin violated two of the four rules, rooibos and its polyphenols remain attractive therapeutic options to alleviate oxidative stress in biological systems; therefore, importance should be placed on the study of rooibos and its polyphenols (Joubert *et al.*, 2011).

2.5 ORGAN SYSTEMS: HISTOLOGY AND PATHOLOGY

2.5.1 Pancreas histology

The rodent pancreas is a highly diffuse, multilobulated structure that spreads from the end of the duodenal loop into the gastrosplenic omentum (Kara, 2006). Topographically, the rat pancreas can be observed with the removal of the stomach and duodenum. Once these structures are removed three distinct portions are seen namely the biliary, duodenal and gastrosplenic portions (Kara, 2005).

Histologically, the pancreas consists of both exocrine and endocrine parts that differ in terms of structure and function (Kierszenbaum & Tres, 2015). The functional unit of the exocrine pancreas is the acinus, which secretes digestive enzymes (Wieczorek *et al.*, 1998; Young *et al.*, 2006; Kierszenbaum & Tres, 2015). The acinus is a pyramid shaped cluster of secretory cells that surround the centroacinar cells, recognised by their central location and pale staining nuclei in the lumen (Kierszenbaum & Tres, 2015). Each centroacinar cell is surrounded by the acinar cells, of which the

apical portion is occupied by dark staining zymogen granules containing the pancreatic enzymes (Kierszenbaum & Tres, 2015). These cells are continuous with the duct systems forming the intercalated ducts, the smallest tributary of the duct system, followed by the intralobular ducts and the interlobular ducts. These ducts are differentiated by the amount of connective tissue. The bigger the duct, the more connective tissue (Young *et al.*, 2006; Kierszenbaum & Tres, 2015).

Both the exocrine and endocrine portions are highly vascularised and are supplied by the acinar vascular system and insuloacinar portal systems, respectively (Kim *et al.*, 2009; Kierszenbaum & Tres, 2015). Different types of models have been proposed for islet microvasculature, mainly the mantle to core, core to mantle and artery to vein models, which differ according to the cell types and their function within the pancreatic islets (Murakami *et al.*, 1997; Kim *et al.*, 2009). However, this is beyond the scope of this research.

Embedded within the exocrine tissue are the pancreatic islets forming approximately 2% of the total organ mass (Wieczorek *et al.*, 1998). Each islet is surrounded by a delicate capsule made up of reticulin fibres and is formed by anastomosing cords of endocrine cells. These endocrine cells include glucagon secreting α -cells, insulin secreting β -cells, somatostatin secreting δ -cells and pancreatic polypeptide secreting PP-cells (Elayat *et al.*, 1995; Wieczorek *et al.*, 1998; Young *et al.*, 2006; Kierszenbaum & Tres, 2015). Each islet in the human and rat vary in terms of composition, architecture, location, and size (Figure 2.7) (Wieczorek *et al.*, 1998; Steiner *et al.*, 2010).

In humans, the α -cells form the majority (82%) of the islet, compared to β -cells (13%), δ -cells (4%), and PP-cells which comprise the minority (1%) (Steiner *et al.*, 2010). The various cell types are dispersed within the islet and do not form a specific pattern. Various studies have noted that the composition of pancreatic islets may vary according to location within the organ. Brissova *et al.* (2005) demonstrated that the body, neck, and tail portions of the pancreas contained greater numbers of α -cells and β -cells, whereas the head portion had a greater number of PP-cells. Kim and colleagues (2009) noted that smaller islets have a larger number of β -cells in comparison to larger islets.

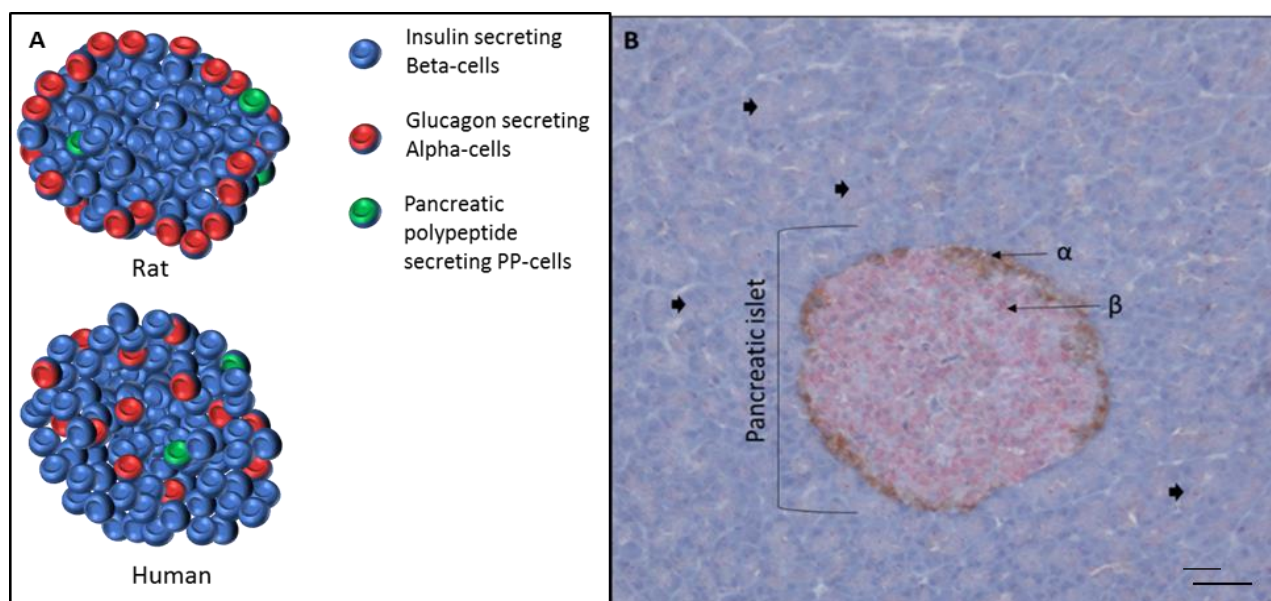


Figure 2.7: Graphical representation of the islets of Langerhans. A) shows the variation in human and rat pancreatic islets, rat pancreatic islets show insulin secreting β -cells forming the majority, and are surrounded at the mantle by the glucagon secreting α -cells. Dorsal aspect of the islet contains several PP-cells with few δ -cells. In the human islets, the various cells are dispersed throughout the islet and do not follow a specific pattern Adapted from (Suckale *et al.*, 2008); B) a double immunohistochemically labelled rat pancreatic islets using insulin and glucagon antibodies to identify α -cells and β -cells within the pancreatic islet embedded within the acinus (black arrows) (100x magnification) bar=100 μ m.

Unlike human islets, the rat islet is predominately composed of β -cells (forming 60-80% of the total islet mass), followed by the α -cells (15-20%), δ -cells (<10%) and PP-cells (1%) (Steiner *et al.*, 2010). On two-dimension histological sections the pancreatic islets show α -cells forming a continuous mantle around a core of β -cells (Wieczorek *et al.*, 1998; Steiner *et al.*, 2010). Like humans, a significant difference in the number of islets were present in different regions of the rat pancreas. Eleyat *et al* (1995) noted that PP-cell rich islets were predominantly found in duodenal portion of the pancreas while α -cell rich islets were mainly situated in the upper duodenal, gastric, and splenic portions. The size of the islets vary throughout the pancreas (Eleyat *et al.*, 1995). One of the resounding notes stated by Kim *et al* (2009) and Steiner *et al* (2010), is that the pancreas is not a static structure and is able to respond to various physiological conditions and that islet structure and architecture is compromised in various pathological conditions.

2.5.2 Pancreas pathology

The pancreas is prone to various metabolic changes affecting both the exocrine and endocrine portion. Damage to the exocrine portion of the pancreas is termed pancreatitis of which there are two forms, namely acute and chronic (Cross, 2013). Pancreatitis generally refers to inflammation of the pancreas which may develop due to infection, hyperlipidaemia, trauma, alcohol abuse, or with the use of certain drugs (Cross, 2013). Zhang and colleagues (2010) demonstrated the early manifestation of

damage in a pancreatitis induced rat model. The pancreas presented with mild inflammatory cell infiltration, intestinal congestion and oedema, including instances of focal necrosis (Zhang *et al.*, 2010). The continuation of this insult to the pancreas leads to chronic pancreatitis which may result in fibrosis or complete destruction of pancreatic tissue (Kierszenbaum & Tres, 2015).

The endocrine portion may be affected by immunosuppressive drugs tacrolimus and cyclosporine leading to degenerative changes of pancreatic islets (Drachenberg *et al.*, 1999). These degenerative changes present as cytoplasmic changes and vacuolations of β -cells (Drachenberg *et al.*, 1999). In STZ induced diabetic rats, Adewole *et al* (2007) noted the breakdown of micro-anatomical features, namely the dysregulation of β -cells, decreased cellular density, and necrotic changes. In STZ treated mice, Michels *et al* (1986) noted a higher volume of pancreatic islets however, the study noted decreases in β -cell volume compared to controls.

It should further be noted that all these disease states may be a result of oxidative stress. The β -cell is particularly prone to oxidative stress as these cells contain very low levels of natural antioxidants (Sakuraba *et al.*, 2002). These disease states demonstrate the morphological changes and histopathological representations that may occur.

2.5.3 Liver histology

The liver is multifunctional metabolic organ, where fats are oxidised to triglycerides producing energy and plasma lipoproteins are synthesised forming cholesterol and phospholipids (Young *et al.*, 2006). Through the actions of glycogenesis, glycogenolysis and gluconeogenesis, the liver is able to regulate blood glucose concentrations, and metabolise carbohydrates to fatty acids and triglycerides (Young *et al.*, 2006). It further functions to synthesize and produce plasma proteins, clotting factors, and non-essential amino acids. In addition, the liver functions to eliminate and detoxify various drugs and toxins including alcohol. In this regard the liver plays an important role in drug metabolism (Young *et al.*, 2006).

The rat liver consists of four lobes, namely the median lobe, caudate lobe, right lateral lobe and left lateral lobe (Suckow *et al.*, 2005). One of the main differences between the rat and human liver is that the former lacks a gall bladder. In rats the bile ducts from each caudate lobe, anastomose forming the common bile duct (Suckow *et al.*, 2005). Although, anatomically the number and pattern of the liver lobes varies between species, histologically the liver follows a similar structure.

There are two types of cells in the liver, namely the parenchymal cells which are the hepatocytes and non-parenchymal cells (Kupffer, stellate and endothelial cells) (Bouwens *et al.*, 1992; Wisse *et al.*, 1996). Hepatocytes are the pyramidal or rounded shaped cells that form the bulk of the liver parenchyma (80%) and provide both exocrine and endocrine functions (Baratta *et al.*, 2009). These cells are generally mononucleated; however, binucleated hepatocytes are common as well (Gupta, 2000). A network of collagen type I, II and III, IV and V is found throughout the liver and is particularly rich in type III reticulin fibres, providing an architectural base in which the hepatocytes sit (Kierszenbaum & Tres, 2015). The hepatocytes form the limiting plates of the hepatic sinusoids. Kupffer cells are predominantly found within the blood sinusoids, however the cells are more frequent around the periportal areas (Wisse *et al.*, 1996). Separating the blood sinusoids from the hepatocytes is the space of Disse (Kierszenbaum & Tres, 2015). Of which some of the non-parenchymal cells such as stellate cells (peri-sinusoidal cells) are found (Wisse *et al.*, 1996). These cells are activated in the early stages of liver injury (Wisse *et al.*, 1996). Finally, endothelial cells line, blood vessels and sinusoids within the liver (Kierszenbaum & Tres, 2015).

The structural and functional unit of the liver is the hepatic lobule. The classical structure of the hepatic lobule is discerned by the central vein surrounded by six portal triads forming a hexagon (Figure 2.8) (Young *et al.*, 2006; Kierszenbaum & Tres, 2015). The classic hexagonal shape of the lobule is not easily seen in the human or rat however, this structure is clearly defined in other mammals including the pig (Kierszenbaum & Tres, 2015). The portal lobule is defined by three central veins where the bile canaliculi drain into the same bile duct forming, the hepatic lobule (Cross, 2013). The final structure of the liver and commonly referred to in pathology, is the liver acinus. The liver acinus is the smallest functional unit of the liver and is structured based on arterial blood flow between bordering central veins and the portal triad. Essentially, the acinus is made up of two wedged shaped masses consisting of a portal triad at the centre and are surrounded by two neighbouring central veins. Each acinus consist of three zones; zone one (periportal region) consisting of highly oxygenated hepatocytes, zone two (midzonal) forming the intermediate layer, and zone three (centrilobular) consisting of poorly oxygenated hepatocytes prone to hypoxia (Kierszenbaum & Tres, 2015).

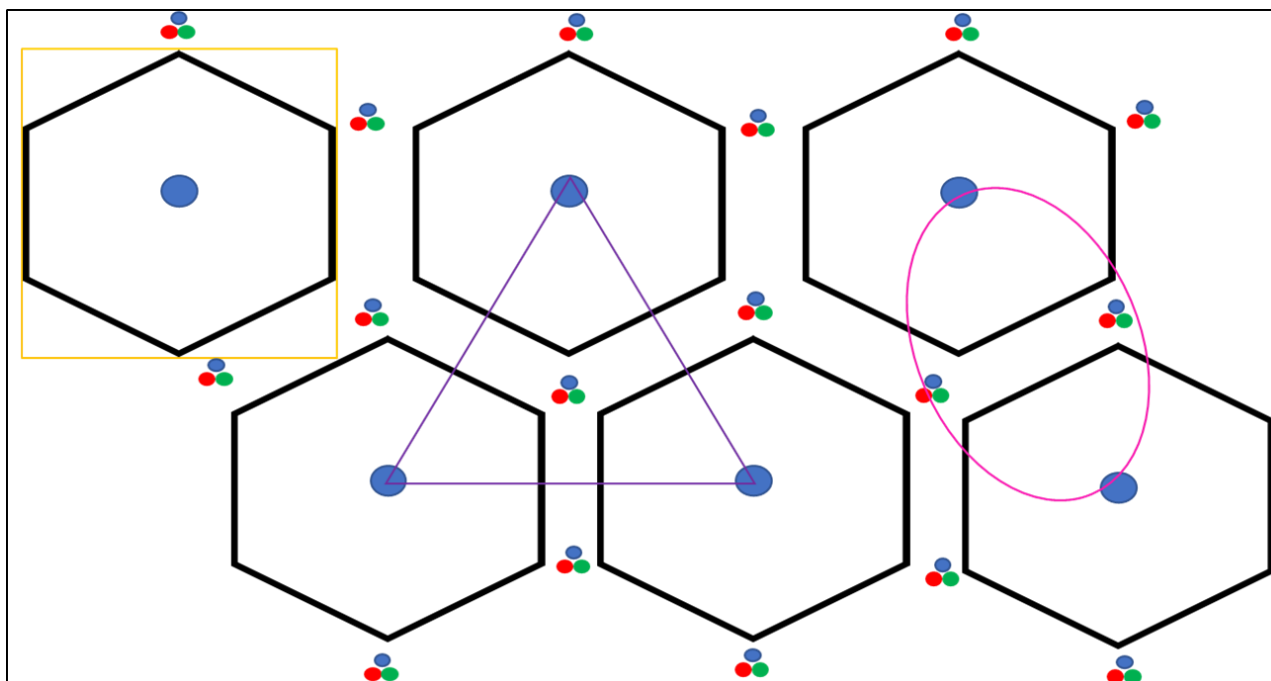


Figure 2.8: Graphical representation of the functional units of the liver. The hepatic lobule is the hexagonal shaped structure (orange) consisting of a central vein (large blue circle) at the centre and is surrounded by the portal triad (triangle shaped circles) consisting of the hepatic vein (small blue circle), hepatic artery (red circle) and bile duct (green circle). The portal lobule (large purple triangle) is formed by the central veins which drain into a single central bile duct. The acinus (pink oval) is formed by neighbouring central veins and consist of three zones, zone three closest to the central vein and zone one is the furthest from the central vein.

2.5.4 Liver pathology

The liver is a highly regenerative organ and able to adapt quickly to stressors (Nayak *et al.*, 1996; Michanalopoulos, 2007). However, due its multifunctionality, the liver is prone to various types of damage, for the majority of this section focus is placed on the diagnosis of hepatic liver injury as a result of drug administration. It should be noted that these liver injuries all follow a common pathway; generally resulting in fibrotic changes (Alcolado *et al.*, 1997), unless these insults lead to degenerative changes such as necrosis. The major histological lesions in the liver are fatty changes, hepatocellular death or hepatobiliary lesions (Amacher, 1998). There are two types of fatty changes, namely microvesicular or macrovesicular steatosis, which are differentiated by the displacement of the nucleus (Amacher, 1998). Microvesicular steatosis is characterised by the formations of small lipid vacuoles within the cytoplasm of hepatocytes. Generally, this formation does not cause the displacement of the nucleus. Macrovesicular steatosis is described as the formation of one large lipid vacuole displacing the nucleus of the hepatocytes (Amacher, 1998). Another form of damage that may result, is fibrosis. Fibrosis is characterised by an increase collagen fibres within the parenchyma (Alcolado *et al.*, 1997). With increasing severity fibrosis, will result in cirrhosis (Cross, 2013). One of the principle staining techniques used to observe fibrosis in the liver is Masson's trichrome stain,

which is able to distinguish type I collagen fibres allowing histopathologists to examine the extent of the fibrotic change (Saxena, 2010). Cellular damages will occur where large portions of the liver parenchyma are disrupted leading to necrosis. Necrosis leads to the severe disruption and subsequent collapse of liver architecture specifically reticulin fibres. The reticulin stain is routinely used by histopathologist to examine the extent of architectural damage and regeneration occurring in the liver (Saxena, 2010).

Liver injuries share common diagnostic feature in that they lead to liver enzyme elevations specifically ALT and AST. These serum biomarkers are the gold standard in determining liver toxicity and are the single most commonly used diagnostic feature for hepatocellular injury (Amacher, 1997; Ozer *et al.*, 2008). When damage occurs hepatocytes release ALT and AST into the extracellular space, thus entering circulation (Ozer *et al.*, 2008). Both these serum markers provide an indication of damage in other areas of the body, for example AST may also be used as a biomarker for heart and skeletal muscle injury, while ALT may be used as marker for muscle necrosis (Nathwani *et al.*, 2005). However, it is the ratio of AST:ALT that allow pathologists to determine liver injury from other types of tissue damage (Ozer *et al.*, 2008). Serum AST and ALT are routinely used diagnostic features used in experimental and clinical studies, and are often referred to in studies evaluating the liver (Siest *et al.*, 1975).

2.5.5 Kidney histology

The kidney forms part of the urinary system and primarily functions to filtrate and excrete waste products (Kierszenbaum & Tres, 2015). It regulates blood and water homeostasis through the absorption of small molecules, such as amino acids and glucose (Kierszenbaum & Tres, 2015). Through the renin-angiotensin-aldosterone system the kidney maintains blood pressure (Young *et al.*, 2006; Cross, 2013; Kierszenbaum & Tres, 2015). Due to its many functions, the kidney is comprised of unique systems of complex structures allowing for the filtration and excretion of waste products from the blood (Cross, 2013).

The urinary system of the human and rat comprises of two paired bean-shaped kidneys (Green, 1955). Anatomically, the rat kidney is unilobular while the human is multilobular (Kierszenbaum & Tres, 2015). However, the kidney does not vary histologically and is composed of four distinct segments divided into a cortex and medulla. The cortex is further divided into the outer cortex and medullary cortex and then into the outer and inner medulla (Young *et al.*, 2006; Kierszenbaum & Tres, 2015). The medulla consists of cone or pyramid shaped structures that form the renal medullary pyramid. The pyramid extends from the calyx to the cortex, forming the corticomedullary zone (Kierszenbaum

& Tres, 2015). The renal medullar pyramids to the corticomedullary zone form the renal lobe (Young *et al.*, 2006; Kierszenbaum & Tres, 2015) these structures form the bulk of the kidney.

Blood is supplied to the kidney by a single renal artery, consisting of a dorsal and ventral branch, which in turn, subdivide into the cranial and caudal branches (Yoldas & Dayan, 2014; Kierszenbaum & Tres, 2015). These vessels then branch out into the juxtamedullary cortex forming the arcuate arteries (Kierszenbaum & Tres, 2015). These arteries then ascend into the cortex forming the interlobular arteries and afferent arterioles giving rise to the glomerular capillary network (Kierszenbaum & Tres, 2015). This unique network of glomerular capillaries, form a part of the nephron. The nephron is the functional unit of the kidney and is comprised of the renal corpuscle and renal tubules (Young *et al.*, 2006).

Situated within the cortex is the spherical-shaped renal corpuscle, which is composed of a glomerulus surrounded by a Bowman's capsule (Young *et al.*, 2006; Calado, 2013). The glomerulus is a mass of anastomosing glomerular capillaries that are situated within the renal space (Kierszenbaum & Tres, 2015). The glomerulus is composed of the glomerular capillaries, podocytes and the mesangium (a mixture of mesangial cells and mesangium matrix) (Kierszenbaum & Tres, 2015). The Bowman's capsule is made up of visceral and parietal layers, it is the parietal layer that forms the basement membrane of the capsule. The renal space is the space between the visceral and parietal layer of the Bowman's capsule which is generally filled by plasma ultrafiltrate (Young *et al.*, 2006; Calado, 2013; Kierszenbaum & Tres, 2015). The renal space is continuous with the second portion of the nephron, the renal tubule (Young *et al.*, 2006; Kierszenbaum & Tres, 2015).

The renal space joins with the PCTs which descend into the medulla forming the loop of Henle, which then ascend back to the cortex forming the distal convoluted tubules (DCT). Via a connecting tube, the DCTs attach to the collecting duct. Facing the afferent and efferent arterioles is an area of dense cells termed the macula densa, which form part of the DCT (Kierszenbaum & Tres, 2015).

The PCT and DCT are distinctly different, and can be differentiated by the pattern of the epithelial cells, and the presence or absence of a brush border (Young *et al.*, 2006; Kierszenbaum & Tres, 2015). The brush border allows for a substantial increase in the absorption capacity of the PCT. Due to the high glycogen content of the brush border, the periodic acid schiff (PAS) stain provides a good indication of the differences between the PCT and DCTs. Due to the increased mitochondria within the cytoplasm, the PCTs generally stain more intensely using the PAS method. Situated within the cortex, amongst the PCTs, are the DCTs. These tubules arise from the ascending limb of the loop of

Henle and are distinguished from the PCT by the clearer larger lumen, increased number of nuclei and the absence of a brush border (Young *et al.*, 2006; Kierszenbaum & Tres, 2015). The various functions of the kidney will determine the resulting injurious lesion and the structure affected in the kidney.

2.5.6 Kidney pathology

The nature of the kidney is highly complex; thus, the resulting pathology may affect various structures. Figure 2.9 summarises the types of diseases affecting the glomerular corpuscle and PCT. The size and width of the glomerulus is implicated in various diseases (Kotyk *et al.*, 2015). These injuries present as increased glomerular surface area and expansion of the renal space due to a thickening basement membrane. These have been observed in numerous pathological conditions including drug induced toxicities. Glomerular disease may occur as a consequence of a high fat diet, diabetes, blood pressure, or drug use. A study conducted by Goumenos *et al.* (2009) on obese individuals, found that obese patients presented with enlarged glomeruli and early stages of diabetic nephropathy. In rats, large intravenous doses of human basic fibroblast growth factor (FCE 26184) resulted in enlarged and vacuolated podocytes and cast formation in the PCT and DCT (Mazué *et al.*, 1993). In STZ-induced diabetic rats the kidneys presented with increased glomerular volume, tubule length and volume compared to the control animals (Rasch & Dørup, 1997). A similar study noted an enlarged renal space with thickening of tubular and glomerular basement membranes in obese dogs compared to controls (Henegar *et al.*, 2001). A study evaluating drug toxicity of cyclosporine and FK505 (antibiotics) noted that short term drug toxicity was associated with PCT and DCT vacuolations not exceeding 20% of the total diameter (Randhawa *et al.*, 1993). Thus, various injuries may lead to quantitative and qualitative measurable changes within the kidney.

CHAPTER THREE: RESEARCH DESIGN

3.1 RESEARCH QUESTIONS

- Does ART have a histologically discernible damaging effect on the histology of the pancreas, liver, and kidney?
- If so, what is the extent of the histological damage in the various organs?
- Does the administration of rooibos (*A. linearis*) tea, attenuate the potentially damaging effects of the antiretroviral drug combination (Efavirenz, Emtricitabine, and Tenofovir) on the histology of the pancreas, liver, and kidney in male Wistar rats?

3.2 AIM

To assess the effects of antiretroviral drugs, and rooibos tea on the histology of the pancreas, liver, and kidney in the male Wistar rat.

3.3 OBJECTIVES

To achieve the above mentioned aim the following steps will be taken:

1. To histologically assess the morphology of the pancreas and kidney using light microscopy and quantitative morphometric measurements in the following four groups:
 - Untreated control (C);
 - Control animals receiving ART (C-ARV);
 - Control animals receiving rooibos tea (C-R);
 - Experimental animals receiving ARV drugs and rooibos tea (ARV+R).
2. To analyse the pancreas, liver, and kidney for pathology using semi-quantitative methods of grading and scoring in the four treatment groups.
3. To measure blood glucose levels in the four experimental groups and to compare differences between the groups.
4. To measure alanine aminotransferase (ALT) and aspartate aminotransferase (AST) levels including the ratio of ALT:AST of the four experimental groups and to compare the differences between these groups.

3.4 HYPOTHESES

H₀: Rooibos does not have a restorative effect on the histomorphology of the pancreas, liver, and kidney of male Wistar rats following antiretroviral therapy.

H_a: Rooibos has restorative effects on the histomorphology of the pancreas, liver, and kidney of male Wistar rats following antiretroviral therapy.

CHAPTER FOUR: MATERIALS AND METHODS

4.1 ETHICAL APPROVAL

Ethical approval for the following study has been obtained from Stellenbosch University Research Ethics Committee. Ethical approval was granted for the housing of animals under SU-ACUD14-00021, and for the use of animal tissue under the ethics number SU-ACUD15-0003.

4.2 STUDY GROUPS AND ANIMAL CARE

Male Wistar rats (*Rattus norvegicus*) (N=40) were obtained from the Central Animal Unit of the Faculty of Medicine and Health Sciences of Stellenbosch University. The rats were randomly selected and sorted into four groups. Three groups of control animals were prepared, consisting of untreated control (C) (n=10), rooibos control (C-R) (n=10) and ART control (C-ARV) (n=10) rats. Finally, one experimental group was prepared, receiving a combination of ART and rooibos tea (ARV+R) (n=10) (Figure 4.1).

Housing and care of the rats were conducted ethically and under the conditions set out by the Research Ethics Committee: Animal Care and Use (REC: ACU) of Stellenbosch University using the South African National Standards (SANS) document. Rats were reared as pups for four weeks, and kept under observation for signs of stress, illness, or injury for a period of two weeks on standard breeders feed (*Nutritionhub* (Pty) Ltd, Stellenbosch, South Africa) and water until reaching a weight of 180 g. The animals then underwent experimentation for nine weeks prior to euthanasia. The life span of the rats totalled 15 weeks.

During experimentation, rats were housed at room temperature (± 23 °C) following 12-hour light and dark cycles (06:00 to 18:00) with 40% humidity at the Central Research Facility, Stellenbosch University. All groups had access to standard breeders feed, consisting of 1.272 kJ/100 g and water or rooibos tea *ad libitum* from the start of the intervention.

4.3 ANTIRETROVIRAL ADMINISTRATION

Weight dependent dosage of one Odimune[®] (*Cipla Medpro* (Pty) Ltd, Bellville, Western Cape) Tablet containing 600 mg Efavirenz, 200 mg Emtricitabine, and 300 mg Tenofovir was administered to C-ARV and ARV+R groups.

Antiretroviral dosage for the rats was calculated per the guidelines set out by the United States Food and Drug Administration (Centre for Drug Evaluation and Research, 2005). Specific doses were calculated using the average weight of the rats in individual cages. A final dose of 51.6 mg/kg/day of

EFV, 17.4 mg/kg/day of FTC, and 25.8 mg/kg/day was given to the rats. This was then multiplied by the weight of the rat. Exact dose and weight calculations are supplied in Appendix C.

Single Odimmune[®] tablets were crushed and suspended in 1 mL water and thoroughly vortexed. Each prepared sample was refrigerated at 4 °C and administered via oral gavage daily to C-ARV and ARV+R groups. The C and C-R groups were gavaged using tap water to maintain consistency between animals. Gavage was conducted by a professional technician at the animal unit of Stellenbosch University.

4.4 SUPPLEMENTATION OF ROOIBOS

Dried rooibos (*A. linearis*) leaves were obtained from the Carmiën[®] tea company Pty, Ltd (Brakfontein, South Africa). A 2% aqueous solution was made using 20 g of fermented (red tea) rooibos leaves and added to 1 L boiling water. Leaves were steeped for 30 min, filtered through a layer of cheese cloth, followed by Whatman No.4 and No.1 filter papers. The preparation was stored in light limiting bottles and wrapped in aluminium foil per the methods described by Marnewick *et al.*, 2003. This limited the effects of light exposure to the polyphenols in the tea, as light exposure is known to cause decreased levels of polyphenols. The tea was provided in place of water to the C-R and ARV+R groups. Fluid intake of the animals was measured and recorded weekly.

4.5 PROCEDURES

4.5.1 Anaesthesia and euthanasia

Prior to harvesting, animals were weighed using an automated scale. Anaesthesia was administered via intra-peritoneal injection using sodium pentobarbitone (Eutha-naze[®], Bayer (Pty), Ltd, Isando, Gauteng) at a dose of 2 mg/mL/kg prior to surgery. Anaesthesia was conducted by a trained professional authorised by the South African Veterinary Council (SAVC). Full anaesthetisation was ascertained by testing pedal, withdrawal, and corneal reflexes.

4.5.2 Tissue harvesting

Tissue was received from the Medical Physiology Department of Stellenbosch University, Faculty of Medicine and Health Sciences from a study entitled: Effect of *Aspalathus linearis* supplementation, during anti-retroviral treatment, on the heart and aortas of male Wistar rats and the effects of drinking rooibos on the cardiovascular profile of patients on ART (Imperial, 2017). This study forms part of the aim to minimise the impact of experimentation on animals and to acquire as much information as possible from organs that would otherwise be discarded after death.

Tissue was harvested nine weeks from the start of the experiment. Once fully anaesthetised the heart was removed rendering the animal dead. The abdominal cavity was exposed allowing for the removal of the pancreas, liver, and left kidney. A portion of the left lateral lobe was dissected and immediately placed in 5% paraformaldehyde fixative. The pancreas was immediately placed in the fixative once removed to immediately suspend the autolytic process. The left kidney was transversely halved prior to placement in the fixative allowing for maximum infiltration of the fixative.

4.5.3 Blood sampling

Once the abdominal cavity and thoracic cavity were open and the heart removed, blood was harvested from the abdominal and thoracic cavity using disposable pasteurised plastic pipettes and placed into MiniCollect[®] 1 mL red top serum tubes (*The Scientific Group, (Pty), Ltd, Milnerton, Western Cape*). Within two hours of blood collection, the clotted blood samples were centrifuged at 1 300 revolutions per minute for 20 minutes using a Biofuge pico centrifuge (*Heraeus, Kendro Laboratory products, Germany*). Blood serum was collected from each tube using a P100 micro-pipette and stored at -80 °C in preparation for blood analysis. The prepared serum samples were sent to the National Health Laboratory Services (NHLS) at Tygerberg Hospital, where aspartate aminotransferase (AST) and alanine aminotransferase (ALT) levels were tested under NHLS standard operating procedures (Appendix D). An AST:ALT ratio was calculated to determine liver function.

4.6 HISTOLOGICAL PROCEDURES

Fixed portions of the of the pancreas, liver, and kidney were added to labelled embedding cassettes and processed under standard histological procedures, using the Shannon Elliot Duplex Processor (*OptoLaboratory, Cape Town*). Tissue was processed to ensure complete dehydration and rigidity for sectioning (Appendix E). Processed tissues were embedded in paraffin wax using the Leica EG 116 Embedder (*SMM instruments, Germany*). The tissue blocks were then placed in the freezer to cool for 20 minutes before sectioning. A Leica RM 2125 RT microtome (*SMM Instruments, Germany*) was used for sectioning of the various tissues.

4.6.1 Sectioning and staining of the pancreas

Pancreatic sections were prepared in duplicate for routine automated haematoxylin and eosin (H&E) stain using the Leica Auto Stainer XL (*SMM Instruments, Johannesburg*) (Appendix F) and standard immunohistochemistry labelling techniques. Tissues that were sectioned at 5 µm were placed on frosted slides and stained using H&E. Immunohistochemical labelling of pancreatic tissue was conducted per the standard operating procedures of the South African Medical Research Council (MRC), ICC\B7-V01 (Appendix G). Due to the specificity of the immunohistochemistry stain, the

pancreas was sectioned at 3 μm and placed on positively charged slides, which allowed for the complete infiltration of the stain into pancreatic tissue.

A standard double labelling immunohistochemical (IHC) approach was conducted using the Dako EnVision G/2 system/AP rabbit/mouse link (K5355, *Dako*, Denmark, Inc), using anti-insulin and anti-glucagon antibodies. The EnVision kit is specifically recommended for detecting antigens at very low concentrations. Sections of pancreas were deparaffinised and dehydrated to water which allowed for the even distribution of the stain. Following the blocking of endogenous peroxidases using 3% hydrogen peroxide (Merck (Pty) Ltd, Modderfontein, Gauteng), a 1:20 dilution of normal goat serum (NGS) was applied to block charged sites. Slides were then placed in a moisture chamber for 30 minutes to prevent drying out of reagent. Once the excess serum was blotted, a 1:100 dilution of the polyclonal anti-glucagon primary antibody was added binding to the antigen of interest (K5355, *Dako*, North America, Inc) and incubated at room temperature for 30 min. Sections were then jet washed and a 1:200 dilution of the biotinylated goat anti-rabbit IgG and Vectastain ABC (*Vector Laboratories*, Ak-5010) was applied, sections were incubated for one hour in a moisture chamber. Sections were then dried around the edges and the liquid DAB-Chromogen solution (K5355, *Dako*, North America, Inc) was applied for visualisation of the antigen-antibody complexes. Slides were then jet washed and rinsed and a 1:20 dilution of Normal Horse Serum (NHS) was applied. Once complete a 1:10 000 dilution of the monoclonal anti-insulin antibody (K5355, *Dako*, North America, Inc) was added and incubated overnight at 4 °C. Following incubation, a biotinylated rabbit/mouse link (K5355, *Dako*, North America, Inc) was applied. The EnVision and AP Enhancer (K5355, *Dako*, North America, Inc) were used to observe the antibody labelling. Pancreatic tissue from the control group was used as an internal positive control for the staining procedure. External and internal positive controls were used to validate the stains. This technique labels insulin secreting β -cells pink/red and glucagon secreting α -cells brown (Figure 4.2).

4.6.2 Sectioning and staining of the liver

Four slides at different specified section thicknesses were made for hepatic tissue, which allowed for various staining techniques to be applied. To ensure that different areas of the liver were studied a 15 μm trim was made between sections. Haematoxylin and eosin stains were made for each animal, on a 5 μm tissue sections, using the Leica Auto Stainer XL. The H&E stain was used to control for all the special stains applied to the tissue, as well as acting a primary reference point for any observable pathology.

The Gordan and Sweet silver impregnation technique was applied to 4 μm thick sections and placed on positively charged slides (Appendix H). Positively charged slides were used to allow maximum adherence of the silver solution to the tissue for a more robust stain. This technique stains reticulin fibres black, and was used to determine subtle architectural changes that would otherwise not be observable in the H&E stained tissue. A Periodic Acid Schiff (PAS) stain was applied to 4 μm thick sections (Appendix I). The PAS stain is routinely used to determine glycogen deposits in liver sections as glycogen accumulation may signify pathology. Finally, a Masson's Trichrome (MT) stain was applied to 5 μm thick sections. Masson's Trichrome is routinely used by histopathologists to determine fibrotic changes associated with liver pathology (e.g. fibrosis). This stain is used to differentiate smooth muscle fibres and stains collagen type I blue (Appendix J). These stains were applied to observe the potential progression of liver pathology by staining various histological structures. Human skin was used as an external positive control for the MT and silver impregnation, as skin contain high amounts of collagen. Rat colon was used as an external positive control for PAS. The C-group was used as an internal control for all stains.

4.6.3 Sectioning and staining of the kidney

Two slides, 5 and 3 μm thick, were made for the kidney. To ensure that different parts of the kidney were studied, 15 μm trims were made between sections of tissue. Tissue was stained using H&E and PAS. In the kidney, PAS was used to stain the basement membrane magenta, and nuclei blue. This stain specifically allowed for better differentiation of the proximal and distal convoluted tubules. Periodic Acid Schiff is routinely used by histopathologists to identify impairments in the basement membrane. Rat colon was used as an external positive control for PAS, sections acquired from the C-group was used as internal positive controls.

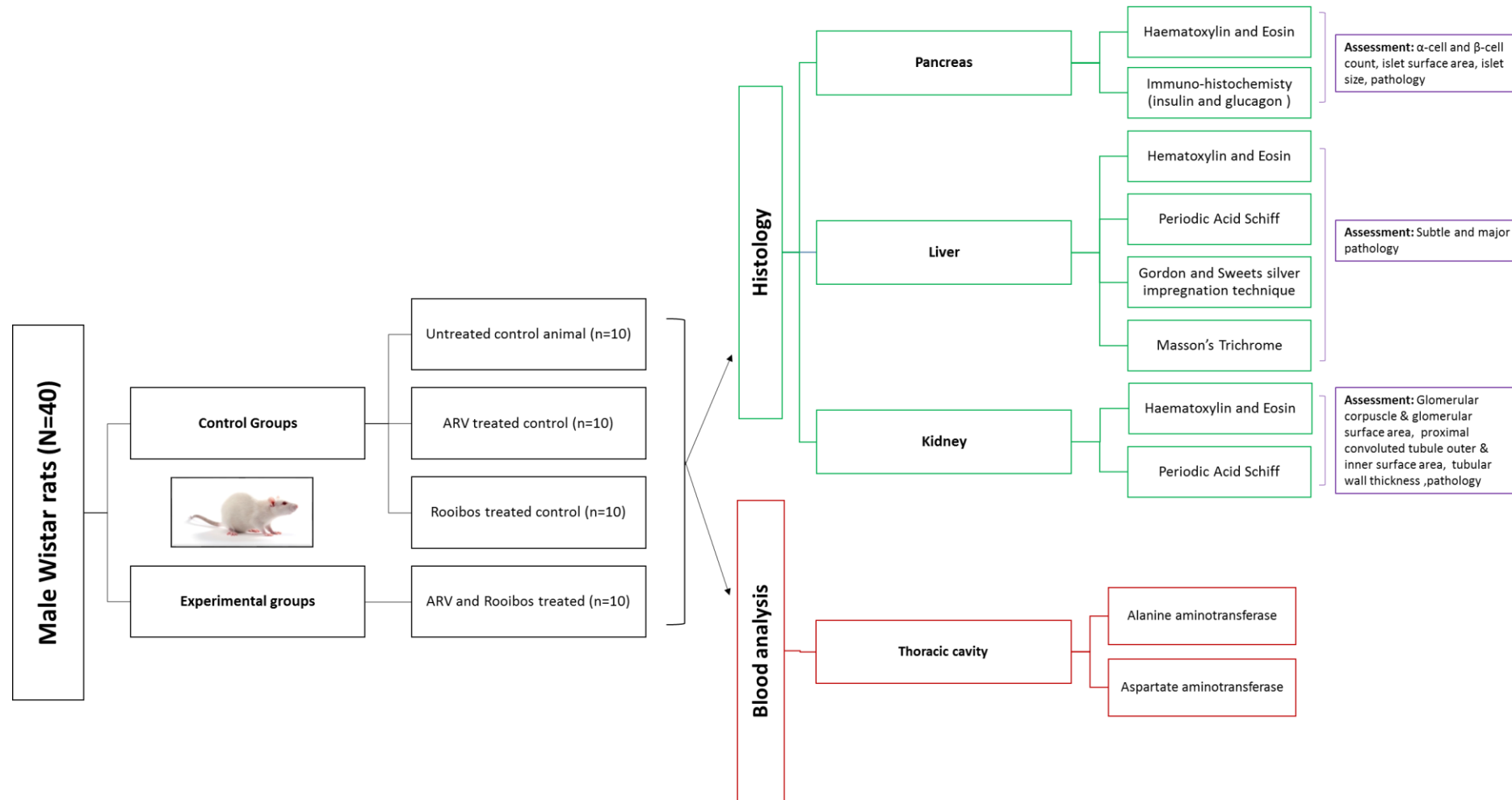


Figure 4.1: Summary of methodology. Male Wistar rats were divided into four groups where the pancreas, liver, and kidney were removed. Each tissue was subjected to haematoxylin and eosin staining as well as other various immunohistochemical and special stains. Each organ was morphometrically analysed and graded and scored for pathology. Additionally, liver function tests, aspartate and alanine aminotransferase, were performed.

4.7 STEREOLOGY AND MORPHOMETRY

Each tissue section was examined under the light microscope, using a Nikon Eclipse Ti Automated scanning microscope (*Nikon Instruments Inc*, Walt Whitman Road Melville, New York) with inbuilt camera (Nikon Digital Sight DS-Fic, *Nikon corporation*, Japan). The analytical techniques differed with each organ which are further elaborated in Sections 4.7.1-4.7.3.

4.7.1 Pancreas

Immunohistochemically labelled sections of the pancreas were captured using a 10 x objective lens in conjunction with the Nikon NIS Imaging Software version 4.40 (*Nikon Instruments Inc*, Copyright 1991-2015). The whole section was scanned with a 15% overlap area. Once scanning was complete the images were stitched forming a complete image of the total section.

To quantify the amount of glucagon-and insulin-positive cells, sections of the pancreas were subject to a red/green/blue colour segmentation. This caused images to be converted to a binary image. The total section areas and the total islet areas (μm^2) were determined. The total islet number was quantified using the Leica Qwin professional software (*Leica Microsystems*, United Kingdom), which was calibrated to 0.7 μm /pixel. The software was additionally used to determine the specific areas (μm^2) of glucagon positive α -cells (brown) and insulin positive β -cells (red) within each islet (Figure 4.2). The area of β -cells and α -cells was expressed as a percentage of the total islet area. Due to the percentage overlap that occurred during image capturing, islets that fell in the borders of the micrographs were excluded thereby preventing double analysis of the islets.

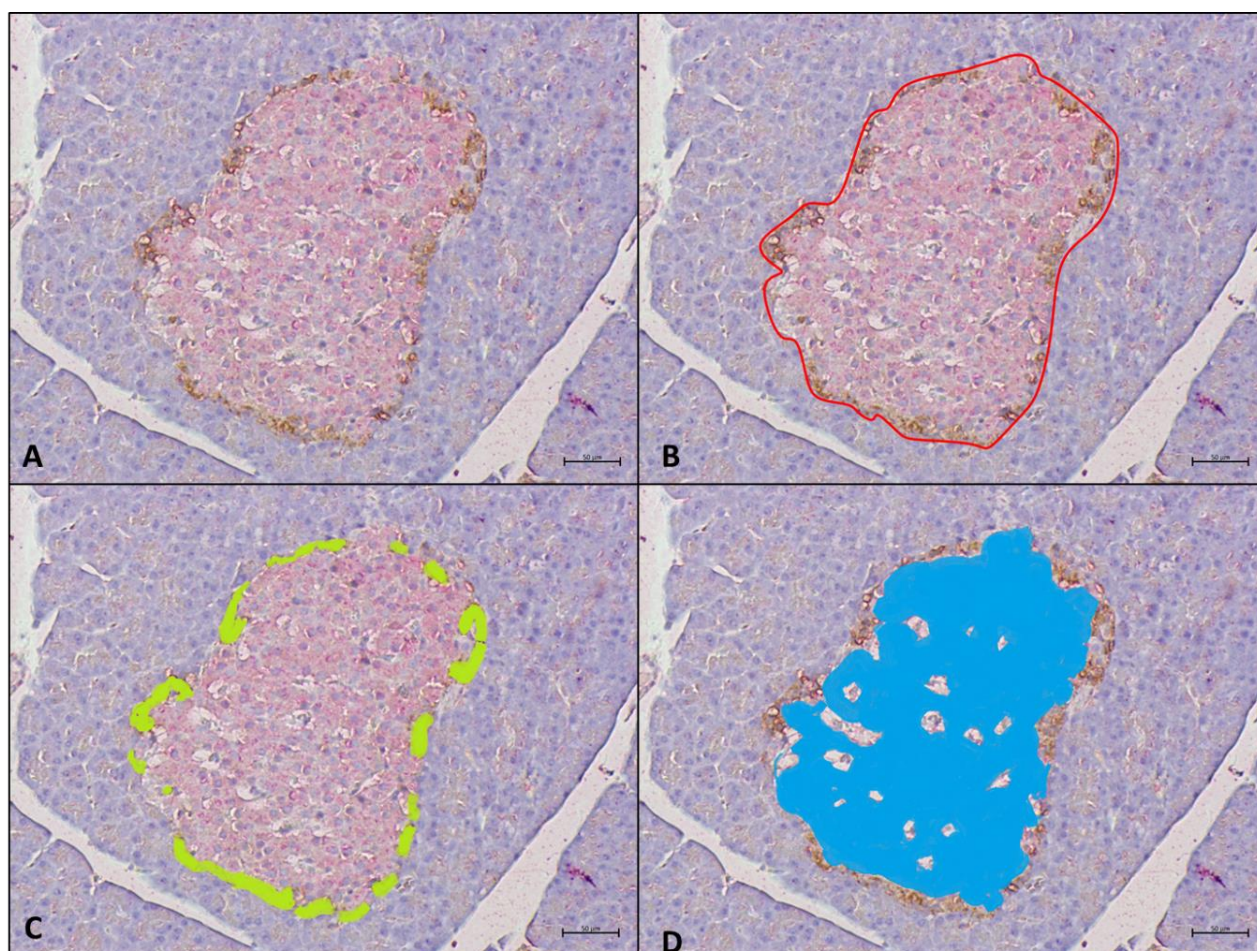


Figure 4.2: Morphometric analysis of the islets of pancreatic islets using immunohistochemical labelling.

A) Demonstrates a pancreatic islet in a control animal, with α -cells (labelled brown with anti-glucagon antibodies) and β -cells (labelled pink/ red with anti-insulin antibodies); B) The surface area of the islet were measured in μm^2 (red) by drawing around the perimeter of the islet; C) Using colour segmentation the area of α -cells (green) were highlighted then quantified; D) The area of β -cells (blue) are quantified. Bar=50 μm , 100 x objectives.

4.7.2 Liver

Liver sections were photographed at 100 x magnification with the Nikon NIS Imaging software version 4.40 (*Nikon Instruments Inc*, Copyright 1991-2015) for subtle pathology. The tissue section was graded and scored as described in Table 4.1. An average score was obtained from all the stains used and compared between the various groups. The H&E stains were used as a confirmatory slide for overall pathology. First, the whole tissue section of each stain was evaluated, then by lobule, followed by the portal areas, central vein and hepatocyte. Evaluators of pathology were blinded as to which group was under study. The histological features were grouped into three main categories namely architectural, glycogen, and fibrotic changes. Trends in areas affected were noted. Disruptions were evaluated and the severity of the disruption was scored.

Table 4.1: Definitions and scoring of liver pathology.

Stain	Definition	Score
Gordon and Sweet's Reticulin stain	Measuring architectural changes in reticulin fibres	
	• Normal	0
	• Slight disruption to architecture	1
	• Moderate disruption to architecture	2
	• Severe disruption to architecture	3
Periodic Acid Schiff Stain	Measuring glycogen deposits based on staining intensity	
	• Normal	0
	• Slight glycogen deposits	1
	• Moderate glycogen deposits	2
	• Severe glycogen deposits	3
Masson's Trichrome	Measuring fibrotic changes	
	• Normal	0
	• Slight fibrotic lesions	1
	• Moderate fibrotic lesions	2
	• Severe fibrotic lesion	3

4.7.3 Kidney

Sections of the kidney were photographed at 200 x magnification with Nikon NIS Imaging Software version 4.40 (*Nikon Instruments Inc*, Copyright 1991-2015). Kidney sections stained using PAS were scanned with a 15% overlap in the images. Images were stitched forming a composite image of the whole section.

Once all individual photographs were obtained, a total of 30 glomerular corpuscles were randomly selected and were measured using Zen10 software (*Carl Zeiss Microscopy*, Oberkochen), (see randomisation protocol in Appendix K). The surface area of each chosen corpuscle was measured following methods adapted from Sedek *et al* (2013). The surface area (μm^2) of the glomerular corpuscle and the glomeruli were measured by tracing around the perimeter of the glomerular corpuscle and glomeruli. From these measurements, the diameter (μm) and perimeter (μm) of the corpuscle and glomeruli was generated using the Zen software. The surface area (μm^2) of the renal space was quantified according to Equation 4.1. Finally, the outer surface area (OSA) and luminal surface areas (LSA) of three of the nearest proximal convoluted tubules (PCTs) to the glomerular corpuscle were measured (Figure 4.3). Both the diameter (μm) and perimeter (μm) of these areas were generated on the Zen software. To quantify tubular wall thickness in the PCTs, the difference of the OSA and LSA was found (Equation 4.2).

$$RS = GCSA - GSA$$

RS: Renal space

BCSA: Glomerular corpuscle Surface Area (μm^2)

GSA: Glomerular Surface Area (μm^2)

Equation 4.1: Equation demonstrating the surface area in (μm^2) of the Bowman's space.

$$\text{Tubule wall area} = \text{OSA} - \text{LSA}$$

OSA: Outer Surface area (μm^2)

LSA: Luminal Surface Area (μm^2)

Equation 4.2: Quantifying tubular wall area (μm^2).

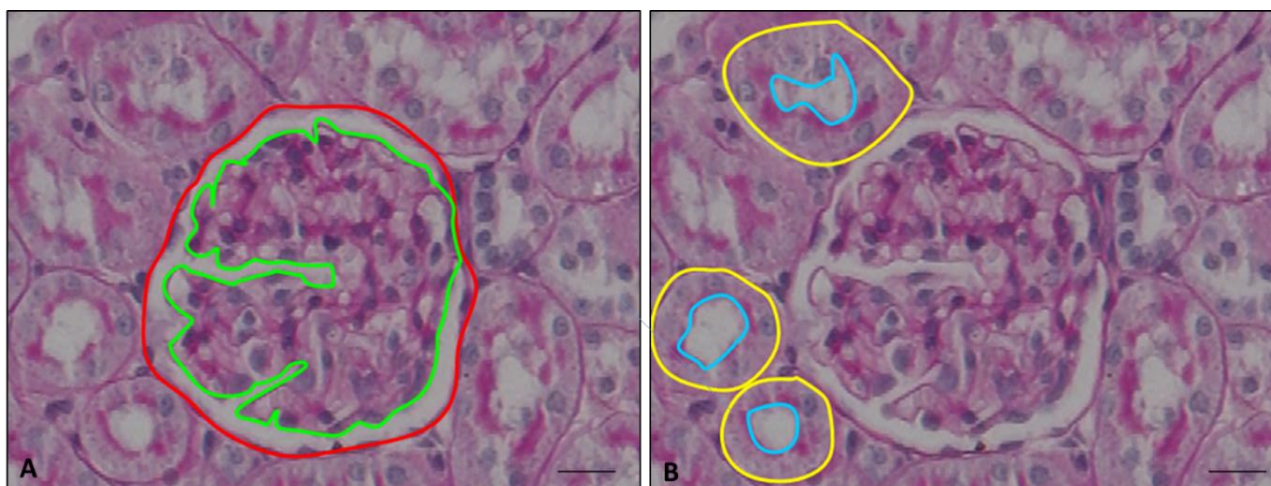


Figure 4.3: Morphometric measurement of the glomerular corpuscle and proximal convoluted tubules. The highlighted regions demonstrate the site of the surface area measurements of; A) glomerular corpuscles (μm^2) (red) and glomerular surface areas in μm^2 (green); B) The proximal convoluted tubules outer surface area in μm^2 (yellow) and inner surface area in μm^2 (blue) (100x magnification) Bar=100 μm .

4.8 PATHOLOGICAL SCORING OF THE PANCREAS, LIVER, AND KIDNEY

Each slide was thoroughly assessed for pathology and variations in cellular components. Each organ system was analysed using semi-quantitative methods of grading and scoring specifically looking at early manifestations of cellular damage. Study participants were blinded to the groups analysed. Three individuals, including two histologists scored the tissue. A veterinary histopathologist Dr E.C. Du Plessis (IDEXX laboratories, Onderstepoort campus, Faculty of Veterinary Science, University of Pretoria) was consulted for the confirmation of findings.

Whole tissue sections were analysed for early manifestations of cellular damage and scored (Table 4.2). These early manifestations of cellular damage were defined as follows: Cellular swelling or granular cytoplasm is defined by a “cloudy” or “ground glass” appearance in the cytoplasm of the cell. Hydropic degenerations are referred to as “vacuolar degeneration”, is the appearance of vacuoles within the cell; as membrane permeability decreases, water accumulations increase, producing clear vacuoles within the cell. Fatty changes are characterised by the accumulation of fat deposits within parenchymal cell providing a “foamy” appearance. The nucleus in this instance is not displaced within the cells. Severe cases of lipid accumulations cause large fat vacuoles to appear distending the cell and compressing the nucleus against the cell membrane. Advanced stages of fatty change will cause cells to rupture into large fatty cyst. Inflammatory foci was described as the presence of lymphocytes that were dispersed randomly throughout the tissue or localised in specific areas.

Table 4.2: The semi-quantitative methods of grading and scoring including identifying pathological features.

Organ	Score	Scoring system
Pancreas	P0	normal, 0% of tissue is affected
	P1	slight, <5% of tissue is affected
	P2	mild 5%-20% of tissue is affected
	P3	moderate, 20%-60% of tissue is affected
	P4	severe, >60% of tissue is affected
Liver	L0	normal, 0% of tissue is affected
	L1	slight, <5% of tissue is affected
	L2	mild 5%-20% of tissue is affected
	L3	moderate, 20%-60% of tissue is affected
	L4	severe, >60% of tissue is affected
Kidney	K0	normal, 0% of tissue is affected
	K1	slight, <5% of tissue is affected
	K2	mild 5%-20% of tissue is affected
	K3	moderate, 20%-60% of tissue is affected
	K4	severe, >60% of tissue is affected

4.9 POLYPHENOL CHARACTERISATION

A short experiment was conducted to determine the effects of temperature and time on the polyphenol content of the 2% rooibos tea solution. This was conducted to determine whether the concentration of polyphenols given to rats was consistent throughout the week. Each series followed a time pattern in which it was prepared and exposed to the same room conditions as the rat cohorts. Thus, the tea samples would mimic the amount of time rats were exposed to the same tea solution in a specific environment.

Three litres of the tea were made up following the methods described in Section 4.4, and divided into three series of 500 mL each. Series 1 (S1-Fresh) consisted of freshly made tea, series 2 (S2-Fridge) was refrigerated at 4 °C for one week and series 3 (S3-Frozen) consisted of tea that was stored in a freezer (-20 °C) for two weeks. All tea groups were stored in light limiting bottles.

Each series was then further divided into two sub-groups day 1 (D1) and day 7 (D7) of 300 mL each respectively (Figure 4.4). The D1 sub-groups were immediately freeze dried after the specified storage times for each series (Appendix L). The D7 groups were placed at room temperature following 12-hour light and dark cycles at 40% humidity in light limiting bottles wrapped in aluminium foil for a period of one week. The bottles mimicked the same procedures as given to the animal cohorts. Each tea series (150 mL) was subsequently frozen with liquid nitrogen in virtis

cryogenic flasks and lyophilized using a Labcoco™ (*Vacutec*, Roseveld park, South Africa) freeze dryer for 24 to 48 hours, or until completely freeze dried. Freeze dried samples were stored at room temperature in airtight plastic containers, covered in aluminium foil and placed in a dark dry cupboard until all samples were completed. Samples were sent for polyphenol characterization using liquid chromatography-mass spectrometry (LC-MS) techniques.

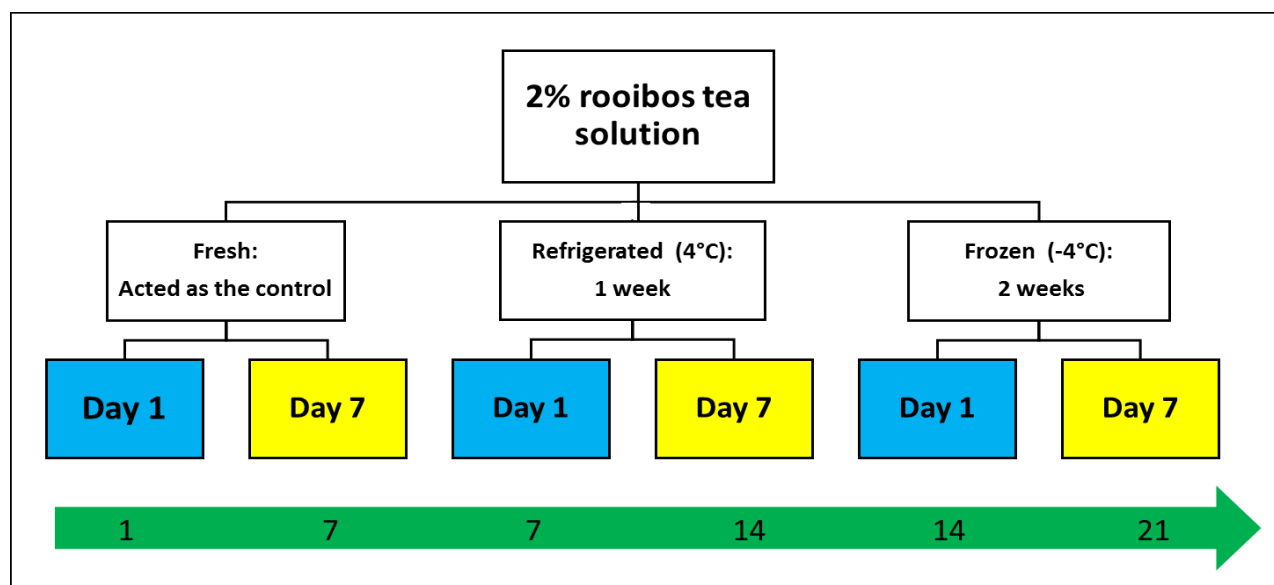


Figure 4.4: Rooibos tea allocation. Day 1 samples followed the specified storage times and were immediately freeze-dried, groups marked day 7 (yellow) were kept at room temperature following 12-hour light and dark cycles, at 40% humidity, to mimic the condition the rats were exposed to during experimentation. The green arrow demonstrates the time sequence in days from the making of the tea until freeze drying.

Polyphenolic characterisation was conducted at the Central Analytical Facility (CAF) at Stellenbosch University per their standardised methods. Liquid chromatography-mass spectrometry analysis was conducted using a Waters Synapt G2 quadrupole time-of-flight mass spectrometer. The spectrometer was fitted with a Waters ultra-pressure liquid chromatograph and photo diode array detection. Polyphenol separation was attained using a Waters HSS T3, 2.1x150 mm column with 1.7 μm particles. A 0.1% formic acid (solvent A) and acetonitrile containing 0.1% formic acid (solvent B) gradient was applied. A linear gradient was exercised starting at 100% using solvent A for one minute and was then changed to solvent B for 22 minutes. Once complete, the gradient was changed, where 40% of solvent B was used for 50 seconds. A wash step was conducted for one and a half minutes at 100% of solvent B. Following this, re-equilibration to initial conditions was applied for 4 minutes. A flow rate was established at 0.3 mL/min, the column was kept at 55 $^{\circ}\text{C}$. An injection volume of 1 μL was used.

Data was captured in MS^E mode which consisted of a low collision energy scan of 6 V from m/z 150 to 1500 and a high collision energy scan from m/z 40 to 1500. The high collision energy scan was done using a collision energy ramp of 30-60 V. The photo diode array detector was set to scan from 220-500 nm.

The mass spectrometer sensitivity was optimized at a cone voltage of 15 V. Nitrogen was used as the desolvation gas at a rate of 650 l/hr at a temperature of 275 °C. The instrument ran with an electrospray ionization probe in the negative mode. The negative mode is used to identify negatively charged compounds like polyphenols. Calibration was established using sodium formate. Leucine encephaline was infused in the background as a lock mass for accurate mass determination.

4.10 STATISTICAL ANALYSIS

For statistical analysis, a biostatistician, Professor Martin Kidd at the Centre for Statistical Consultation, Department of Statistics and Actuarial Sciences, Stellenbosch University, was consulted for quantitative and descriptive statistics. Statistical analysis was conducted with the Statistica[®] version 13.2 (Dell, 2014, USA) software. The raw data is plotted against a theoretical normal (linear graph) which differentiated outliers that may have influenced statistical significance.

Descriptive statistics were performed for all data collected; mean values, standard deviations and standard errors were obtained. From this data, graphs were constructed to visually represent the data at a confidence interval of 95%.

An analysis of variance (ANOVA) was conducted. This is a statistical technique used to determine the variance of normally distributed independent samples. This technique is used to test variations in sample groups by assuming each sample group is equal to the other (null hypothesis). A significant difference is found when the null hypothesis is rejected at $p\text{-value} \leq 0.05$. Lavene's test was used to determine the homogeneity of variance between samples by assuming the variance is equal across groups.

Fischer's Least Significant Difference (LSD) post hoc test was additionally conducted. The LSD is a test to identify which means are significant. Additionally, this test provides an indication of trends between two variables. A trend was defined at a $LSD < 0.05$.

CHAPTER FIVE: RESULTS

The following section will provide graphical, statistical and descriptive evidence on the effects of ART and rooibos on the pancreas, liver, and kidney. A section reporting on pathology and additional findings is given. Using ANOVA, statistical significance was determined at a p-value less than 0.05. Trends were reported at an LSD value less than 0.05.

5.1 DESCRIPTIVE AND STATISTICAL ANALYSIS ON BODY MASS

No changes in body mass were observed between the treatment groups; however, a trend was observed where the C-R had a higher body mass (Table 5.1) compared to the other treatment groups (LSD= 0.032).

Table 5.1: Number of samples (n-value), and mean body mass (g) between the different groups (\pm Std. Dev).

Group	n-value	Mean body mass (g)
C	10	277.10 \pm 37.09
C-ART	10	284.70 \pm 26.07
C-R	10	307.10 \pm 32.02*
ART+R	10	284.00 \pm 32.02

* Indicates a trend observed with an LSD < 0.05. Control (C); Control antiretroviral therapy (C-ART); Control rooibos (C-R), Experimental (ART+R).

5.2 THE EFFECTS OF TREATMENT ON PANCREATIC ISLETS

The number of pancreatic islets, as well as morphometric measurements on islet area including α and β -cell areas were determined, to investigate the effects of treatment on islet architecture. Using absolute values, pancreatic islet size (measured in μm^2) did not vary significantly between groups (Figure 5.1 A). No differences were found between the number of islets per section area (total size of tissue measured) (Figure 5.1 B). When α -cell area was expressed as a percentage of the mean islet area (Figure 5.2 A), the LSD post hoc test demonstrated a trend where the ART+R group had a smaller percentage of α -cells compared to the C-R group (LSD =0.028). However, these groups did not vary from the control. When β -cell area was expressed as a percentage of the mean islet area (Figure 5.2 B), a significant difference was found where the ART+R group had a larger percentage of β -cells compared to the C-ART and C-R group. Yet, neither group varied from the control. Absolute values and descriptive statistics for all measurements can be found in Appendix M.

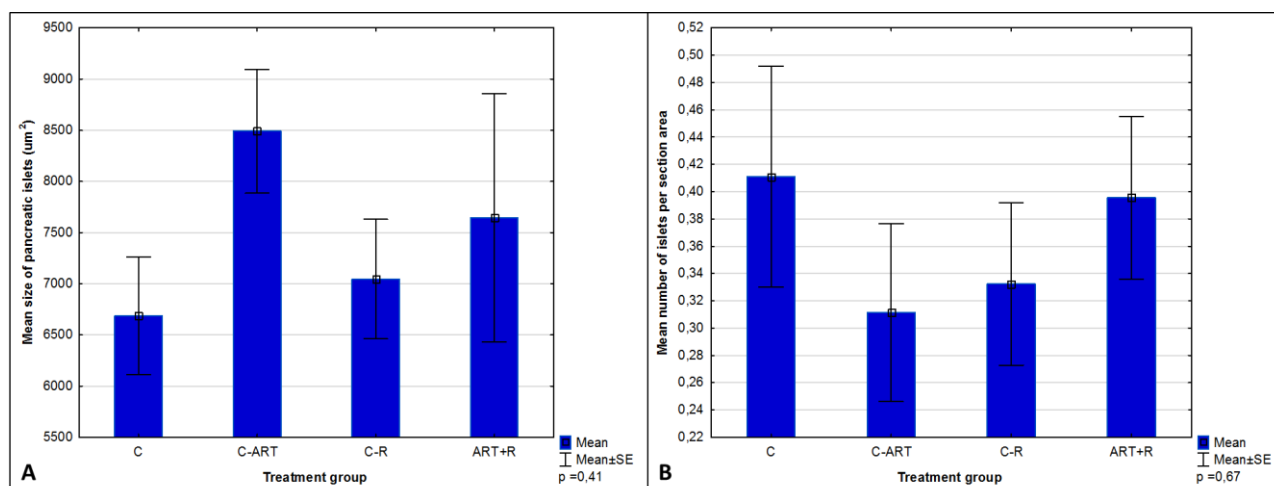


Figure 5.1: Effects of treatment on pancreatic islet size and number. A) Mean pancreatic islet size across groups (um²) did not vary significantly ($p=0.41$); B) Mean number of islets per section area did not vary significantly ($p=0.67$). Vertical bars denote standard errors of the mean. Control (C); Control antiretroviral therapy (C-ART); Control rooibos (C-R), Experimental (ART+R).

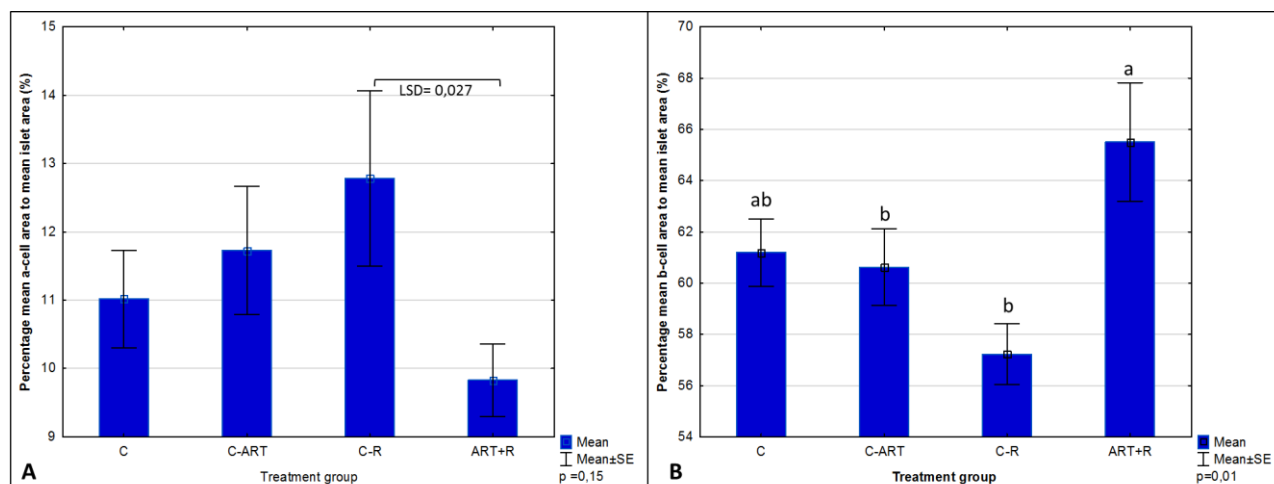


Figure 5.2: Effects of treatment on the percentage of α - and β -cells areas. A) Percentage of α -cells to mean islet area did not vary significantly between groups ($p=0.15$), a trend (LSD=0.027) was found where the C-R had a higher α -cell area to total islet area compared to the ART+R group; B) Percentage of β -cells varied significantly between groups ($p=0.01$) where the ART+R had a significantly greater percentage of β -cells compared to the C-ART and C-R groups. No group varied significantly from the C group. Vertical bars denote standard errors of the mean. Control (C); Control antiretroviral therapy (C-ART); Control rooibos (C-R), Experimental (ART+R).

5.3 THE EFFECTS OF TREATMENT ON THE LIVER

The aspartate aminotransferase (AST) and alanine aminotransferase (ALT) serum biomarkers did not differ significantly between groups (ALT; $p=0.98$; AST; $p=0.89$; AST:ALT; $p=0.92$), indicating that neither ART nor rooibos caused major changes to liver function compared to the control (Figure 5.3). All absolute values and LSD post hoc values are presented in Appendix M.

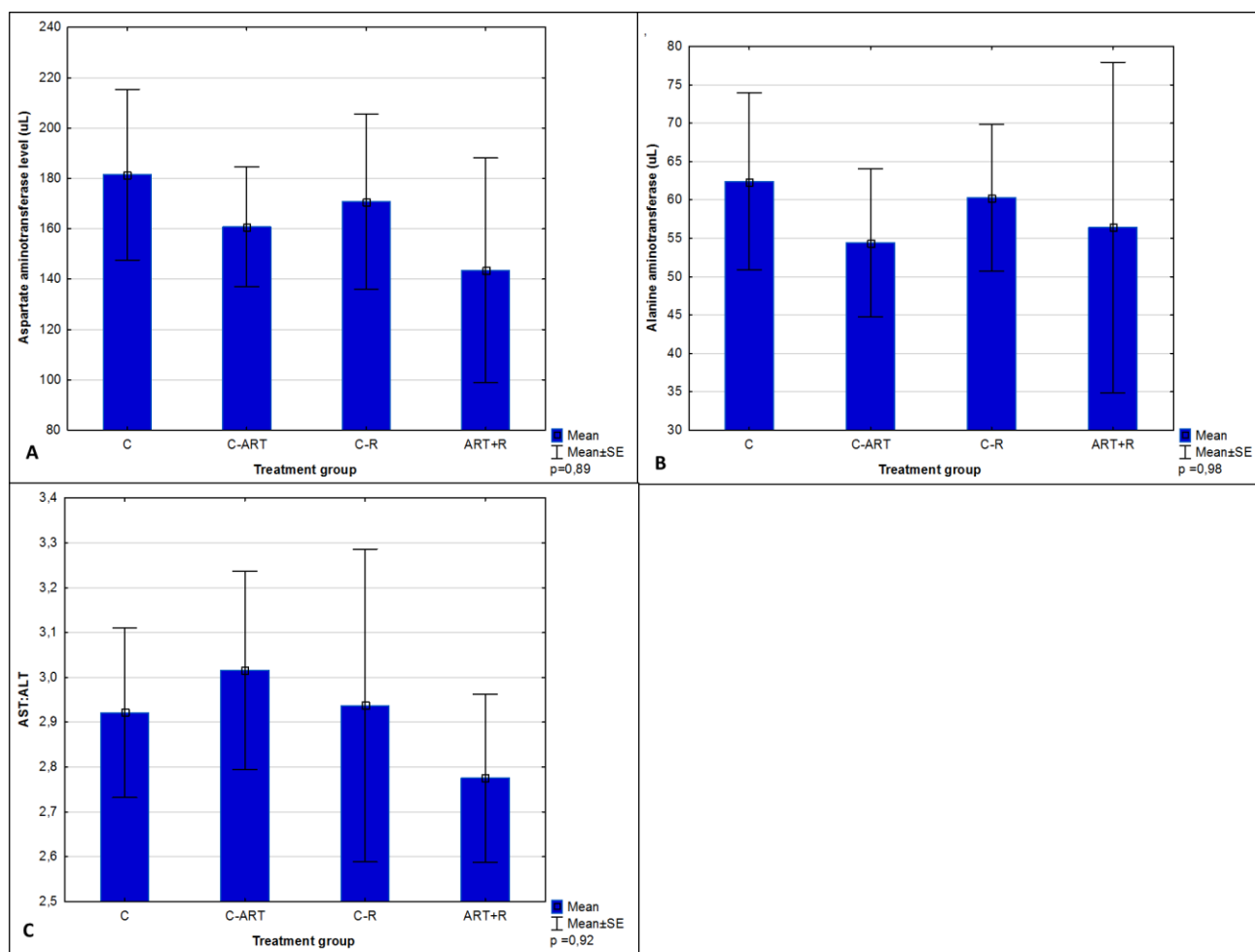


Figure 5.3: Effects of treatment on liver function biomarkers. A) Aspartate aminotransferase values were not significantly different between groups ($p=0.89$). B) Alanine aminotransferase levels were not significant between groups ($p=0.98$). C) The AST: ALT ratio which indicates liver function, were not significant between groups ($p=0.92$). Vertical bars denote standard errors of the mean. Control (C); Control antiretroviral therapy (C-ART); Control rooibos (C-R), Experimental (ART+R).

5.4 THE EFFECTS OF TREATMENT ON THE KIDNEY

Surface area measurements of the corpuscle were made by measuring around the perimeter of the Bowman's capsule. A trend was present between the C-R group and ART+R group, where the glomerular corpuscle tended to be larger in the C-R group ($LSD=0.017$). This was consistent with the diameter measurements ($LSD=0.029$) (Figure 5.4 A, B). Despite this, the size of the corpuscle was not significantly different to the control. The surface area and diameter of the glomerulus did not vary significantly between groups (Figure 5.4 C, D) Absolute values and LSD post hoc values are presented in Appendix M.

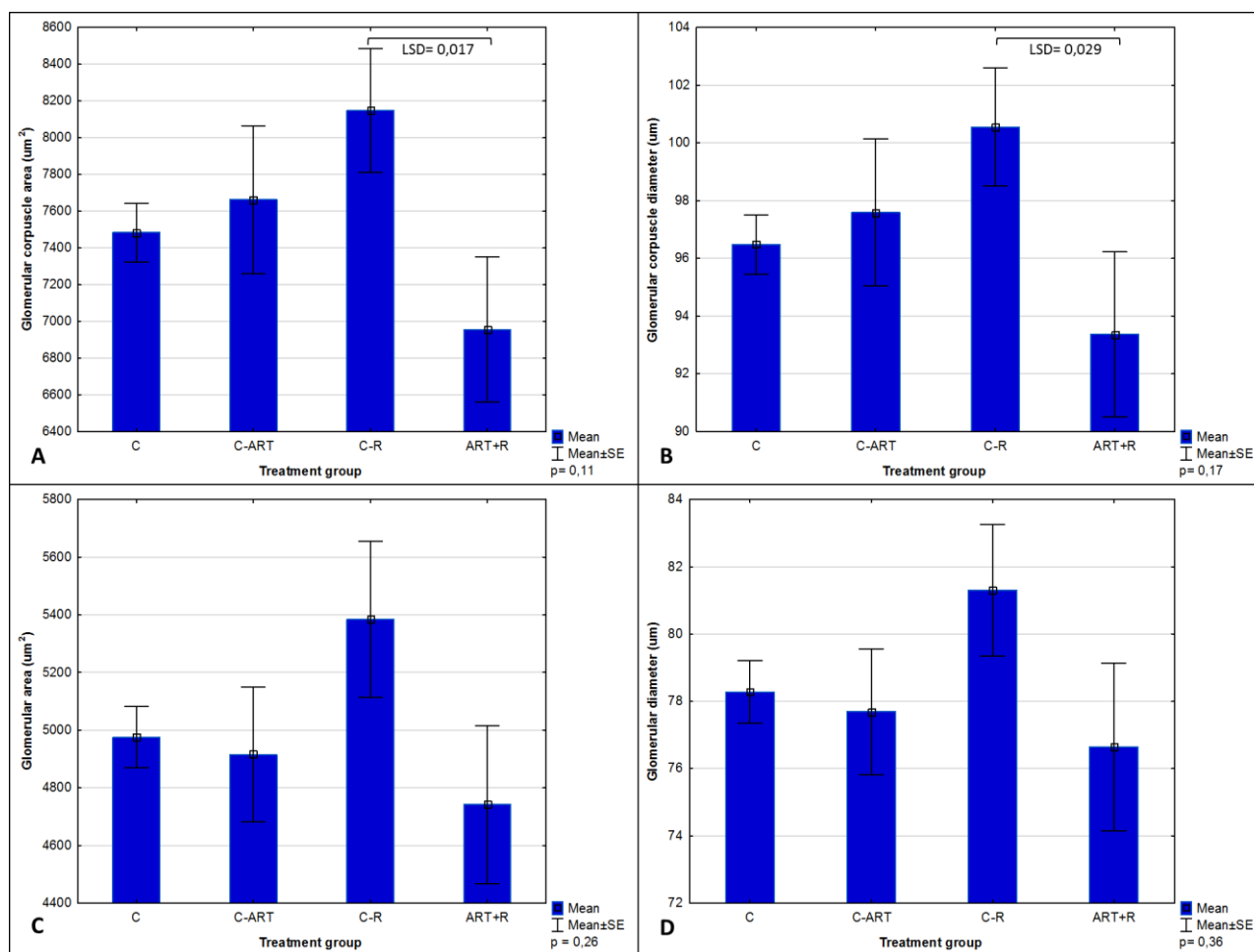


Figure 5.4: Effects of treatment on the size of the glomerular corpuscle and glomeruli. A) The surface area ($p=0.11$); B) and diameter ($p=0.17$) did not vary significantly between groups, however, trends were observed between the C-R and ART+R groups ($LSD=0.017$ and $LSD=0.029$) respectively. There was no statistical significance present in; C) the glomerular surface area ($p=0.26$) and; D) glomerular diameter ($p=0.36$). Vertical bars denote standard errors of the mean. Control (C); Control antiretroviral therapy (C-ART); Control rooibos (C-R), Experimental (ART+R).

The size of the renal space was determined by finding the difference between the corpuscle and glomerular surface area. Trends were observed between the ART+R and both C-ART ($LSD=0.034$) and C-R ($LSD=0.029$) groups. The ART+R group tended to have a smaller renal space, area compared to the C-R group. However, these were not significantly different from the control (Table 5.2). A similar trend was observed between the C-ART and ART+R groups where the renal space width was smaller in the ART+R group ($LSD=0.036$). Although, these changes were not statistically significant different from the control. Absolute values and LSD post hoc values are detailed in Appendix M.

Table 5.2: The space and width of the renal space (\pm Std. Dev).

Treatment group	Size of the renal space (μm^2)	Renal space width (μm)
C	2507.42 \pm 284.83	18.20 \pm 1.89
C-ART	2747.18 \pm 637.98*	19.90 \pm 3.49*
C-R	2763.14 \pm 680.75*	19.25 \pm 3.49
ART+R	2212.90 \pm 473.95*	19.25 \pm 4.51*

* Indicates trend in the groups. Control (C); Control antiretroviral therapy (C-ART); Control rooibos (C-R), Experimental (ART+R).

The size of the proximal convoluted tubules (PCT) were determined by measuring the outer surface area (OSA) and luminal surface area (LSA). The size of the tubule wall was determined by finding the difference between the OSA and LSA. Table 5.3 details the area and diameter of the OSA and LSA, as well as tubule wall area and wall thickness for all groups. Statistical significance was observed in the luminal surface area and diameters between the C-R and ART+R groups. This significance shows that the C-R groups had the largest luminal surface area and diameter, while the ART+R had the smallest. Neither the C-R nor the ART+R groups were significantly different from the control. In general, the PCT of the C-R group were larger compared to the other groups. However, the tubular wall thickness was consistent throughout the groups, thus the size of the tubule remained constant compared to the control.

Table 5.3: The average surface area and diameter of the proximal convoluted tubules of antiretroviral therapy and rooibos treated rats (\pm Std. Dev).

	C	C-ART	C-R	ART+R
Outer surface				
Area (μm^2)	2359.41 \pm 256.41	2403.60 \pm 494.60	2528.53 \pm 293.21	2276.37 \pm 397.49
Diameter (μm)	53.57 \pm 4.33	54.03 \pm 2.79	55.37 \pm 5.34	53.11 \pm 3.09
Luminal surface				
Area (μm^2)	586.73 \pm 192.28 ^{ab}	592.53 \pm 125.01 ^{ab}	734.65 \pm 245.04 ^a	496.75 \pm 173.62 ^b
Diameter (μm)	25.73 \pm 2.73 ^{ab}	25.79 \pm 5.07 ^{ab}	28.92 \pm 3.61 ^a	23.90 \pm 3.61 ^b
Tubule wall				
Area (μm^2)	1772.67 \pm 236.20	1811.07 \pm 264.72	1793.89 \pm 199.31	1779.62 \pm 292.08
Diameter (μm)	27.85 \pm 3.28	28.24 \pm 1.41	28.24 \pm 2.67	29.20 \pm 3.14

Differing letters indicate significant differences. Groups sharing letters do not indicate statistical significance. Control (C); Control antiretroviral therapy (C-ART); Control rooibos (C-R), Experimental (ART+R).

5.5 PATHOLOGY

5.5.1 Scoring of the pancreas

No pathological lesions nor subtle morphological changes, such as granular cytoplasm, vacuolations, fatty changes or inflammatory foci were observed. The arrangement of α - and β -cells, as seen through immunohistochemistry, correspond to what has been classically described. The β -cells labelled

pink/red were centralised forming the bulk of the islet and were surrounded by the α -cells, labelled brown with anti-glucagon antibody at the periphery (Figure 5.5). This pattern was followed in each treatment group and did not vary from the control. Thus, pancreatic islet morphology was maintained with no instances of subtle changes between groups. A summary of all observations is presented in Appendix M.

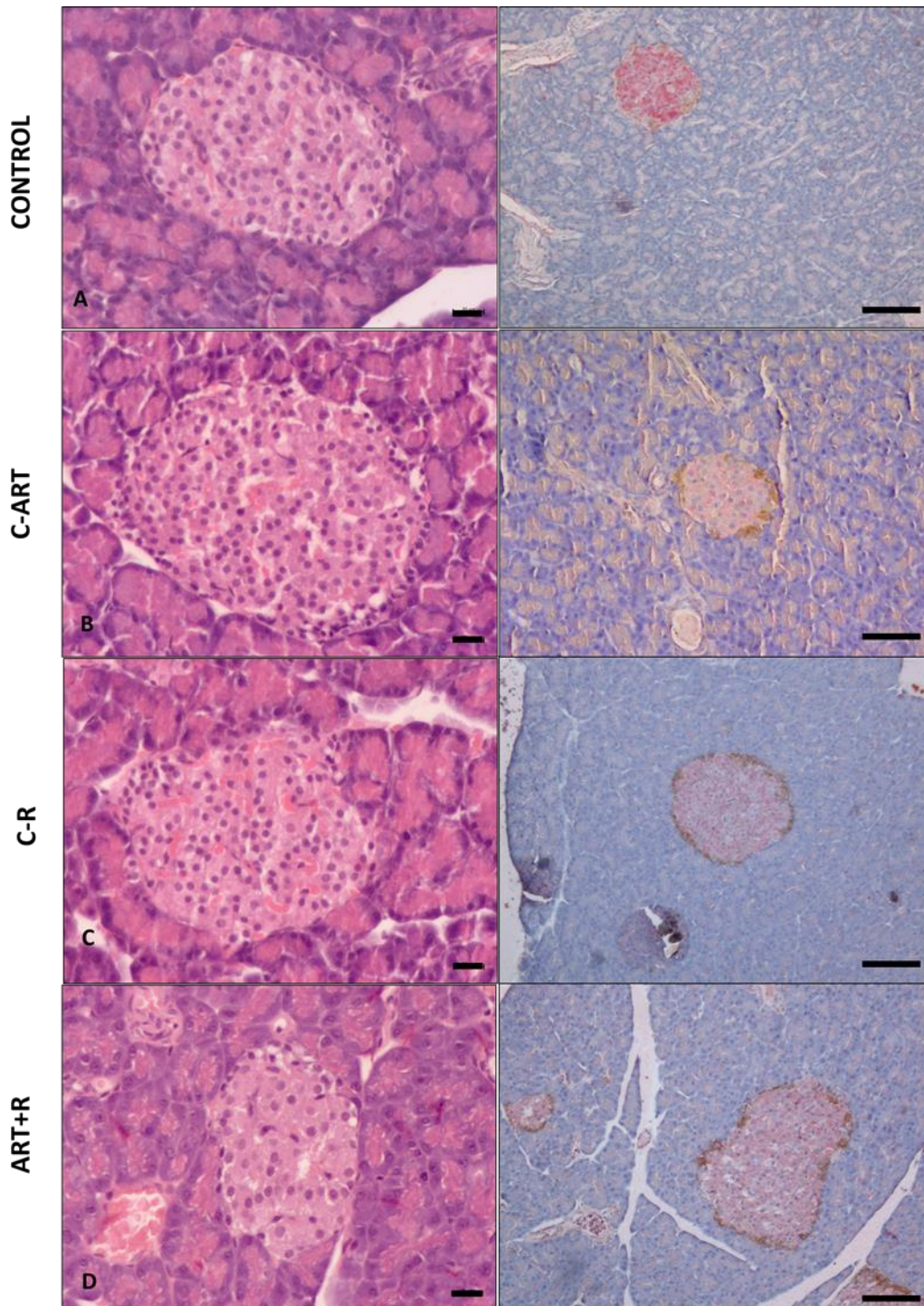


Figure 5.5: Pancreatic islet micrographs showing islet histomorphology in the various groups. H&E stained and immunohistochemistry labelled pancreatic islets of A) control (200 x magnification); B) C-ART C) C-R and D) ART+R animal. No major changes were observed in the labelled islets. (100 x magnification), bar= 20 μ m.

Instances of lymph nodes with active centres were observed (Figure 5.6). The lymph nodes were mildly active and were found in the paracortical regions of the pancreatic acinus, one in the control group, two in the C-ART and C-R group, and three in the ART+R group. The inclusions of the lymph nodes were incidental, the activity of the nodes was mild and not considered a lesion. Thus, the pancreas was scored normal for each group.

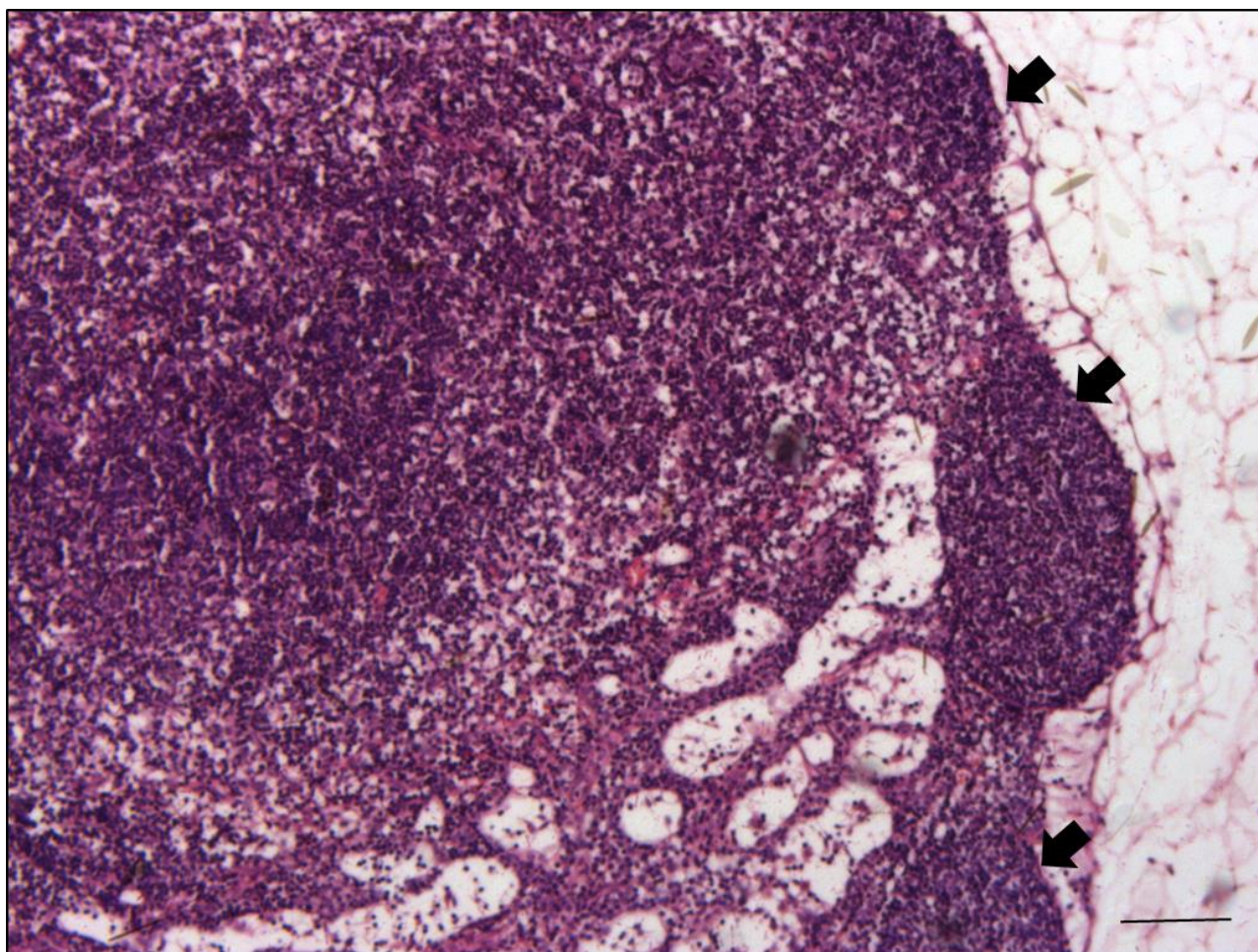


Figure 5.6: Haematoxylin and eosin stained pancreatic lymph node. Black arrows show the mildly active centres at the paracortical region of the lymph node (50 x magnification) Bar=100 μ m.

5.5.2 Scoring of the liver

Detailed pathological examination of H&E stained slides demonstrated that the liver was consistent in all groups to what is classically described. Subtle histological changes were observed in all groups, including granular cytoplasmic changes (Figure 5.7), vacuolations (Figure 5.8), and inflammatory foci (Figure 5.9). Of the total sample, 44% had granular cytoplasmic changes, consisting of 8% from the C group, 13% from C-ART, 15% from C-R, and 10% from ART+R. The most predominant histological change observed was vacuolation with 64% of the sample affected, where the C-ART group constituted 20% of the total. Inflammatory foci were rarely observed affecting only 13% of the

total sample of which the C-ART group contributed 8%. It should be noted that these were scored a level 1 indicating the subtleness of the change.

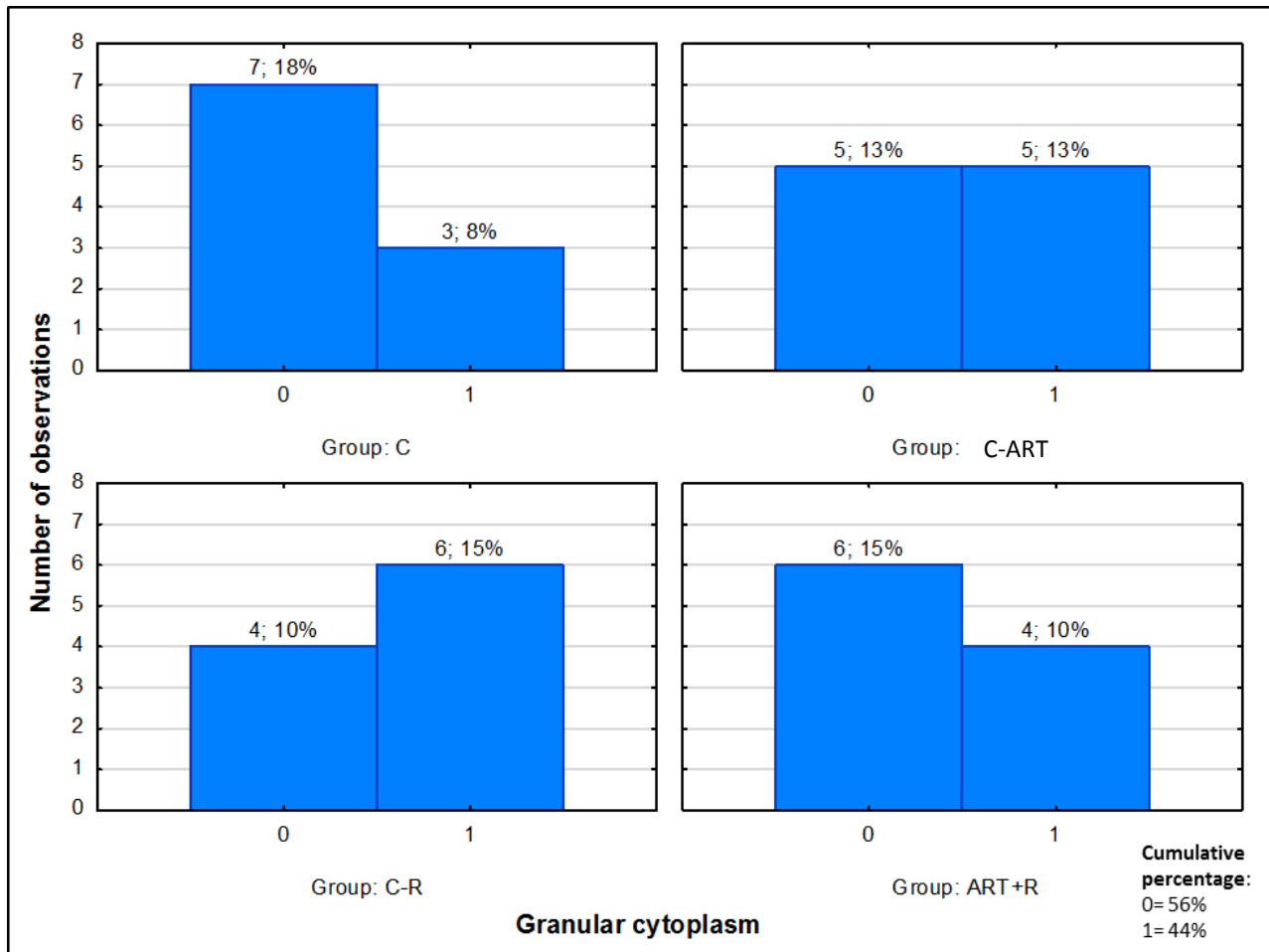


Figure 5.7: Occurrence of granular cytoplasm in the treatment groups. The percentages indicate the presence of granular changes across groups. Each percentage was calculated from the total sample size. The cumulative percentage is indicated. The total 44% affected was distributed as follows; 8% C, 13% C-ART, 15% C-R, and 10% ART+R. Control (C); Control antiretroviral therapy (C-ART); Control rooibos (C-R), Experimental (ART+R).

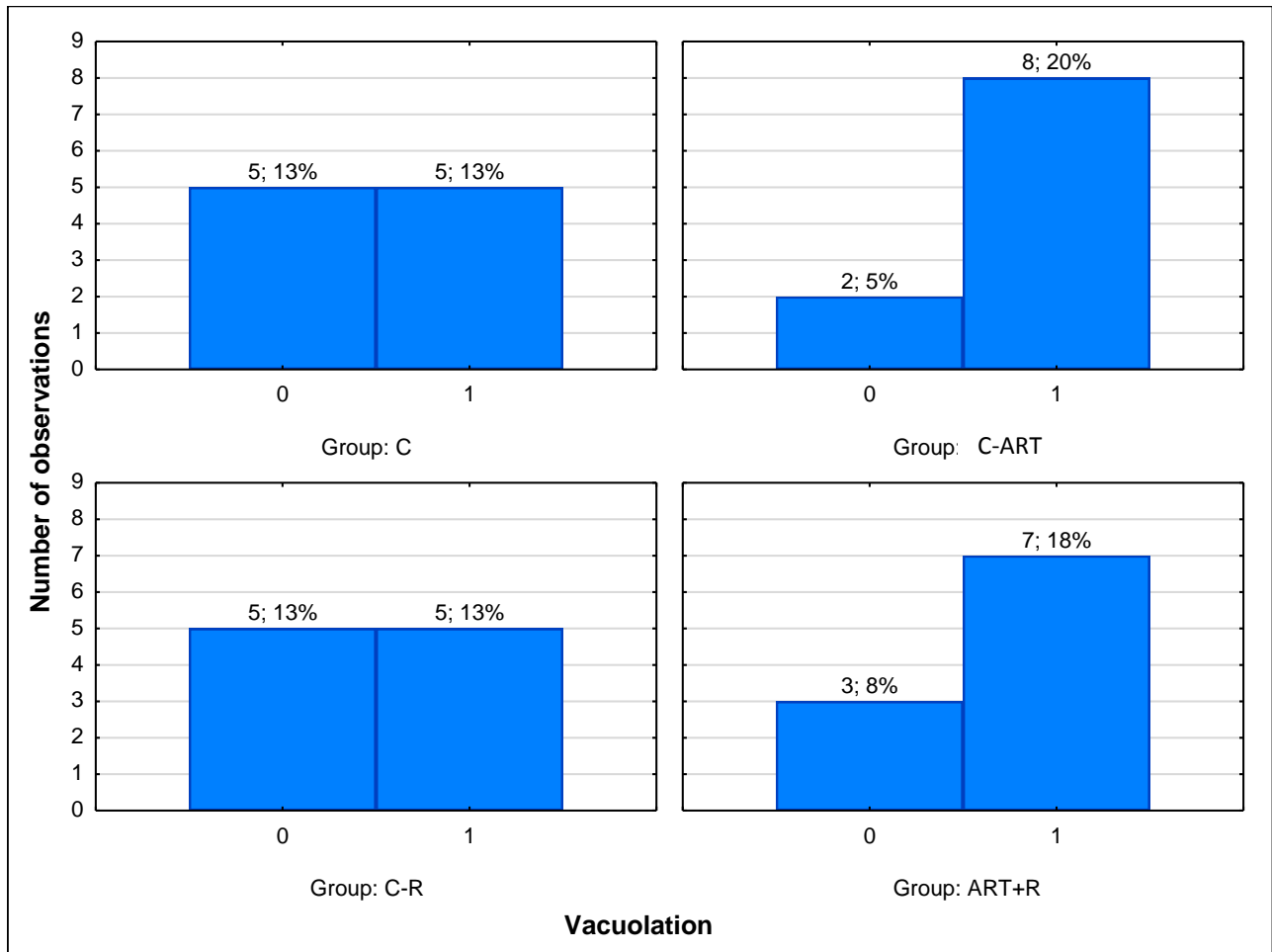


Figure 5.8: Occurrence of vacuolation in the treatment groups. The percentages indicate the presence of vacuolation across groups. Each percentage was calculated from the total sample size (N=40). The cumulative percentage is indicated. Of the total 64%, 13% of the C group was affected followed by, 20% in the C-ART, 13% in the C-R and 18% in the ART+R groups. Control (C); Control antiretroviral therapy (C-ART); Control rooibos (C-R), Experimental (ART+R).

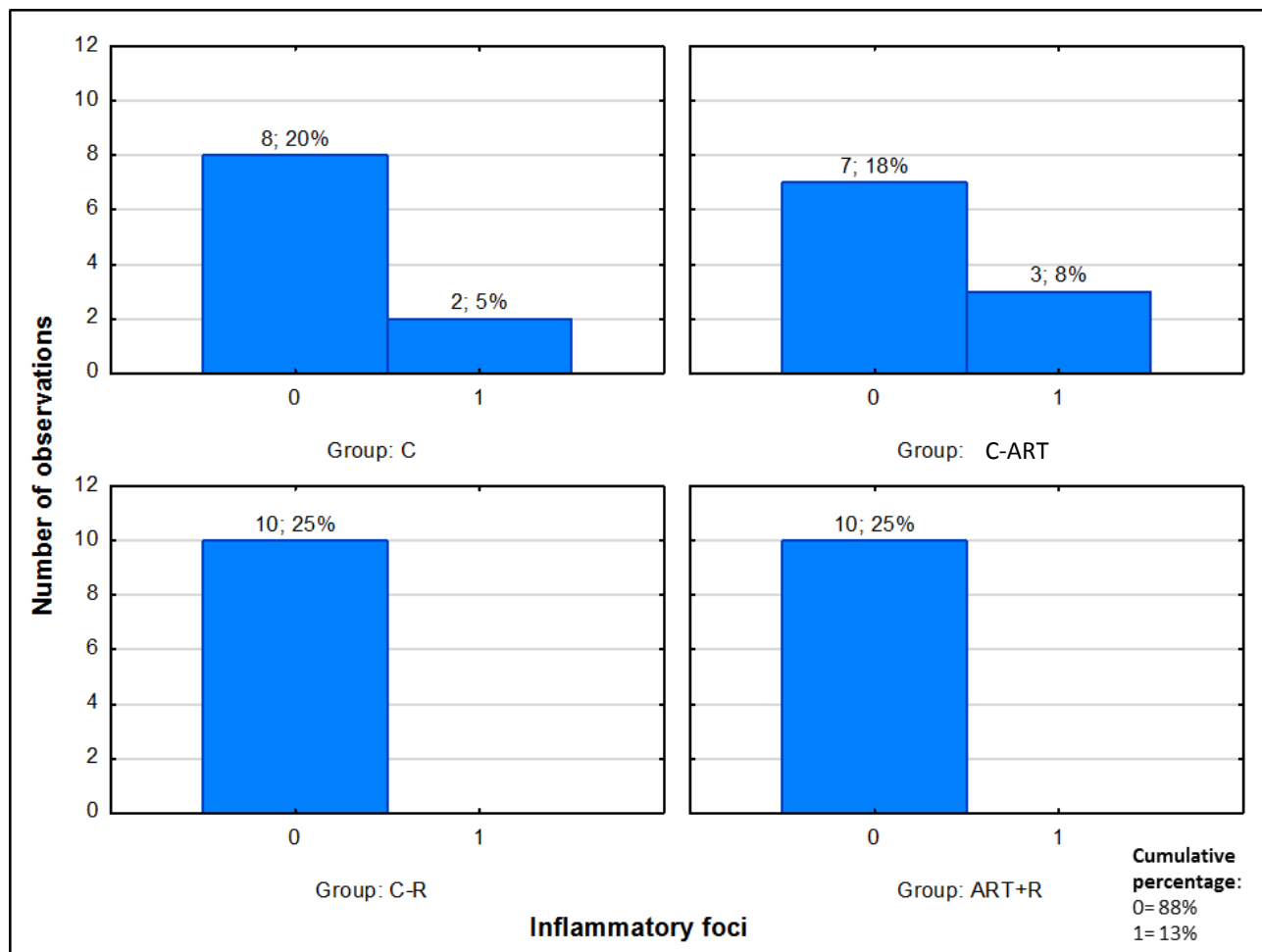


Figure 5.9: Occurrence of inflammatory foci in the treatment groups. The percentages indicate the presence of inflammatory foci across groups. Each percentage was calculated from the total sample size (N=40). The cumulative percentage is indicated. Of the total 13% affected, 5% was derived from the C followed by, 8% in the C-ART, the C-R, and ART-R were unaffected. Control (C); Control antiretroviral therapy (C-ART); Control rooibos (C-R), Experimental (ART+R).

Granular cytoplasmic changes and vacuolations in liver hepatocytes were present in all groups including the control (Figure 5.10). These changes were localised around the central vein and periportal regions, however these changes were mostly diffuse. The presence of inflammatory foci was observed in the liver parenchyma and were confined to two groups, namely the C and C-ART. The presence of these inflammatory foci is, however, negligible as the presence was too insignificant to indicate inflammation and was scored a level 1 (Figure 5.11 A, B).

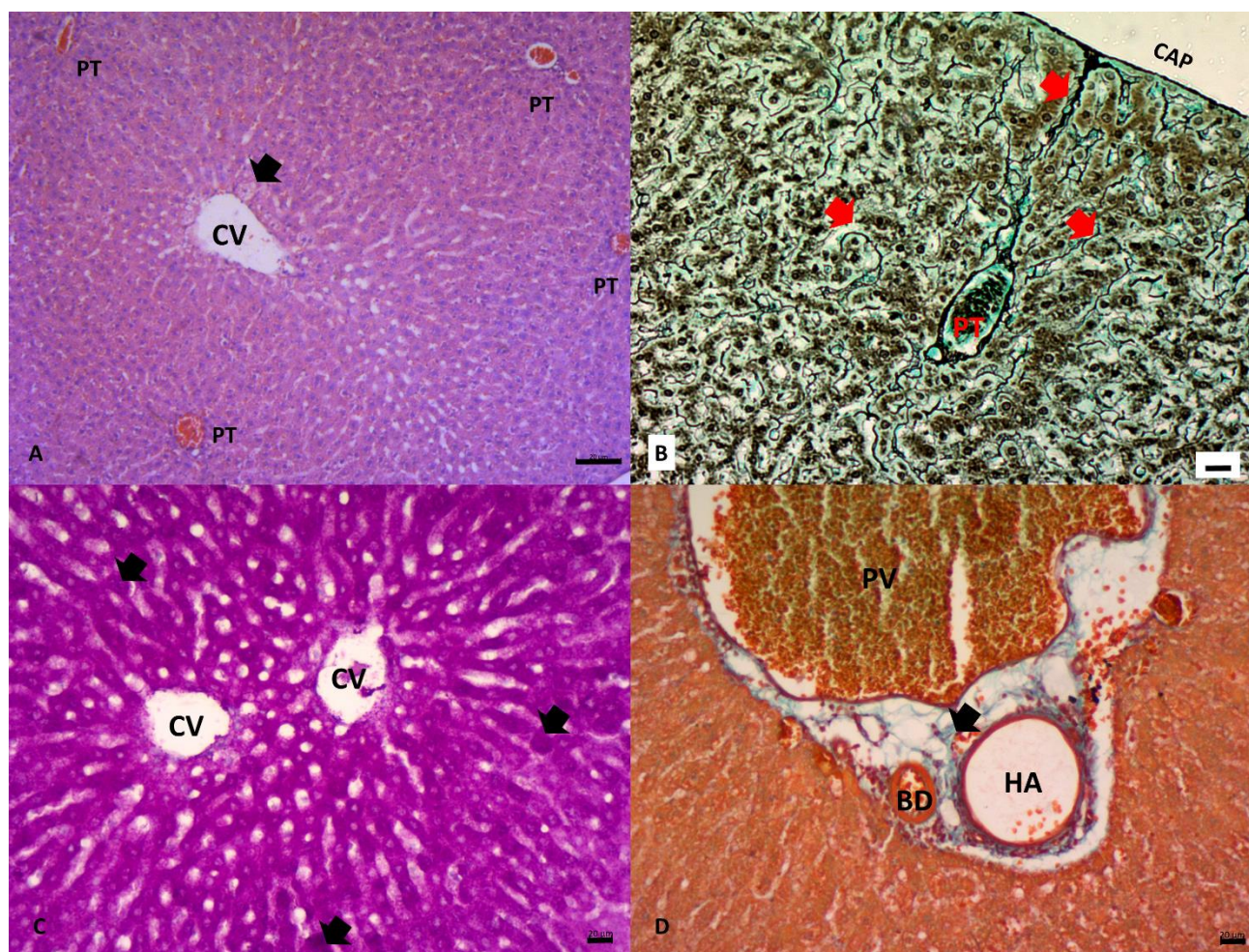


Figure 5.10: Photomicrographs depicting liver histology in a control animal. A) H&E stained (50 x magnification) slide of a hepatic lobule showing a central vein surrounded by portal tracts. Black arrows denote slight vacuolation around the central vein; B) Reticulin stained micrograph (100 x magnification) demonstrating liver architecture; hepatocytes are lined by a continuous network of black reticulin fibres (red arrows); C) PAS stained central veins (100 x magnification) with black arrows showing glycogen dense hepatocytes; D) Masson's Trichrome (MT) stained portal tract (100 x magnification) showing the light blue stained collagen fibres (black arrows). Bar=20 µm. CV=Central vein, PT=Portal tract, HA=Hepatic artery, PV=Portal vein, BD=Bile duct, CAP=Capsule.

Analysis of the reticulin stain revealed slight disruptions in reticulin fibres, around central veins, towards the capsule or areas where granular and vacuolar changes were present (Figure 5.11 C, D). These disruptions were very mild and the liver was scored as normal. No instances of pathological glycogen accumulations were found in PAS stained livers and these were scored as normal (Figure 5.11 E). No major accumulation of collagen fibres indicative of fibrosis was observed using the MT stain (Figure 5.11 F). Overall, normal liver morphology was maintained. A summary of all observations is presented in Appendix M.

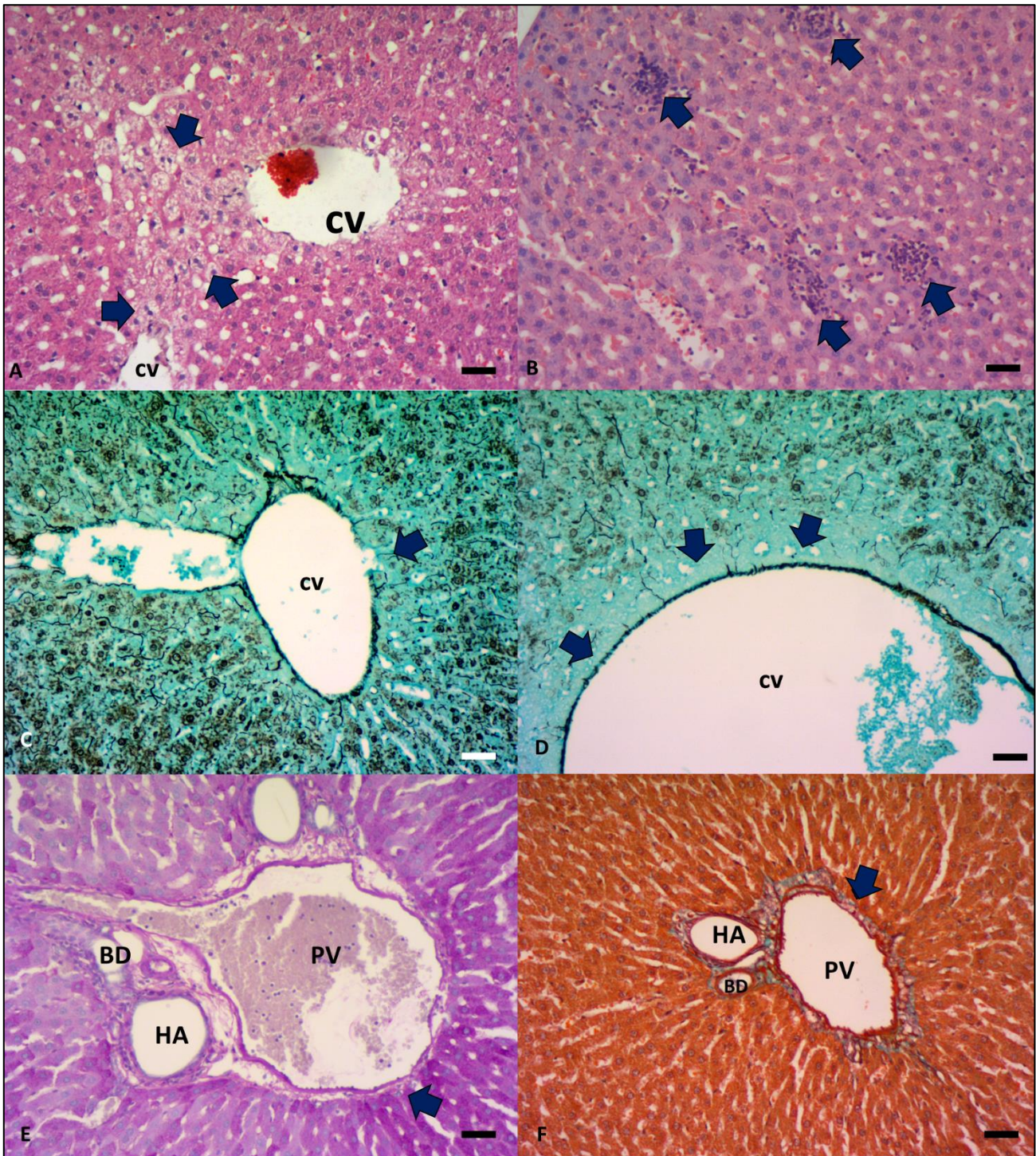


Figure 5.11: Photomicrographs of subtle tissue changes in the liver. A) H&E stained central vein showing slight vacuolation in the liver (100x magnification); B) H&E stained hepatic lobule showing inflammatory foci (black arrows) (100x magnification); C & D) Reticulin stained liver showing slight disruption of reticulin fibres around the central vein where vacuolation occurred (black arrow) (100x magnification); E) PAS stained portal tract showing glycogen rich hepatocytes (black arrow) (100x magnification); F) MT stained liver showing collagen fibres (black arrow) (100x magnification) were maintained. CV=Central vein, PV= Portal vein, HA= Hepatic artery, BD= Bile duct. Bars= 20 μ m.

5.5.3 Scoring of the kidney

Detailed pathological examination using H&E slides showed no instances of kidney lesions, which would have been indicative of nephrotoxicity (Figure 5.12 A). Granular cytoplasmic changes were not observed, however vacuolations were observed in the proximal convoluted tubules (PCT) in all groups. The presence of vacuolations were so slight and random that they were not quantifiable and the kidney was scored as normal (Figure 5.12 B). Slight instances of proteinaceous material (Figure 5.12 C) were found throughout the kidney, specifically in the proximal convoluted tubules and medullary region, however did not indicate pathology. Examination of PAS stained slides demonstrated no indication of basement membrane thickening within the glomerulus. These findings correlate to the lack of changes observed in the glomerular corpuscle and PCT when measured. A summary of all observations is presented in Appendix M.

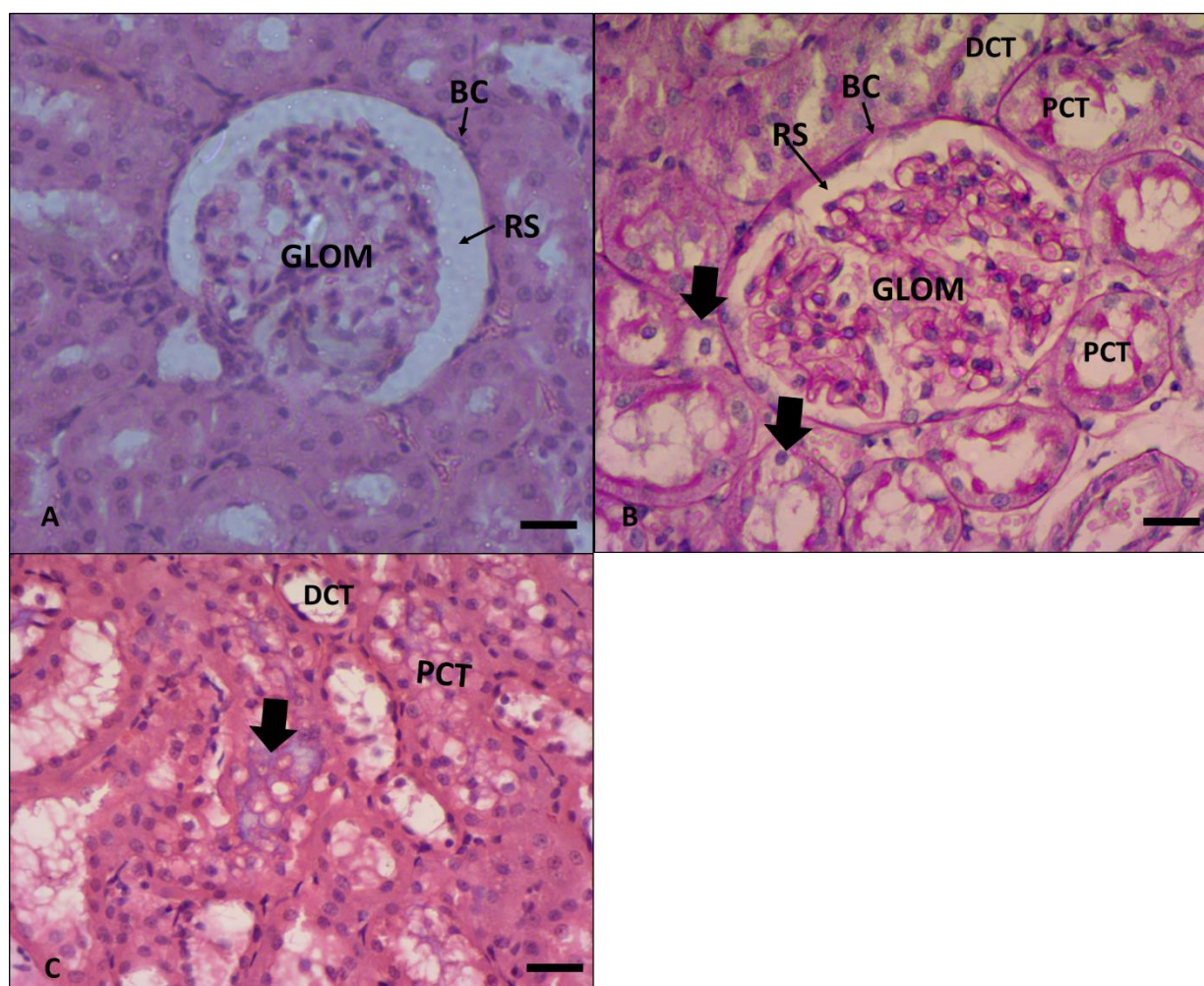


Figure 5.12: Photomicrographs (200 x magnification) of the rat kidney. A) H&E stained glomerular corpuscle of a control animal showing normal glomerular structure; B) PAS stained glomerular corpuscle showing the slight vacuolation (black arrow) in the proximal convoluted tubules; C) H&E stained kidney showing proteinaceous material in the proximal convoluted tubules (black arrow). Bars= 20 μ m. PCT= proximal convoluted tubules, DCT=Distal convoluted tubules, GLOM=Glomerulus, RS=Renal space, BC=Bowman's capsule.

5.6 ROOIBOS TEA STANDARDS

The quantity of polyphenols remained constant throughout all groups (Figure 5.13 A, B, C). However, some changes were observed between the Day 1 and Day 7 samples in each group. Aspalathin, the most abundant rooibos polyphenol, had one of the highest peaks (449, 451) in all groups. Quercetin-3-O-robinobioside/rutin (609), orientin (447) and iso-orientin (447) showed some decreases within groups. However, when superimposed (Figure 5.13 D), no major observable differences were found in aspalathin concentrations (449, 451) in the refrigerated and frozen samples when compared to the control fresh sample. The results indicate that rooibos tea can be stored for a period of four weeks refrigerated or frozen at $-4\text{ }^{\circ}\text{C}$ without drastic changes in rooibos polyphenol concentrations, indicating that the rats received similar concentrations of rooibos polyphenols throughout the week. Singular chromatograms of each group are provided in Appendix M.

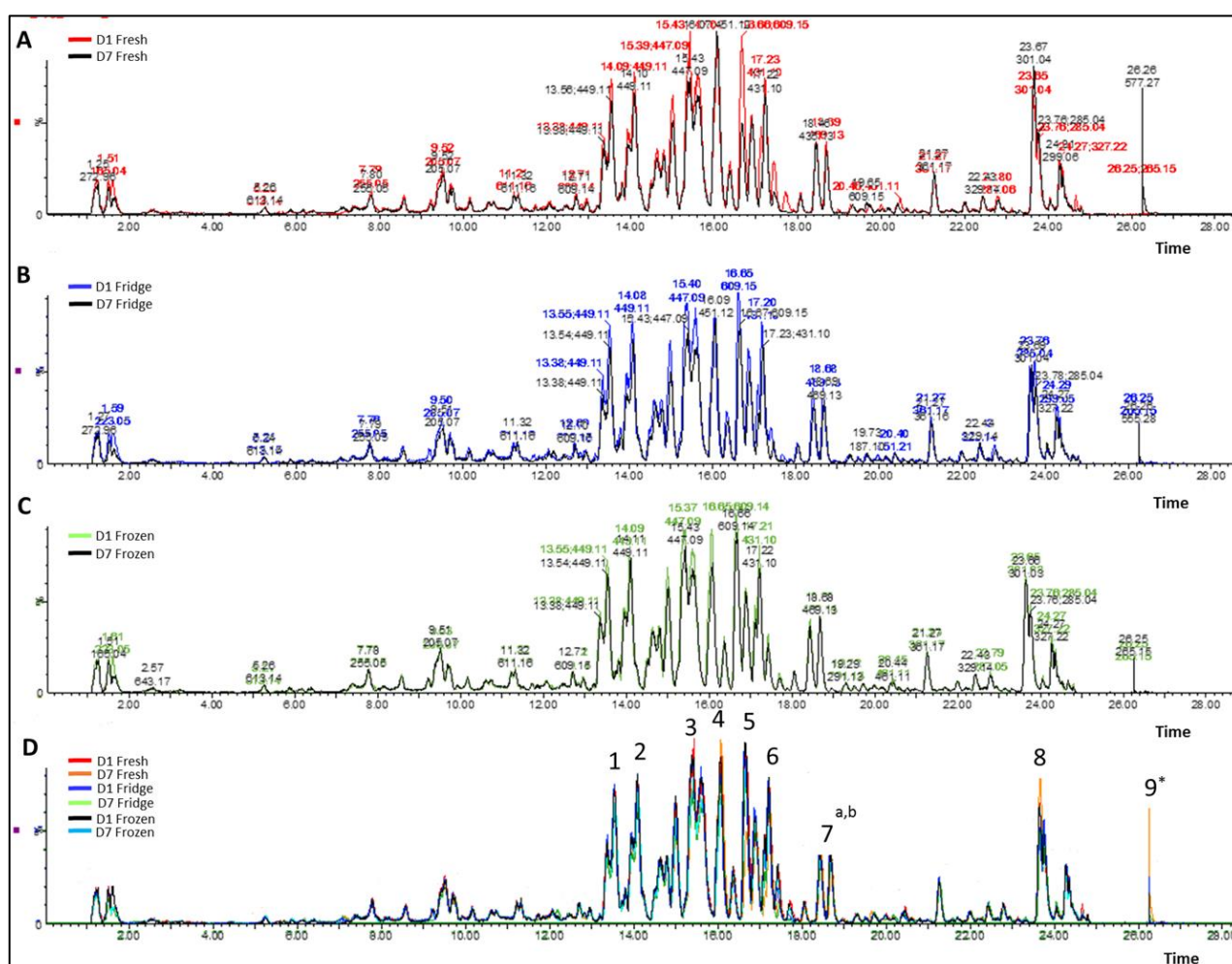


Figure 5.13: Rooibos chromatograms showing the amount of rooibos polyphenols. A) Day 1 and day 7 fresh; B) Day 1 and day 7 refrigerated; C) Day 1 and Day 7 frozen; D) super imposed image of all groups 1, 2= 449 (Aspalathin found in fermented samples), 3= 447 (Orientin and iso-orientin), 4= 451 (Aspalathin in fermented and unfermented samples), 5= 609 (Quercetin-3-O-glucoside), 6= 431 (Apigenin-8-C-glucoside) 7a= 435 (Nothofagin), 7b= 469 (unknown substance), 8= 301 (Quercetin found in fermented rooibos samples) 9*= Unknown substance. Flow rate=0.3 $\mu\text{l}/\text{min}$, column=Waters HSST3, 201x150 nm, column temperature=55 $^{\circ}\text{C}$, detection wavelength=220-500 nm, injection volume= 1 μl .

CHAPTER SIX: DISCUSSION

Antiretroviral drugs are widely-used and administered specifically for the treatment of human immunodeficiency virus (HIV) (Herlitz *et al.*, 2010; Meintjes *et al.*, 2017). The severity of the epidemic has led to accelerated licencing of many antiretroviral drugs without considering the potential risks of long term treatment (Carr & Cooper, 2000). Increasing reports of antiretroviral adverse drug reactions (ADRs) in affected individuals is concerning, often resulting in the discontinuation of treatment (Monforte *et al.*, 1999; Ammassari *et al.*, 2001; Carr, 2003). Numerous studies have reviewed the overall adverse effects of antiretroviral drugs, yet, most ADRs were reported in HIV-positive individuals or individuals receiving alternate drug combinations to the one used in the current study (Brinkman *et al.*, 1998; Fellay *et al.*, 2001; Rudorf & Krikorian, 2005; Carr & Cooper, 2010; Jao & Wyatt, 2010; Neuman *et al.*, 2013). Human immunodeficiency virus causes several adverse reactions in the body such as HIV associated nephropathy (HIVAN) (Winston *et al.*, 1998). Other adverse reactions, as a result of HIV, may be due to immune compromise, leading to the manifestation of opportunistic infections. Lee *et al.* (1993) showed that HIV-infected individuals are especially prone to ADRs as a consequence of HIV altering the metabolism of oxidative pathways, which could potentially be worsened with the introduction of ART (Styrt *et al.*, 1996). The present study had the opportunity to investigate the effects of a specific ART combination, commonly used in South Africa, on the histomorphology of the pancreas, liver, and kidney in a HIV-negative rat model. The study simultaneously introduced a 2% weight over volume (w/v) fermented rooibos tea solution to determine whether the histologically observable effects of ART could be attenuated. In an effort to curb the number of animals used in research, the current study used tissue from rats obtained from the Medical Physiology Department of Stellenbosch University, in a study that observed the physiological effects of a 2% rooibos tea solution on the hearts and aortas of antiretroviral treated male Wistar rats (Imperial, 2017). Reference is made to the results found in that study to support the findings here.

Numerous studies (Carr *et al.*, 2000, Guzik *et al.*, 2006; Lagathu *et al.*, 2007; Stein *et al.*, 2007; Lugassy *et al.*, 2010) have been published on the metabolic effects of ART. The exact mechanism of weight gain caused by ART is a multifactorial process and may be correlated to the reversal of HIV associated wasting (Dorey-Stein *et al.*, 2008) and adipocyte dysfunction (Carr *et al.*, 1998). The lack of significant changes in body weight in the C-ART group, in this study, agrees with current literature, where no significant body mass gain was observed in patients receiving a daily dose of Efavirenz (FTC), Emtricitabine (EMT), Tenofovir (TDF) (Deeks & Perry, 2010). The lack of a significant weight reduction in the C-ART group in the current study could be dose dependant, as significant body weight reductions were observed by Lebrecht *et al.* (2009) in rats given a dose of 100 mg/kg/day of TDF for 8 weeks. Additionally, weight gain is primarily associated with the use of the nucleoside

reverse transcriptase inhibitors (NRTIs) namely, stavudine, zidovudine and protease inhibitors (PIs) (Martinez *et al.*, 2001). The drug combination used in the current study does not contain PIs or the NRTIs mentioned by Martinez *et al.* (2001), thus, significant weight loss or weight gain was not expected and confirmed by the results of this study. Though fluid consumption remained constant between groups (Imperial, 2017), rooibos tended to increase the body weights of the rats, although these were not significantly different from the control groups. Rooibos has been reported to improve appetite (Morton, 1983) which could have resulted in the slightly elevated body weights observed. Food consumption in the present study was not measured, thus the slight increase in body weight cannot be confirmed as a change in appetite alone. The fact that these changes were not significant agrees with the current literature given that rats fed fermented (Baba *et al.*, 2009) and unfermented (Ajuwon *et al.*, 2013) rooibos tea infusions did not gain weight.

The current study is operating under the premise that antiretroviral drugs are causing oxidative stress (Jian *et al.*, 2007) leading to histological observable changes. The lack of significant findings in the pancreas, liver, and kidney suggest that the FTC, EMT, and TDF combination is relatively safe in HIV-negative rodents. Thiobarbituric acid reactive substances (TBARS) is a common analytical test used to measure lipid peroxidation, thereby providing a measure for oxidative stress (Janero, 1990). Ideally, an increase in TBARS was expected to be observed in the C-ART group with a subsequent decrease to control levels in the ART+R group. However, no significant differences, indicated by the following values (C=7.69±0.55; C-R=7.49±0.39; C-ART=7.54±0.79; ART+R=5.39±0.53 µmol/L), were observed between groups in the animals used in the current study, conducted by Imperial (2017). The absence of a potent oxidative stressor to induce a change could suggest the lack of histologically observable differences in the current study.

Both the exocrine and endocrine portions of the pancreas have been reported to be affected with the use of ART, including pancreatic acinar atrophy, and increases in islet size and volume, respectively (Chehter *et al.*, 2000; Neuman *et al.*, 2012; Barbosa *et al.*, 2013; Ferreira *et al.*, 2015). No major histological changes such as acinar atrophy, indicating exocrine pancreatic damage, was observed in the current study. The size of pancreatic islets and the number of pancreatic islets per section area did not vary in the present study. This could be due to the size of the tissue section, as size could have led to increases in the number of islets measured between groups. Since tissue was taken from the gastrosplenic portion of the pancreas, the area in which the sample was taken could have further influenced results, as size and number of islets are greater in this area of the rat pancreas (Elayat *et al.*, 1995). Barbosa *et al.* (2013) and Ferreira *et al.* (2015) have correlated ART to enlarged islets. Both studies associated these changes to long-term use of ART. The lack of significant changes in islet

size in the current study suggests that the experimental period was not sufficient to cause a change. This is further supported by the lack of changes in the percentage of α and β -cells compared to the control group.

There is an increased incidence of diabetes in HIV-positive individuals receiving ART (Carr *et al.*, 1998; Brown *et al.*, 2005). In the pancreas, diabetes is associated with changes in islet size (Froulob *et al.*, 2010), number (Taniyama *et al.*, 1999), increased β -cell dysfunction, and decreased β -cell volumes (Michels *et al.*, 1986). Pancreatic β -cells contain very low levels of cellular antioxidants (Sakuraba *et al.*, 2002), resulting in a reduction in β -cell function due to oxidative stress. The current study did not observe a change in percentage of α -or β -cells compared to the control group. Further illustrating the failure of ART, in the present study, to cause significant oxidative stress to lead to changes in β -cell size, number, and distribution. To our knowledge, no study has reported on the changes in α -and β -cells with the EMT, TDF, FTC combination. This could be due, firstly, to the relative safety of this combination as adverse events leading to discontinuation are seldom with the EMT, TDF, FTC combination (Zolopa *et al.*, 2013). Secondly, antiretrovirals are not causing significant amounts of oxidative stress to induce a change in the number of α and β -cells in this HIV-negative rat model. Lastly, the lack of a viral load or the duration of treatment was not sufficient to warrant a change in the current study. Other factors such as dietary and lifestyle differences could account for the increased incidence of diabetes in HIV-infected individuals receiving ART, since reports of diabetic complications were prevalent among HIV-infected individuals before the introduction of ART (Hadigan & Grinspoon, 2008). Other studies have directly associated insulin resistance and concomitantly diabetes, to the actions of PIs (Brown *et al.*, 2005), concluding that these drugs inhibit the actions of glucose transporter 4 (GLUT-4). Moreover, pancreatic involvement could be directly linked to the actions of HIV itself (Chehter *et al.*, 2000). Therefore, the lack of significant results could be due to the absence of external variables that would otherwise lead to significant changes to pancreatic islet histomorphometry in HIV-positive humans.

The lack of changes in the C-R group was expected, as rooibos has shown to attenuate instances of oxidative stress (Francisco, 2010; Awoniyi *et al.*, 2012; Chen *et al.*, 2013) in diabetic complications (Ulcina *et al.*, 2006; Francisco, 2010; Muller *et al.*, 2012) by improving β -cell function (Son *et al.*, 2013; Kamakura *et al.*, 2015) and overall oxidative status (Marnewick *et al.*, 2003). A common feature of these studies is that an oxidative stressor was induced, either by the introduction of streptozotocin (STZ) (Ulcina *et al.*, 2006) or a high fat diet (Mathijs *et al.*, 2014), to observe the potential therapeutic effect of the antioxidant agent. β -cell vacuolation has been observed in diabetic rat models with the simultaneous restoration of β -cells with added polyphenols (Adewole *et al.*,

2007). This was further observed by Chellan *et al* (2014), where the introduction of an unfermented version of honeybush tea increased β -cell proliferation in STZ diabetic rats, comparable to the actions of the antidiabetic drug, metformin. The same study concluded that β -cell protection was due to the actions of the antioxidants (magiferin, isomangiferan and xanthose) present in honeybush (Chellan *et al.*, 2014). Kajimoto and Kaneto (2004) further noted that in oxidative conditions, β -cell mass significantly increased when mice were treated with antioxidants. No instances of β -cell vacuolations were observed in the present study with either ART or rooibos administration. Rooibos polyphenols in the current study did not show attenuating effects in pancreatic β -cells comparable to those observed in other studies (Kajimoto & Kaneto, 2004; Adewole *et al.*, 2007, Chellan *et al.*, 2014). This may be due to the fact that ART, in the current study, did not cause major oxidative stress to warrant a significant histomorphological change to pancreatic α - and β -cells. Similarly, rooibos could not demonstrate an attenuating effect as no oxidative stress was induced correlating to the lack of changes observed in the experimental group compared to the control. Overall, islet histomorphometry remained constant in the present study.

The likelihood of these changes to be expressed in other organs is slight; however, as drugs are metabolised and excreted by target enzymes in the liver and kidney, their effects may be more evident in these areas. Severe liver dysfunction is defined as a grade five times greater than baseline (Soriano *et al.*, 2008). In rats, baseline is recorded at ALT: 17.5-30.2 μ /L and AST: 45.7-80.8 μ /L (Thapa & Walia, 2007). Elevations in liver transaminases are associated with the use of ART (Núñez, 2006). Aspartate aminotransferase and ALT serum levels in the current study, were only slightly elevated above baseline; however, these were not significantly different compared to the control group. The present study did not find any significant changes in the liver indicative of hepatotoxicity. These liver function tests are the most common diagnostic feature for liver function (Amacher, 1998; Ozer *et al.*, 2008). Both AST and ALT have specificity outside the liver and may specify instances of damaged myocytes (Ozer *et al.*, 2008).

The ratio of AST:ALT provides a better indication of liver function (Ozer *et al.*, 2008). The ratio of liver transaminases in the present study indicates that no major liver alterations occurred. Liver enzyme elevations have been reported with the use of all ARTs (Wit *et al.*, 2002; Núñez, 2006) with nevirapine (Sanne *et al.*, 2005; Neuman *et al.*, 2012) and PIs, being the greatest offenders often leading to hepatotoxicity in HIV-infected individuals receiving cART. In clinical settings, liver enzyme elevations need to be critically analysed as a significant proportion of elevations may be due to hepatitis B infection flares, and not necessarily the actions of ART (Soriano *et al.*, 2008). It should be noted that liver enzyme elevations are not the sole indicator of liver toxicity. In clinical trials, liver

enzyme elevations are often accompanied and confirmed histologically by the presence of hepatotoxic lesions (Amacher, 1998). No histopathological lesions in the present study was observed that were indicative of hepatotoxicity, corresponding to the lack of liver enzyme elevations. Zimmerman (1999) stated that hepatotoxicity may present as necro-inflammatory changes similar to that observed in chronic viral hepatitis. Additionally, major distortion to liver architecture, specifically the collapse of the reticulin network and enlargement of hepatocyte may occur with the use of ART (Neuman *et al.*, 2012). Instances of necrosis and severe congestion of the portal and venous system have additionally been reported with the use of ART (Adaramoye *et al.*, 2012). The specialised stains, specifically the reticulin stain, used in the present study, would single out more subtle changes that would be difficult to see on standard H&E stained tissue. No major distortion to the reticulin network of the liver was observed in the current study which would indicate ART induced hepatotoxicity, although very subtle histological changes, including granular cytoplasm and vacuolations were present. The incidence of these changes within the liver are normal and often reversible (Robins & Angell, 1976; Wit *et al.*, 2002), however, it may signify early hepatic damage, hypoxia, or mitochondrial injury in some instances (Nayak *et al.*, 1996). It should be noted that liver dysfunction in HIV-infected individuals may be exacerbated by the presence of co-opportunistic infections including hepatitis A, B, C, D and E (Núñez, 2006). Therefore, the presence of severe histopathology would only occur in cases of severe toxicity. The liver is a highly regenerative organ able to adapt rapidly to cellular stressors and attenuate toxic bioproducts (Michanalogoulos, 2007). A study conducted by Nayak *et al* (1996) concluded that vacuolated hepatocytes are adapted to resist further damage.

The presence of cellular changes in the C-R is negligible. As literature has shown the attenuating effects of rooibos against hydrogen peroxide (Ajuwon *et al.*, 2013), carbon tetrachloride (Ulcina *et al.*, 2008) and tert-butyl hydroperoxide (Canda *et al.*, 2014) induced hepatotoxicity in rats, by reducing elevated AST and ALT liver enzymes. Arguably, these changes could be slightly injurious as rooibos has shown hepatotoxic effects in isolated instances of excessive intake (Sinsalo *et al.*, 2010, Engels *et al.*, 2013, Zacharia & Whitlach, 2013). While Marnewick *et al* (2011) noted increased AST and ALT levels in individuals drinking six cups of rooibos daily, these levels were within physiologically relevant ranges. Additionally, Joubert *et al* (2005), cautioned against flavonoid rich fractions of fermented rooibos as these contained pro-oxidants that could, in turn, lead to pro-oxidative stress. Studies reporting on ART induced hepatotoxicity, have attributed these changes to alcohol abuse, direct liver injury, and the occurrence of co-morbid infections including hepatitis B and hepatitis C infections (Sulkowski *et al.*, 2000; Wit *et al.*, 2000; Carr, 2003; Dieterich *et al.*, 2004; Núñez, 2006). While Mendes and Correia (2008) reason that liver damage exists in HIV patients,

independent of ART and that hepatic injury occurs in ART patients regardless of treatment. Thus, ART associated hepatotoxicity is complex and should not be credited exclusively to its use.

Tenofovir is eliminated by glomerular filtration and tubular secretions (Ray *et al.*, 2006; Post *et al.*, 2010) implicating it in renal disease (Kohler *et al.*, 2009; Lebrecht *et al.*, 2009; Herlitz *et al.*, 2010). Renal damage caused by TDF presents as proximal convoluted tubule (PCT) dysfunction (Post *et al.*, 2010), glomerular filtration rate changes (Fabien *et al.*, 2013) or tubular ectasia with the loss of brush borders in PCT (Jao & Wyatt, 2010). Vrouenraets *et al.* (2011) attributed glomerular filtration changes to tubular secretion and not to the actions of the glomerulus. Various diseases cause changes to the size, diameter, and width of the glomerular corpuscle and PCTs (Kotyk *et al.*, 2016). Histopathological analysis of the kidney in the present study showed no pathological changes such as enlarged glomeruli, increased renal space area and width, or changes in the size of the glomerular corpuscle, indicative of nephrotoxicity. Preclinical studies using large doses of tenofovir, often ten to 12 times larger than an average human dose (Hoesley, 2008) noted renal toxicities; yet, these changes were often reversible (Röling *et al.*, 2006; Zimmerman *et al.*, 2006; Hoesley, 2008).

In rats, Lebrecht (2009) demonstrated that a dose of 100 mg/kg/day of tenofovir resulted in increased PCT diameter and concluded that the changes were associated with mitochondrial DNA depletions. The lack of significant changes in the PCT in the present study could be dose dependent as only 25.8 mg/kg/day of TDF was administered, approximately four times less than that used by Lebrecht *et al.* (2009). Although, the drugs administered in this study were combined, Mathias *et al.* (2007) stated that the combination EFV/FTC/TDF actions were equivalent to their individual components. While histopathological analysis revealed the presence of vacuolations, these were so mild in the present study that the kidney was scored as normal. Although, vacuolation may signify the presence of early kidney damage, such as those seen with the use of the chemotherapy drug, cisplatin (Shea *et al.*, 2014). The lack of histological observable changes agrees with Kohler *et al.* (2009), who observed no histological changes in the glomeruli and PCT using light microscopy in mice receiving a 100 mg/kg/day dose of tenofovir. However, the same study found mitochondrial changes in the PCT lumen using electron microscopy, suggesting mitochondrial dysfunction as a possible cause for renal damage in patients receiving ART (Kohler *et al.*, 2009). Mitochondrial toxicities with the use of TDF was further noted by Herlitz *et al.* (2010). Furthermore, renal damage may depend on the patients profile (Kalyesubula & Perazella, 2011), such as having diabetes, kidney disease, using nephrotoxic drugs, or HIV-related pathologies (including HIVAN) (Kalyesubula & Perazella, 2011) that could exacerbate kidney injury.

To our knowledge this study is the first to morphometrically quantify the effects of rooibos on the histology of the kidney. Rooibos in this study did not cause any changes to the glomerular corpuscle or the PCT that could indicate damage. Rooibos is not expected to have a damaging effect on the kidney as it has shown attenuating effects in various other organs (Baba *et al.*, 2009; Awoniyi *et al.*, 2011; Ajuwon *et al.*, 2013). Limited research has been conducted on the effects of rooibos on the kidney; however, Opuwari & Monsees (2014) showed increased levels of creatinine with the use of fermented and unfermented rooibos tea solutions, suggesting changes in kidney function. However, no changes were observed histologically (Opuwari & Monsees, 2014; Monsees & Opuwari, 2017), agreeing with the lack of changes observed in the current study.

Numerous health benefits have been reported with the use of rooibos (Ulcina *et al.*, 2006; Joubert *et al.*, 2008; Baba *et al.*, 2009; Marnewick *et al.*, 2009; Beltran-Debon *et al.*, 2011; Joubert & de Beer, 2011; Muller *et al.*, 2016). Most of these studies attributed these changes to the actions of aspalathin, the rooibos plants most abundant polyphenol (Snijman *et al.*, 2007, Snijman *et al.*, 2009). Although aspalathin has shown potent antioxidant activity *in vitro* (von Gadow *et al.*, 1997, Bramati *et al.*, 2003; Joubert *et al.*, 2008; Krafczyk *et al.*, 2009; Chen *et al.*, 2013), *in vivo* studies using pure aspalathin have often lacked such positive results (Muller *et al.*, 2016). Aspalathin ingested orally is not highly bioavailable and fails to follow Lipinski's rule of five for the bioavailability of substances (Lipsinki *et al.*, 2012), which points to its inability to cause significant changes *in vivo* (Muller *et al.*, 2016). In fact, aspalathin has shown to be metabolised by the intestine as C-glucosidases (Kreuz *et al.*, 2008; Stalmach *et al.*, 2009; Briter *et al.*, 2011) and not in its original form. Recent research is moving towards evaluating the combined actions of rooibos polyphenols, as their synergistic action could increase the therapeutic potential of rooibos. For example, quercetin, nothofagin and orientin, well-known plant polyphenols, also found in rooibos have shown therapeutic effects *in vivo* (Eybl *et al.*, 2008; Ku *et al.*, 2015; Himpe *et al.*, 2016). Thus, the therapeutic potential of rooibos polyphenols could be attributed to its multiple polyphenols each exerting its own effect (Snijman *et al.*, 2007). Furthermore, fermented and unfermented extract versions are gaining prominence, as interests rise on the nutraceutical potential of rooibos (Joubert & de Beer, 2011). The lack of histological observable changes in the rooibos group, in the present study, could be accredited to the bioavailability of rooibos or the lack of a potent toxic drug to induce a change, that would allow the attenuating effects of rooibos to be observed.

Rooibos polyphenols, specifically aspalathin, are prone to degradation when exposed to light, pH fluctuations and oxidation (Joubert, 1996; Standley *et al.*, 2001). The current study investigated the effects of temperature and time on rooibos polyphenols in an aqueous solution, in an attempt to

elucidate whether the polyphenols would degrade before being administered to rats during experimentation. The main aim of this additional aspect of the study was to determine whether the rats in the current study would attain the same quantity of polyphenols throughout the week when kept in light limiting bottles. To our knowledge, no study has been conducted on the phenolic viability of the tea once fed to a rat cohort. Liquid chromatography-mass spectrometry was used to investigate the concentration and types of polyphenols found within the rooibos tea solutions. This is a high throughput method used to detect compounds in a solution such as serum and tea (Pitt, 2009). The present study did not find major difference between the fresh sample that was made up and the sample that remained for a week following the study protocol. The main polyphenols, aspalathin, its isomers, orientin and iso-orientin, quercetin-3-o-glucoside, apigenin-8-glucoside and nothofagin, were compared to the established quantified fermented samples conducted by Beelders *et al* (2012). No major changes in these polyphenols were observed between the control sample (Day 1 fresh) of the current study to those quantified by Beelders *et al* (2012). Although slight deviations were observed in Day 7 samples to the control, no major depreciation in these rooibos polyphenols were observed. Thus, we can adequately show that the animals used in the current study received similar quantities of polyphenols each week.

To save research time, the study wanted to test if the phenolic concentrations would decrease if the samples were stored, as commercial iced tea versions of rooibos tended to have a lower antioxidant capacity (Joubert *et al.*, 2009; de Beer *et al.*, 2011). This is due to the fact that aspalathin is unstable in aqueous solutions. Although, studies have mentioned storing the tea at -20 °C (de Beer *et al.*, 2011), none to our knowledge have tested the tea once stored and given to rats in a research environment. The lack of drastic changes between refrigerated and frozen samples indicate that rooibos could be stored for up to a period of two weeks without a major compromise to the phenolic viability if light is limited and oxidation is prevented. The lack of change between groups could be attributed to the fact that light was limited and the tea was kept from being oxidised (de Beer *et al.*, 2011). Although aspalathin rich extract versions of rooibos are available and under investigation, aqueous solution such as the one used in this study are still used to test anecdotal evidence (Snijman *et al.*, 2009), as fermented versions are still the most commonly consumed (South African Rooibos Council, 2011).

CHAPTER SEVEN: CONCLUSION

In conclusion, by suggesting that rooibos can attenuate the histological observable effects of ART is an overreach, if cART is not causing significant increases in oxidative stress, to warrant significant changes to organ histomorphology. No changes were observed at a histological level in any of the organs studied, that would indicate damage caused by ART or rooibos intake. There was a non-significant increase in body weight with rooibos, thus, metabolic changes are unlikely. This was further reiterated by the lack of histological changes in the pancreas, liver, and kidney. Although, the liver demonstrated signs of potential damage, presenting as vacuolations, granular cytoplasmic changes, and in very rare instances, lymphocyte infiltration. These changes were very subtle and are often reversible (Michanalopoulos, 2007). These changes were additionally observed in the C-R group, which could indicate slight damage, as isolated reports have mentioned toxicity with chronic intake (Sinsalo *et al.*, 2010, Engels *et al.*, 2013, Zacharia & Whitlach, 2013). Additionally, this could be due to the pro-oxidant activities of rooibos (Joubert *et al.*, 2005). Perhaps with a prolonged treatment period and increased dose, the histomorphological changes associated with ART would have been more overt.

From the current study, we can deduce that the ADRs noted in the literature may be exacerbated by external variable such as the oxidative role of HIV, the occurrence of co-opportunistic infections, metabolic variations, or drug-drug interaction (Núñez, 2005; Meintjes *et al.*, 2017). Furthermore, we can soundly state that a 2% rooibos tea solution and ART does not cause deleterious or attenuating effects to an extent that it would lead to individual and diverse changes to organ histomorphometry in rodents. Thus, answering the research questions, ART is not causing major histological changes over the period tested in this model. The co-administration of rooibos cannot be seen to attenuate ADRs as no major stressor occurred. This study upholds that ART, when given to rats for a nine week period does not cause overt histomorphological changes that would indicate damage, while the co-administration of rooibos tea does not worsen or improve organ histomorphometry.

LIMITATIONS AND FUTURE STUDIES

The inability to induce oxidative stress with ART limited the ability to observe any attenuating effects of rooibos. Analysis of TBARS was conducted on the same animals by another researcher, this oxidative measure is primarily used to test for lipid peroxidation. Future studies should focus on investigating total antioxidant capacity or measuring glutathione levels between groups as these would provide better indication of the oxidative stress or lack thereof.

Tissue was shared with the Medical Physiology Department of Stellenbosch University in the effort to attain as much information as possible from animals in research. However, this limited the ability to obtain adequate amount of blood to conduct additional analyses, such as amylase in the pancreas or creatinine in the kidney. These tests would have provided an indication of pancreatic and kidney function, which could have validated the changes observed in these organs. As the animals were shared by many researchers the ability to retrieve samples at an optimum time may have led to autolysis which may further account for the slight pathological changes observed in these animals. Furthermore, the size of the sample and the fixation time may not have been sufficient.

Keeping animals for longer period of times was not possible due to the incurred costs. Thus, the experimental period (9 weeks) may have been insufficient to allow for significant changes to be observed at a tissue level.

Rooibos polyphenols are highly unstable in aqueous solutions, although, all efforts were ensured to maintain similar levels of polyphenols future studies could focus on using extract versions of the tea with an appropriate medium to be introduced to the animals. This will ensure that all animals received the same quantity of polyphenols daily. Future studies testing the therapeutic potential of rooibos could use unfermented rooibos leaves or extracts as these have increased concentrations of rooibos polyphenols.

The study could have benefited from a longer experimental period, as this would have allowed for electron microscopic (EM) studies to be conducted. Mitochondrial toxicities have been described with the use of ART. Thus, analysis of the number, size, and shape of mitochondria at an EM level would provide an indication of mitochondrial toxicities and whether these changes could be averted with rooibos administration.

REFERENCES

- Adaramoye, O.A., Adesanoye, O.A., Adewumi, O.M. & Akanni, O. 2012. Studies on the toxicological effect of nevirapine, an antiretroviral drug, on the liver, kidney and testis of male Wistar rats. *Human and Experimental Toxicology*, 31(7):676-685.
- Adewole, S., Salako, A., Doherty, O. & Naicker, T. 2007. Effect of melatonin on carbon tetrachloride-induced kidney injury in Wistar rats. *African Journal of Biomedical Research*, 10(2):153-164.
- Ajuwon, O.R., Katengua-Thamahane, E., Van Rooyen, J., Oguntibeju, O.O. & Marnewick, J.L. 2013. Protective effects of rooibos (*Aspalathus linearis*) and/or red palm oil (*Elaeis guineensis*) supplementation on tert-butyl hydroperoxide-induced oxidative hepatotoxicity in Wistar rats. *Evidence-Based Complementary and Alternative Medicine*, 2013:1-19.
- Alcolado, R., Arthur, M.J.P. & Iredale, J.P. 1997. Pathogenesis of liver fibrosis. *Clinical Science*, 92(2):103-112.
- Amacher, D.E., Schomaker, S.J. & Burkhardt, J.E. 1998. The relationship among microsomal enzyme induction, liver weight and histological change in rat toxicology studies. *Food and Chemical Toxicology*, 36(9):831-839.
- Ammassari, A., Murri, R., Pezzotti, P., Trotta, M.P., Ravasio, L., De Longis, P., Caputo, S.L., Narciso, P., Pauluzzi, S., Carosi, G. & Nappa, S. 2001. Self-reported symptoms and medication side effects influence adherence to highly active antiretroviral therapy in persons with HIV infection. *Journal of Acquired Immune Deficiency Syndromes*, 28(5):445-449.
- Andersen, V., Sonne, J. & Andersen, M. 2001. Spontaneous reports on drug-induced pancreatitis in Denmark from 1968 to 1999. *European Journal of Clinical Pharmacology*, 57(6):517-521.
- Atripla*[®] product information. 2017. Bristol-Myers Squibb & Gilead Sciences.
- Awoniyi, D.O., Aboua, Y.G., Marnewick, J. & Brooks, N. 2012. The Effects of Rooibos (*Aspalathus linearis*), Green Tea (*Camellia sinensis*) and Commercial Rooibos and Green Tea Supplements on Epididymal Sperm in Oxidative Stress-induced Rats. *Phytotherapy Research*, 26(8):1231-1239.
- Baba, H., Ohtsuka, Y., Haruna, H., Lee, T., Nagata, S., Maeda, M., Yamashiro, Y. & Shimizu, T. 2009. Studies of anti-inflammatory effects of Rooibos tea in rats. *Pediatrics International*, 51(5):700-704.
- Baratta, J.L., Ngo, A., Lopez, B., Kasabwalla, N., Longmuir, K.J. & Robertson, R.T. 2009. Cellular organization of normal mouse liver: a histological, quantitative immunocytochemical, and fine structural analysis. *Histochemistry and Cell Biology*, 131(6):713-726.
- Barbosa, A.G., Chehter, E.Z., Bacci, M.R., Mader, A.A. & Fonseca, F.L. 2013. AIDS and the pancreas in the HAART era: a cross sectional study. *International Archives of Medicine*, 6(28):1-6. DOI 10.1186/1755-7682-6-28

- Barré-Sinoussi, F., Ross, A.L. & Delfraissy, J.F. 2013. Past, present and future: 30 years of HIV research. *Nature Reviews: Microbiology*, 11(12):877-883.
- Beelders, T., Sigge, G.O., Joubert, E., de Beer, D. & de Villiers, A. 2012. Kinetic optimisation of the reversed phase liquid chromatographic separation of rooibos tea (*Aspalathus linearis*) phenolics on conventional high performance liquid chromatographic instrumentation. *Journal of Chromatography A*, 1219:128-139.
- Beltrán-Debón, R., Rull, A., Rodríguez-Sanabria, F., Iswaldi, I., Herranz-López, M., Aragonès, G., Camps, J., Alonso-Villaverde, C., Menéndez, J.A., Micol, V. & Segura-Carretero, A. 2011. Continuous administration of polyphenols from aqueous rooibos (*Aspalathus linearis*) extract ameliorates dietary-induced metabolic disturbances in hyperlipidemic mice. *Phytomedicine*, 18(5):414-424.
- Bissell, D.M., Gores, G.J., Laskin, D.L. & Hoofnagle, J.H. 2001. Drug-induced liver injury: Mechanisms and test systems. *Hepatology*, 33(4):1009-1013.
- Bleibel, W., Kim, S., D'Silva, K. & Lemmer, E.R. 2007. Drug-induced liver injury. *Digestive Diseases and Sciences*, 52(10):2463-2471.
- Bouwens, L., De Bleser, P., Vanderkerken, K., Geerts, B. & Wisse, E. 1992. Liver cell heterogeneity: functions of non-parenchymal cells. *Enzyme*, 46:155-168.
- Bramati, L., Aquilano, F. & Pietta, P. 2003. Unfermented rooibos tea: quantitative characterization of flavonoids by HPLC–UV and determination of the total antioxidant activity. *Journal of Agricultural and Food Chemistry*, 51(25):7472-7474.
- Brinkman, K., ter Hofstede, H.J., Burger, D.M., Smeitink, J.A. & Koopmans, P.P. 1998. Adverse effects of reverse transcriptase inhibitors: Mitochondrial toxicity as common pathway. *AIDS*, 12(14):1735-1744.
- Brissova, M., Fowler, M.J., Nicholson, W.E., Chu, A., Hirshberg, B., Harlan, D.M. & Powers, A.C. 2005. Assessment of human pancreatic islet architecture and composition by laser scanning confocal microscopy. *Journal of Histochemistry and Cytochemistry*, 53(9):1087-1097.
- Brown, T.T., Cole, S.R., Li, X., Kingsley, L.A., Palella, F.J., Riddler, S.A., Visscher, B.R., Margolick, J.B. & Dobs, A.S. 2005. Antiretroviral therapy and the prevalence and incidence of diabetes mellitus in the multicenter AIDS cohort study. *Archives of Internal Medicine*, 165(10):1179-1184.
- Canda, B.D., Oguntibeju, O.O. & Marnewick, J.L. 2014. Effects of consumption of rooibos (*Aspalathus linearis*) and a rooibos-derived commercial supplement on hepatic tissue injury by tert-butyl hydroperoxide in Wistar rats. *Oxidative Medicine and Cellular Longevity*, 2014:1-9
- Carr, A. & Cooper, D.A. 2000. Adverse effects of antiretroviral therapy. *The Lancet*, 356(9239):1423-1430.

- Carr, A. 2003. Toxicity of antiretroviral therapy and implications for drug development. *Nature Reviews: Drug Discovery*, 2(8):624-634.
- Chehter, E.Z., Longo, M.A., Laudanna, A.A. & Duarte, M.I.S. 2000. Involvement of the pancreas in AIDS: A prospective study of 109 post-mortems. *AIDS*, 14(13):1879-1886.
- Chellan, N., Joubert, E., Strijdom, H., Roux, C., Louw, J. & Muller, C.J. 2014. Aqueous extract of unfermented honeybush (*Cyclopia maculata*) attenuates STZ-induced diabetes and β -cell cytotoxicity. *Planta Medica*, 80(09):622-629.
- Chen, W., Sudji, I.R., Wang, E., Joubert, E., van Wyk, B.E. & Wink, M. 2013. Ameliorative effect of aspalathin from rooibos (*Aspalathus linearis*) on acute oxidative stress in *Caenorhabditis elegans*. *Phytomedicine*, 20(3):380-386.
- Courts, F.L. & Williamson, G. 2009. The C-glycosyl flavonoid, aspalathin, is absorbed, methylated and glucuronidated intact in humans. *Molecular Nutrition and Food Research*, 53(9):1104-1111.
- Cross, S. (ed) 2013. *Underwood's Pathology*. 6th Edition. Glasgow: Churchill Livingstone.
- D'Autréaux, B. & Toledano, M.B. 2007. ROS as signalling molecules: mechanisms that generate specificity in ROS homeostasis. *Nature Reviews: Molecular Cell Biology*, 8(10):813-824.
- de Beer, D., Joubert, E., Viljoen, M. and Manley, M. 2012. Enhancing aspalathin stability in rooibos (*Aspalathus linearis*) ready-to-drink iced teas during storage: the role of nano-emulsification and beverage ingredients, citric and ascorbic acids. *Journal of the Science of Food and Agriculture*, 92(2):274-282.
- Deavall, D.G., Martin, E.A., Horner, J.M. & Roberts, R. 2012. Drug-induced oxidative stress and toxicity. *Journal of Toxicology*, 2012:1-13
- Deeks, E.D. & Perry, C.M. 2010. Efavirenz/Emtricitabine/Tenofovir Disoproxil Fumarate Single-tablet Regimen (Atripla®). *Drugs*, 70(17):2315-2338.
- DeJesus, E., Young, B., Morales-Ramirez, J.O., Sloan, L., Ward, D.J., Flaherty, J.F., Ebrahimi, R., Maa, J.F., Reilly, K., Ecker, J. & McColl, D. 2009. Simplification of antiretroviral therapy to a single-tablet regimen consisting of efavirenz, emtricitabine, and tenofovir disoproxil fumarate versus unmodified antiretroviral therapy in virologically suppressed HIV-1-infected patients. *Journal of Acquired Immune Deficiency Syndromes*, 51(2):163-174.
- Dieterich, D.T., Robinson, P.A., Love, J. & Stern, J.O. 2004. Drug-induced liver injury associated with the use of nonnucleoside reverse-transcriptase inhibitors. *Clinical Infectious Diseases*, 38(2):80-89.
- Dludla, P.V., Muller, C.J.F., Louw, J., Joubert, E., Salie, R., Opoku, A.R. & Johnson, R. 2014. The cardioprotective effect of an aqueous extract of fermented rooibos (*Aspalathus linearis*) on cultured cardiomyocytes derived from diabetic rats. *Phytomedicine*, 21(5):595-601.

- Dorey-Stein, Z., Amorosa, V.K., Kostman, J.R., Lo Re, V. & Shannon, R.P. 2008. Severe Weight Gain, Lipodystrophy, Dyslipidemia, and Obstructive Sleep Apnea in a Human Immunodeficiency Virus-Infected Patient Following Highly Active Antiretroviral Therapy. *Journal of the Cardiometabolic Syndrome*, 3(2):111-114.
- Drachenberg, C.B., Klassen, D.K., Weir, M.R., Wiland, A., Fink, J.C., Bartlett, S.T., Cangro, C.B., Blahut, S. & Papadimitriou, J.C. 1999. Islet Cell Damage Associated with Tacrolimus and Cyclosporine: Morphological Features in Pancreas allograft biopsies and clinical Correlation. *Transplantation*, 68(3):396-402.
- Elayat, A.A., el-Naggar, M.M. & Tahir, M. 1995. An immunocytochemical and morphometric study of the rat pancreatic islets. *Journal of Anatomy*, 186(3):629-637.
- Engels, M., Wang, C., Matoso, A., Maidan, E. & Wands, J. 2013. Tea not tincture: hepatotoxicity associated with rooibos herbal tea. *ACG Case Reports Journal*, 1(1):58-60.
- Fabian, J., Naicker, S., Goetsch, S. & Venter, W.D.F. 2013. The clinical and histological response of HIV-associated kidney disease to antiretroviral therapy in South Africans. *Nephrology Dialysis Transplantation*, 28(6):1543-1554.
- Fellay, J., Ledergerber, B., Bernasconi, E., Furrer, H., Battegay, M., Hirschel, B., Vernazza, P., Francioli, P., Greub, G., Flepp, M. & Telenti, A. 2001. Prevalence of adverse events associated with potent antiretroviral treatment: Swiss HIV Cohort Study. *The Lancet*, 358(9290):1322-1327.
- Ferreira, F.M., Dos Santos, L.G., Miranda, P.G.D.A., Afonso, R.I., Marques, L.M., Bacci, M., Mader, A.M.A., Barbosa, A.G. & Chether, E.Z. 2015. HIV and Pancreas: Endocrinological Patterns of Pancreatic Morphology. *Journal of Pancreas*, 16(4):369-372.
- Francisco, N.M. 2010. Modulation of postprandial oxidative stress by rooibos (*Aspalathus linearis*) in normolipidaemic individuals. Unpublished doctoral dissertation, Cape Town: Cape Peninsula University of Technology.
- Fraulob, J.C., Ogg-Diamantino, R., Fernandes-Santos, C., Aguila, M.B. & Mandarim-de-Lacerda, C.A. 2010. A mouse model of metabolic syndrome: insulin resistance, fatty liver and non-alcoholic fatty pancreas disease (NAFPD) in C57BL/6 mice fed a high fat diet. *Journal of Clinical Biochemistry and Nutrition*, 46(3):212-223.
- Frick, L. W., Lambe, C. U., St John, L., Taylor, L. C. & Nelson, D. J. (1994). Pharmacokinetics, oral bioavailability, and metabolism in mice and cynomolgus monkeys of (2'R, 5'S)-cis-5-fluoro-1-[2-(hydroxymethyl)-1, 3-oxathiolan-5-yl] cytosine, an agent active against human immunodeficiency virus and human hepatitis B virus. *Antimicrobial Agents and Chemotherapy*, 38(12):2722-2729.
- Gallant, J.E., Parish, M.A., Keruly, J.C. & Moore, R.D. 2005. Changes in renal function associated with tenofovir disoproxil fumarate treatment, compared with nucleoside reverse-transcriptase inhibitor treatment. *Clinical Infectious Diseases*, 40(8):1194-1198.

- Gelderblom, W.C.A., Joubert, E., Gamielien, K., Sissing, L., Malherbe, C.J. & Maritz, G. 2017. Rooibos (*Aspalathus linearis*), honeybush (*Cyclopia intermedia*) and cancer bush (*Sutherlandia frutescens subsp. microphylla*) protect against tobacco-specific mutagenesis *in vitro*. *South African Journal of Botany*, 110:194-200.
- Goumenos, D.S., Kwarar, B., El Nahas, M., Conti, S., Wagner, B., Spyropoulos, C., Vlachojannis, J.G., Benigni, A. & Kalfarentzos, F. 2009. Early histological changes in the kidney of people with morbid obesity. *Nephrology Dialysis Transplantation*, 24(12):3732-3738.
- Gupta, S. 2000. Hepatic polyploidy and liver growth control. *Seminars in Cancer Biology*, 10(3):161-171.
- Hadigan, C. & Grinspoon, S. 2008. Diabetes and Insulin resistance. In Dolin, R., Masur, H. & Saag, M.S (eds) 2007. *AIDS Therapy*. Philadelphia: Churchill Livingstone.
- Hall, A.M. 2013. Update on tenofovir toxicity in the kidney. *Pediatric Nephrology*, 28(7):1011-1023.
- Hendricks, R. & Pool, E.J. 2010. The *in vitro* effects of rooibos and black tea on immune pathways. *Journal of Immunoassay and Immunochemistry*, 31(2):169-180.
- Henegar, J.R., Bigler, S.A., Henegar, L.K., Tyagi, S.C. & Hall, J.E. 2001. Functional and structural changes in the kidney in the early stages of obesity. *Journal of the American Society of Nephrology*, 12(6):1211-1217.
- Herlitz, L.C., Mohan, S., Stokes, M.B., Radhakrishnan, J., D'Agati, V.D. & Markowitz, G.S. 2010. Tenofovir nephrotoxicity: acute tubular necrosis with distinctive clinical, pathological, and mitochondrial abnormalities. *Kidney International*, 78(11):1171-1177.
- Hoesley, C.J. 2008. Tenofovir. In Dolin, R., Masur, H. & Saag, M.S (eds) 2007. *AIDS Therapy*. Philadelphia: Churchill Livingstone.
- Huang, M., du Plessis, J., du Preez, J., Hamman, J. & Viljoen, A. 2008. Transport of aspalathin, a rooibos tea flavonoid, across the skin and intestinal epithelium. *Phytotherapy Research*, 22(5):699-704.
- Imperial, E.G. 2017. Effect of *Aspalathus linearis* supplementation, during anti-retroviral treatment, on the heart and aortas of male Wistar rats and the effects of drinking rooibos on the cardiovascular profile of patients on ART. Unpublished masters dissertation, Stellenbosch: Stellenbosch University.
- Inanami, O., Asanuma, T., Inukai, N., Jin, T., Shimokawa, S., Kasai, N., Nakano, M., Sato, F. & Kuwabara, M. 1995. The suppression of age-related accumulation of lipid peroxides in rat brain by administration of Rooibos tea (*Aspalathus linearis*). *Neuroscience Letters*, 196(1):85-88.
- Iswaldi, I., Arráez-Román, D., Rodríguez-Medina, I., Beltrán-Debón, R., Joven, J., Segura-Carretero, A. & Fernández-Gutiérrez, A. 2011. Identification of phenolic compounds in aqueous and ethanolic rooibos extracts (*Aspalathus linearis*) by HPLC-ESI-MS (TOF/IT). *Analytical and Bioanalytical Chemistry*, 400(10):3643-3654.

- Janero, D.R. 1990. Malondialdehyde and thiobarbituric acid-reactivity as diagnostic indices of lipid peroxidation and peroxidative tissue injury. *Free Radical Biology and Medicine*, 9(6):515-540.
- Jao, J. & Wyatt, C.M. 2010. Antiretroviral medications: adverse effects on the kidney. *Advances in Chronic Kidney Disease*, 17(1):72-82.
- Jiang, B., Hebert, V.Y., Li, Y., Mathis, J.M., Alexander, J.S. & Dugas, T.R. 2007. HIV antiretroviral drug combination induces endothelial mitochondrial dysfunction and reactive oxygen species production, but not apoptosis. *Toxicology and Applied Pharmacology*, 224(1):60-71.
- Joubert, E. & de Beer, D. 2011. Rooibos (*Aspalathus linearis*) beyond the farm gate: From herbal tea to potential phytopharmaceutical. *South African Journal of Botany*, 77(4):869-886.
- Joubert, E. & Ferreira, D. 1996. Antioxidants of Rooibos tea—a possible explanation for its health promoting properties? *South African Journal of Food Science and Nutrition*, 8, pp.79-84.
- Joubert, E. 1996a. HPLC quantification of the dihydrochalcones, aspalathin and nothofagin in rooibos tea (*Aspalathus linearis*) as affected by processing. *Food Chemistry*, 55(4):403-411.
- Joubert, E., Gelderblom, W.C.A., Louw, A. & de Beer, D. 2008. South African herbal teas: *Aspalathus linearis*, *Cyclopia* spp. and *Athrixia phylicoides*—a review. *Journal of Ethnopharmacology*, 119(3):376-412.
- Joubert, E., Viljoen, M., De Beer, D. and Manley, M., 2009. Effect of heat on aspalathin, iso-orientin, and orientin contents and color of fermented rooibos (*Aspalathus linearis*) iced tea. *Journal of agricultural and food chemistry*, 57(10), pp.4204-4211
- Joubert, E., Winterton, P., Britz, T.J. & Gelderblom, W.C. 2005. Antioxidant and pro-oxidant activities of aqueous extracts and crude polyphenolic fractions of rooibos (*Aspalathus linearis*). *Journal of Agricultural and Food Chemistry*, 53(26):10260-10267.
- Kajimoto, Y. & Kaneto, H. 2004. Role of Oxidative Stress in Pancreatic β -Cell Dysfunction. *Annals of the New York Academy of Sciences*, 1011(1):168-176.
- Kalyesubula, R. & Perazella, M.A. 2011. Nephrotoxicity of HAART. *AIDS: Research and Treatment*, 2011:1-11. DOI: 10.1155/2011/562790
- Kamakura, R., Son, M.J., de Beer, D., Joubert, E., Miura, Y. & Yagasaki, K. 2015. Antidiabetic effect of green rooibos (*Aspalathus linearis*). *Cytotechnology*, 67(4):699-710.
- Kara, M.E. 2005. The anatomical study on the rat pancreas and its ducts with emphasis on the surgical approach. *Annals of Anatomy-Anatomischer Anzeiger*, 187(2):105-112.
- Kawano, A., Nakamura, H., Hata, S.I., Minakawa, M., Miura, Y. & Yagasaki, K. 2009. Hypoglycemic effect of aspalathin, a rooibos tea component from *Aspalathus linearis*, in type 2 diabetic model db/db mice. *Phytomedicine*, 16(5):437-443.
- Kearney, B.P., Flaherty, J.F. & Shah, J. 2004. Tenofovir disoproxil fumarate. *Clinical Pharmacokinetics*, 43(9):595-612.

- Kierszenbaum, A.L. & Tres, L. 2015. *Histology and Cell Biology: An Introduction to Pathology*. 4th Edition. Saunders: Philadelphia.
- Kim, A., Miller, K., Jo, J., Kilimnik, G., Wojcik, P. & Hara, M. 2009. Islet architecture: a comparative study. *Islets*, 1(2):129-136.
- Klöppel, G. & Maillet, B. 1993. Pathology of acute and chronic pancreatitis. *Pancreas*, 8(6):659-670.
- Koeppen, B.H. & Roux, D.G. 1966. C-glycosylflavonoids. The chemistry of aspalathin. *Biochemical Journal*, 99(3):604-609.
- Kohen, R. & Nyska, A. 2002. Oxidation of Biological Systems: Oxidative Stress Phenomena, Antioxidants, Redox Reactions, and Methods for Their Quantification. *Toxicologic Pathology*, 30(6):620-650.
- Kohler, J.J., Hosseini, S.H., Hoying-Brandt, A., Green, E., Johnson, D.M., Russ, R., Tran, D., Raper, C.M., Santoianni, R. & Lewis, W. 2009. Tenofovir renal toxicity targets mitochondria of renal proximal tubules. *Laboratory Investigation: A Journal of Technical Methods and Pathology*, 89(5):513-519.
- Kotyk, T., Dey, N., Ashour, A.S., Balas-Timar, D., Chakraborty, S., Ashour, A.S. & Tavares, J.M.R. 2016. Measurement of glomerulus diameter and Bowman's space width of renal albino rats. *Computer Methods and Programs in Biomedicine*, 126:143-153.
- Krafczyk, N. & Glomb, M.A. 2008. Characterization of phenolic compounds in rooibos tea. *Journal of Agricultural and Food Chemistry*, 56(9):3368-3376.
- Kreuz, S., Joubert, E., Waldmann, K.H. & Ternes, W. 2008. Aspalathin, a flavonoid in *Aspalathus linearis* (rooibos), is absorbed by pig intestine as a C-glycoside. *Nutrition Research*, 28(10):690-701.
- Kuwabara, M., Asanuma, T., Niwa, K. & Inanami, O. 2008. Regulation of cell survival and death signals induced by oxidative stress. *Journal of Clinical Biochemistry and Nutrition*, 43(2):51-57.
- Lagathu, C., Bastard, J.P., Auclair, M., Maachi, M., Kornprobst, M., Capeau, J. & Caron, M. 2004. Antiretroviral drugs with adverse effects on adipocyte lipid metabolism and survival alter the expression and secretion of proinflammatory cytokines and adiponectin *in vitro*. *Antiviral Therapy*, 9(6):911-20.
- Lebrecht, D., Venhoff, A.C., Kirschner, J., Wiech, T., Venhoff, N. & Walker, U.A. 2009. Mitochondrial tubulopathy in tenofovir disoproxil fumarate-treated rats. *Journal of Acquired Immune Deficiency Syndromes*, 51(3):258-263.
- Lee, B.L., Wong, D., Benowitz, N.L. & Sullam, P.M. 1993. Altered patterns of drug metabolism in patients with acquired immunodeficiency syndrome. *Clinical Pharmacology and Therapeutics*, 53(5):529-535.

- Lipinski, C.A., Lombardo, F., Dominy, B.W. & Feeney, P.J. 2012. Experimental and computational approaches to estimate solubility and permeability in drug discovery and development settings. *Advanced Drug Delivery Reviews*, 64:4-17.
- Lugassy, D.M., Farmer, B.M. & Nelson, L.S. 2010. Metabolic and hepatobiliary side effects of antiretroviral therapy (ART). *Emergency Medicine Clinics of North America*, 28(2):409-419.
- Manach, C., Williamson, G., Morand, C., Scalbert, A. & Rémésy, C. 2005. Bioavailability and bioefficacy of polyphenols in humans. I. Review of 97 bioavailability studies. *The American Journal of Clinical Nutrition*, 81(1):230-242.
- Manda, K.R., Banerjee, A., Banks, W.A. & Ercal, N. 2011. Highly active antiretroviral therapy drug combination induces oxidative stress and mitochondrial dysfunction in immortalized human blood-brain barrier endothelial cells. *Free Radical Biology and Medicine*, 50(7):801-810.
- Manfredi, R. & Calza, L. 2008. HIV infection and the pancreas: risk factors and potential management guidelines. *International Journal of STD and AIDS*, 19(2):99-105.
- Marnewick, J.L. 2014. Antioxidant Properties of Rooibos (*Aspalathus linearis*)—*in vitro* and *in vivo* Evidence. In Laher, I (ed). *Systems Biology of Free Radicals and Antioxidants*: Springer Berlin Heidelberg (4083-4108).
- Marnewick, J.L., Batenburg, W., Swart, P., Joubert, E., Swanevelder, S. & Gelderblom, W.C.A. 2004. *Ex vivo* modulation of chemical-induced mutagenesis by subcellular liver fractions of rats treated with rooibos (*Aspalathus linearis*) tea, honeybush (*Cyclopia intermedia*) tea, as well as green and black (*Camellia sinensis*) teas. *Mutation Research/Genetic Toxicology and Environmental Mutagenesis*, 558(1):145-154.
- Marnewick, J.L., Gelderblom, W.C. & Joubert, E. 2000. An investigation on the antimutagenic properties of South African herbal teas. *Mutation Research/Genetic Toxicology and Environmental Mutagenesis*, 471(1):157-166.
- Marnewick, J.L., Joubert, E., Swart, P., Van der Westhuizen, F. & Gelderblom, W.C. 2003. Modulation of hepatic drug metabolizing enzymes and oxidative status by rooibos (*Aspalathus linearis*) and honeybush (*Cyclopia intermedia*), green and black (*Camellia sinensis*) teas in rats. *Journal of Agricultural and Food Chemistry*, 51(27):8113-8119.
- Marnewick, J.L., Rautenbach, F., Venter, I., Neethling, H., Blackhurst, D.M., Wolmarans, P. & Macharia, M. 2011. Effects of rooibos (*Aspalathus linearis*) on oxidative stress and biochemical parameters in adults at risk for cardiovascular disease. *Journal of Ethnopharmacology*, 133(1):46-52.
- Marnewick, J.L., Van der Westhuizen, F.H., Joubert, E., Swanevelder, S., Swart, P. & Gelderblom, W.C. 2009. Chemoprotective properties of rooibos (*Aspalathus linearis*), honeybush (*Cyclopia intermedia*) herbal and green and black (*Camellia sinensis*) teas against cancer promotion induced by fumonisin B1 in rat liver. *Food and Chemical Toxicology*, 47(1):220-229.

- Martínez, E., Mocroft, A., García-Viejo, M.A., Pérez-Cuevas, J.B., Blanco, J.L., Mallolas, J., Bianchi, L., Conget, I., Blanch, J., Phillips, A. & Gatell, J.M. 2001. Risk of lipodystrophy in HIV-1-infected patients treated with protease inhibitors: A prospective cohort study. *The Lancet*, 357(9256):592-598.
- Mathias, A.A., Hinkle, J., Menning, M., Hui, J., Kaul, S. & Kearney, B.P. 2007. Efavirenz/Emtricitabine/ Tenofovir Disoproxil Fumarate Single-tablet Regimen Development Team. Bioequivalence of efavirenz/emtricitabine/tenofovir disoproxil fumarate single-tablet regimen. *Journal of Acquired Immune Deficiency Syndromes*, 46(2):167-173.
- Mathijs, I., Da Cunha, D.A., Himpe, E., Ladriere, L., Chellan, N., Roux, C.R., Joubert, E., Muller, "C., Cnop, M., Louw, J. & Bouwens, L. 2014. Phenylpropenoic acid glucoside augments pancreatic beta cell mass in high-fat diet-fed mice and protects beta cells from ER stress-induced apoptosis. *Molecular Nutrition and Food Research*, 58(10):1980-1990.
- May, M.T., Gompels, M., Delpech, V., Porter, K., Orkin, C., Keggs, S., Hay, P., Johnson, M., Palfreeman, A., Gilson, R. & Chadwick, D. 2014. Impact on life expectancy of HIV-1 positive individuals of CD4+ cell count and viral load response to antiretroviral therapy. *AIDS (London, England)*, 28(8):1193.
- Mazibuko, S.E., Muller, C.J.F., Joubert, E., De Beer, D., Johnson, R., Opoku, A.R. & Louw, J. 2013. Amelioration of palmitate-induced insulin resistance in C2C12 muscle cells by rooibos (*Aspalathus linearis*). *Phytomedicine*, 20(10):813-819.
- Mazué, G., Newman, A.J., Scampini, G., Torre, P.D., Hard, G.C., Iatropoulos, M.J., Williams, G.M. & Bagnasco, S.M. 1993. The histopathology of kidney changes in rats and monkeys following intravenous administration of massive doses of FCE 26184, human basic fibroblast growth factor. *Toxicologic Pathology*, 21(5):490-501.
- McKay, D.L. & Blumberg, J.B. 2007. A review of the bioactivity of South African herbal teas: rooibos (*Aspalathus linearis*) and honeybush (*Cyclopia intermedia*). *Phytotherapy Research*, 21(1):1-16.
- Meintjes, G., Moorhouse, M., Carmona, S., Davies, N., Dlamini, S., van Vuuren, C., Manzini, T., Mathe, M., Moosa, Y., Nash, J., Nel, J., Pakade, Y., Woods, J., van Zyl, G., Conradie, F & Venter, F. 2017. Antiretroviral Therapy Guidelines 2017, *South African Journal of HIV Medicine*, 18 (1): A776. Available: <https://doi.org/10.4102/sajhivmed.v18i1.776> [2017, May 7].
- Michalopoulos G.K. & DeFrances M.C. 1997. Liver regeneration. *Science*, 276(5309):60-66.
- Michels, J.E., Bauer, G.E., Johnson, D. & Dixit, P.K. 1986. Morphometric analysis of the endocrine cell composition of rat pancreas following treatment with streptozotocin and nicotinamide. *Experimental and Molecular Pathology*, 44(3):247-258.

- Minzi, O.M.S., Irunde, H. & Moshiro, C. 2009. HIV patients presenting common adverse drug events caused by highly active antiretroviral therapy in Tanzania. *Tanzania Journal of Health Research*, 11(1):5-10.
- Monforte, A.D.A., Lepri, A.C., Rezza, G., Pezzotti, P., Antinori, A., Phillips, A.N., Angarano, G., Colangeli, V., De Luca, A., Ippolito, G. & Caggese, L. 2000. Insights into the reasons for discontinuation of the first highly active antiretroviral therapy (HAART) regimen in a cohort of antiretroviral naive patients. *AIDS*, 14(5):499-507.
- Monforte, A.D.A., Testa, L., Adorni, F., Chiesa, E., Bini, T., Moscatelli, G.C., Abeli, C., Rusconi, S., Sollima, S., Balotta, C. & Musicco, M. 1998. Clinical outcome and predictive factors of failure of highly active antiretroviral therapy in antiretroviral-experienced patients in advanced stages of HIV-1 infection. *AIDS*, 12(13):1631-1637.
- Monsees, T.K. & Opuwari, C.S. 2017. Effect of rooibos (*Aspalathus linearis*) on the female rat reproductive tract and liver and kidney functions *in vivo*. *South African Journal of Botany*, 110:208-215.
- Morton, J.F. 1983. Rooibos tea, *Aspalathus linearis*, a caffeineless, low-tannin beverage. *Economic Botany*, 37(2):164-173.
- Mugavero, M.J, & Wellons, M.F. 2008. Emtricitabine. In Dolin, R., Masur, H. & Saag, M.S (eds) 2007. *AIDS Therapy*. Philadelphia: Churchill Livingstone.
- Muller, C.J., Malherbe, C.J., Chellan, N., Yagasaki, K., Miura, Y. & Joubert, E. 2016. Potential of Rooibos, its Major C-Glucosyl Flavonoids and Z-2-(β -D-Glucopyranoloxo)-3-phenylpropenoic acid in Prevention of Metabolic Syndrome. *Critical reviews in Food Science and Nutrition*, (just-accepted):00-00. DOI: 10.1080/10408398.2016.1157568
- Muller, C.J.F., Joubert, E., De Beer, D., Sanderson, M., Malherbe, C.J., Fey, S.J. & Louw, J. 2012. Acute assessment of an aspalathin-enriched green rooibos (*Aspalathus linearis*) extract with hypoglycemic potential. *Phytomedicine*, 20(1):32-39.
- Mutlib, A.E., Chen, H., Nemeth, G.A., Markwalder, J.A., Seitz, S.P., Gan, L.S. & Christ, D.D. 1999. Identification and characterization of efavirenz metabolites by liquid chromatography/mass spectrometry and high field NMR: species differences in the metabolism of efavirenz. *Drug Metabolism and Disposition*, 27(11):1319-1333.
- Naesens, L., Snoeck, R., Andrei, G., Balzarini, J., Neyts, J. & De Clercq, E. 1997. HPMPC (cidofovir), PMEA (adefovir) and related acyclic nucleoside phosphonate analogues: a review of their pharmacology and clinical potential in the treatment of viral infections. *Antiviral Chemistry and Chemotherapy*, 8(1):1-23.
- Nathwani, R.A., Pais, S., Reynolds, T.B. & Kaplowitz, N. 2005. Serum alanine aminotransferase in skeletal muscle diseases. *Hepatology*, 41(2):380-382.

- Nayak, N.C., Sathar, S.A., Mughal, S., Duttagupta, S., Mathur, M. & Chopra, P. 1996. The nature and significance of liver cell vacuolation following hepatocellular injury—an analysis based on observations on rats rendered tolerant to hepatotoxic damage. *Virchows Archiv*, 428(6):353-365.
- Neuman, M.G., Schneider, M., Nanau, R.M. & Parry, C. 2012. HIV-antiretroviral therapy induced liver, gastrointestinal, and pancreatic injury. *International Journal of Hepatology*, 2012:1-23.
- Núñez, M. 2006. Hepatotoxicity of antiretrovirals: Incidence, mechanisms and management. *Journal of Hepatology*, 44:132-139.
- O'Brien, M.E., Clark, R.A., Besch, C.L., Myers, L. & Kissinger, P. 2003. Patterns and correlates of discontinuation of the initial HAART regimen in an urban outpatient cohort. *Journal of Acquired Immune Deficiency Syndromes*, 34(4):407-414.
- Oliveira, N.M., Ferreira, F.A.Y., Yonamine, R.Y. & Chehter, E.Z. 2014. Antiretroviral drugs and acute pancreatitis in HIV/AIDS patients: is there any association? A literature review. *Einstein (Sao Paulo)*, 12(1):112-119.
- Opuwari, C.S. & Monsees, T.K. 2014. *In vivo* effects of *Aspalathus linearis* (rooibos) on male rat reproductive functions. *Andrologia*, 46(8):867-877.
- Ozer, J., Ratner, M., Shaw, M., Bailey, W. & Schomaker, S. 2008. The current state of serum biomarkers of hepatotoxicity. *Toxicology*, 245(3):194-205.
- Paff, M.T., Averett, D.R., Prus, K.L., Miller, W.H. & Nelson, D.J. 1994. Intracellular metabolism of (-)-and (+)-cis-5-fluoro-1-[2-(hydroxymethyl)-1, 3-oxathiolan-5-yl] cytosine in HepG2 derivative 2.2. 15 (subclone P5A) cells. *Antimicrobial Agents and Chemotherapy*, 38(6):1230-1238.
- Pantsi, W.G., Marnewick, J.L., Esterhuysen, A.J., Rautenbach, F. & Van Rooyen, J. 2011. Rooibos (*Aspalathus linearis*) offers cardiac protection against ischaemia/reperfusion in the isolated perfused rat heart. *Phytomedicine*, 18(14):1220-1228.
- Pérez-Elías, M.J., Moreno, A., Casado, J.L., Dronda, F., Antela, A., López, D., Quereda, C., Navas, E., Hermida, J.M., Del Sol, E. & Moreno, S. 2009. Observational study to evaluate clinical outcomes after first-line efavirenz-or lopinavir-ritonavir-based HAART in treatment-naive patients. *Journal of the International Association of Physicians in AIDS Care*, 8(5):308-313.
- Petrova, A. 2009. Modulation of ultraviolet light induced skin carcinogenesis by extracts of Rooibos and Honeybush using a mouse model: elucidating possible protective mechanisms. Unpublished Masters thesis. Cape Town: Cape Peninsula University of Technology.
- Pitocco, D., Tesaro, M., Alessandro, R., Ghirlanda, G. & Cardillo, C. 2013. Oxidative stress in diabetes: implications for vascular and other complications. *International Journal of Molecular Sciences*, 14(11):21525-21550.
- Pitt, J.J. 2009. Principles and applications of liquid chromatography-mass spectrometry in clinical biochemistry. *The Clinical Biochemist Reviews*, 30(1):19-34.

- Post, F.A., Moyle, G.J., Stellbrink, H.J., Domingo, P., Podzamczer, D., Fisher, M., Norden, A.G., Cavassini, M., Rieger, A., Khuong-Josses, M.A. & Branco, T. 2010. Randomized comparison of renal effects, efficacy, and safety with once-daily abacavir/lamivudine versus tenofovir/emtricitabine, administered with efavirenz, in antiretroviral-naive, HIV-1–infected adults: 48-week results from the ASSERT study. *Journal of Acquired Immune Deficiency Syndromes*, 55(1):49-57.
- Randhawa, P.S., Shapiro, R., Jordan, M.L., Starzl, T.E. & Demetris, A.J. 1993. The histopathological changes associated with allograft rejection and drug toxicity in renal transplant recipients maintained on FK506: clinical significance and comparison with cyclosporine. *The American Journal of Surgical Pathology*, 17(1):60-68.
- Rasch, R. & Dørup, J. 1997. Quantitative morphology of the rat kidney during diabetes mellitus and insulin treatment. *Diabetologia*, 40(7):802-809.
- Ray, A.S., Cihlar, T., Robinson, K.L., Tong, L., Vela, J.E., Fuller, M.D., Wieman, L.M., Eisenberg, E.J. & Rhodes, G.R. 2006. Mechanism of active renal tubular efflux of tenofovir. *Antimicrobial Agents and Chemotherapy*, 50(10):3297-3304.
- Renal corpuscle in kidney*, 2017. [Online]. Available: <https://www.klejonka.info/2017rimage-renal-corpuscle-in-kidney.awp>. [2017, August 20]
- Rudorf, D.C. & Krikorian, S.A. 2005. Adverse effects associated with antiretroviral therapy and potential management strategies. *Journal of Pharmacy Practice*, 18(4):258-277.
- Saag, M.S. 2008. Strategic Use of Antiretroviral Therapy. In Dolin, R., Masur, H. & Saag, M.S (eds) 2007. *AIDS Therapy*. Philadelphia: Churchill Livingstone.
- Sakuraba, H., Mizukami, H., Yagihashi, N., Wada, R., Hanyu, C. & Yagihashi, S. 2002. Reduced beta-cell mass and expression of oxidative stress-related DNA damage in the islet of Japanese Type II diabetic patients. *Diabetologia*, 45(1):85-96.
- Sanderson, M., Mazibuko, S.E., Joubert, E., de Beer, D., Johnson, R., Pheiffer, C., Louw, J. & Muller, C.J. 2014. Effects of fermented rooibos (*Aspalathus linearis*) on adipocyte differentiation. *Phytomedicine*, 21(2):109-117.
- Sanne, I. 2000. Severe liver toxicity in patients receiving two nucleoside analogues and a non-nucleoside reverse transcriptase inhibitor. *AIDS*, 12(5): A566.
- Sanne, I., Mommeja-Marin, H., Hinkle, J., Bartlett, J.A., Lederman, M.M., Maartens, G., Wakeford, C., Shaw, A., Quinn, J., Gish, R.G. & Rousseau, F. 2005. Severe hepatotoxicity associated with nevirapine use in HIV-infected subjects. *The Journal of Infectious Diseases*, 191(6):825-829.
- Sauter, W. 2005. Vergleich antioxidativer Eigenschaften von Extrakten aus *Camellia sinensis*, *Rosmarinus officinalis*, *Cyclopia genistoides*, *Cyclopia sessiliflora* und *Aspalathus linearis*. Unpublished doctoral dissertation, Technische Universität München, Universitätsbibliothek.
- Saxena, R. 2010. Special stains in interpretation of liver biopsies. *Connection*, 92-103.

- Schinazi, R.F., Boudinot, F.D., Ibrahim, S.S., Manning, C., McClure, H.M. & Liotta, D.C. 1992a. Pharmacokinetics and metabolism of racemic 2', 3'-dideoxy-5-fluoro-3'-thiacytidine in rhesus monkeys. *Antimicrobial Agents and Chemotherapy*, 36(11):2432-2438.
- Schinazi, R.F., McMillan, A., Cannon, D., Mathis, R., Lloyd, R.M., Peck, A., Sommadossi, J.P., St Clair, M., Wilson, J. & Furman, P.A. 1992b. Selective inhibition of human immunodeficiency viruses by racemates and enantiomers of cis-5-fluoro-1-[2-(hydroxymethyl)-1, 3-oxathiolan-5-yl] cytosine. *Antimicrobial Agents and Chemotherapy*, 36(11):2423-2431.
- Schloms, L., Storbeck, K.H., Swart, P., Gelderblom, W.C. & Swart, A.C. 2012. The influence of *Aspalathus linearis* (Rooibos) and dihydrochalcones on adrenal steroidogenesis: Quantification of steroid intermediates and end products in H295R cells. *The Journal of Steroid Biochemistry and Molecular Biology*, 128(3):128-138.
- Schmid, S., Opravil, M., Moddel, M., Huber, M., Pfammatter, R., Keusch, G., Ambuhl, P., Wuthrich, R.P., Moch, H. & Varga, Z. 2007. Acute interstitial nephritis of HIV-positive patients under atazanavir and tenofovir therapy in a retrospective analysis of kidney biopsies. *Virchows Archiv*, 450(6):665-670.
- Schouten, J.T., Krambrink, A., Ribaud, H.J., Kmack, A., Webb, N., Shikuma, C., Kuritzkes, D.R. & Gulick, R.M. 2010. Substitution of nevirapine because of efavirenz toxicity in AIDS clinical trials group A5095. *Clinical Infectious Diseases*, 50(5):787-791.
- Sedeek, M., Callera, G., Montezano, A., Gutsol, A., Heitz, F., Szyndralewicz, C., Page, P., Kennedy, C.R., Burns, K.D., Touyz, R.M. & Hebert, R.L. 2010. Critical role of Nox4-based NADPH oxidase in glucose-induced oxidative stress in the kidney: implications in type 2 diabetic nephropathy. *American Journal of Physiology-Renal Physiology*, 299(6):1348-1358.
- Shea, K., Stewart, S. & Rouse, R. 2014. Assessment standards: Comparing histopathology, digital image analysis, and stereology for early detection of experimental cisplatin-induced kidney injury in rats. *Toxicologic Pathology*, 42(6):1004-1015.
- Siest, G., Schiele, F., Galteau, M.M., Panek, E., Steinmetz, J., Fagnani, F. & Gueguen, R. 1975. Aspartate aminotransferase and alanine aminotransferase activities in plasma: statistical distributions, individual variations, and reference values. *Clinical Chemistry*, 21(8):1077-1087.
- Sinisalo, M., Enkovaara, A.L. & Kivistö, K.T. 2010. Possible hepatotoxic effect of rooibos tea: a case report. *European Journal of Clinical Pharmacology*, 66(4):427-428.
- Snijman, P.W., Joubert, E., Ferreira, D., Li, X.C., Ding, Y., Green, I.R. & Gelderblom, W.C. 2009. Antioxidant activity of the dihydrochalcones aspalathin and nothofagin and their corresponding flavones in relation to other rooibos (*Aspalathus linearis*) flavonoids, epigallocatechin gallate, and Trolox. *Journal of Agricultural and Food Chemistry*, 57(15):6678-6684.

- Snijman, P.W., Swanevelder, S., Joubert, E., Green, I.R. & Gelderblom, W.C. 2007. The antimutagenic activity of the major flavonoids of rooibos (*Aspalathus linearis*): Some dose–response effects on mutagen activation–flavonoid interactions. *Mutation Research/Genetic Toxicology and Environmental Mutagenesis*, 631(2):111-123.
- Son, M.J., Minakawa, M., Miura, Y. & Yagasaki, K. 2013. Aspalathin improves hyperglycemia and glucose intolerance in obese diabetic ob/ob mice. *European Journal of Nutrition*, 52(6):1607-1619.
- Soriano, V., Puoti, M., Garcia-Gasco, P., Rockstroh, J.K., Benhamou, Y., Barreiro, P. & McGovern, B. 2008. Antiretroviral drugs and liver injury. *AIDS*, 22(1):1-13.
- South African Rooibos Council. *n.d.* [Online] Available: <https://sarooibos.co.za/faq/#toggle-id-8>. [2017, March 25]
- Standley, L., Winterton, P., Marnewick, J.L., Gelderblom, W.C., Joubert, E. & Britz, T.J. 2001. Influence of processing stages on antimutagenic and antioxidant potentials of rooibos tea. *Journal of Agricultural and Food Chemistry*, 49(1):114-117.
- Staszewski, S. 2008. Efavirenz. In Dolin, R., Masur, H. & Saag, M.S (eds) 2007. *AIDS Therapy*. Philadelphia: Churchill Livingstone.
- Stein, J.H., Komarow, L., Cotter, B.R., Currier, J.S., Dubé, M.P., Fichtenbaum, C.J., Gerschenson, M., Mitchell, C.K., Murphy, R.L., Squires, K. & Parker, R.A. 2008. Lipoprotein changes in HIV-infected antiretroviral-naïve individuals after starting antiretroviral therapy: ACTG Study A5152s. *Journal of Clinical Lipidology*, 2(6):464-471.
- Steiner, D.J., Kim, A., Miller, K. & Hara, M. 2010. Pancreatic islet plasticity: interspecies comparison of islet architecture and composition. *Islets*, 2(3):135-145.
- Styrt, B.A., Piazza-Hepp, T.D. & Chikami, G.K. 1996. Clinical toxicity of antiretroviral nucleoside analogs. *Antiviral Research*, 31(3):121-135.
- Suckale, J. & Solimena, M. 2008. Pancreas islets in metabolic signaling-focus on the beta-cell. *Frontiers in Bioscience*, 13:7156-7171.
- Suckow, M.A., Weisbroth, S.H. & Franklin, C.L. (eds) 2005. *The Laboratory Rat*. 2nd Edition. Burlington: Academic Press.
- Sulkowski, M.S. 2004. Drug-induced liver injury associated with antiretroviral therapy that includes HIV-1 protease inhibitors. *Clinical Infectious Diseases*, 38 (2):90-97.
- Taniyama, H., Hirayama, K., Kagawa, Y., Ushiki, T., Kurosawa, T., Furuoka, H. & Ono, T. 1999. Immunohistochemical demonstration of bovine viral diarrhoea virus antigen in the pancreatic islet cells of cattle with insulin-dependent diabetes mellitus. *Journal of Comparative Pathology*, 121(2):149-157.
- Thapa, B.R. & Walia, A. 2007. Liver function tests and their interpretation. *Indian Journal of Pediatrics*, 74(7):663-671.

- Ulicna, O., Vancova, O., Bozek, P. & Carsky, J. 2006. Rooibos tea (*Aspalathus linearis*) partially prevents oxidative stress in streptozotocin-induced diabetic rats. *Physiological Research*, 55(2):157-164.
- Ulicna, O., Vancova, O., Waczulikova, I., Bozek, P., Janega, P., Babál, P., Liskova, S. & Greksák, M. 2008. Does rooibos tea (*Aspalathus linearis*) support regeneration of rat liver after intoxication by carbon tetrachloride? *General Physiology and Biophysics*, 27(3):179-186.
- United States Food and Drug Administration. *Antiretroviral drugs used in the treatment of HIV infection*. 2016. [Online]. Available: <https://www.fda.gov/forpatients/illness/hiv/aids/treatment/ucm118915.html>. [2016, March 15].
- Van Roey, P., Pangborn, W.A., Schinazi, R.F., Painter, G. & Liotta, D.C. 1993. Absolute Configuration of the Antiviral Agent (-)-cis-5-Fluoro-1-[2-Hydroxymethyl]-1, 3-Oxathiolan-5-yl] Cytosine. *Antiviral Chemistry and Chemotherapy*, 4(6):369-375.
- Villaño, D., Pecorari, M., Testa, M.F., Raguzzini, A., Stalmach, A., Crozier, A., Tubili, C. & Serafini, M. 2010. Unfermented and fermented rooibos teas (*Aspalathus linearis*) increase plasma total antioxidant capacity in healthy humans. *Food Chemistry*, 123(3):679-683.
- von Gadow, A., Joubert, E. & Hansmann, C.F. 1997. Comparison of the antioxidant activity of aspalathin with that of other plant phenols of rooibos tea (*Aspalathus linearis*), α -tocopherol, BHT, and BHA. *Journal of Agricultural and Food Chemistry*, 45(3):632-638.
- Vrouenraets, S.M., Fux, C.A., Wit, F.W., Garcia, E.F., Furrer, H., Brinkman, K., Hoek, F.J., Abeling, N.G., Krediet, R.T., Reiss, P. & Prepare Study Group, 2011. Persistent decline in estimated but not measured glomerular filtration rate on tenofovir may reflect tubular rather than glomerular toxicity. *AIDS*, 25(17):2149-2155.
- Wanjiku, S.M. 2009. Antioxidant status of South African beverages and its role on the chemical parameters in human blood. Unpublished Masters thesis. Cape Town: Cape Peninsula University of Technology.
- Wester, C.W., Thomas, A.M., Bussmann, H., Moyo, S., Makhema, J.M., Gaolathe, T., Novitsky, V. & Essex, M. 2010. Non-Nucleoside Reverse Transcriptase Inhibitor Outcomes Among cART-Treated Adults in Botswana. *AIDS (London, England)*, 24(1):27-36.
- Wieczorek, G., Pospischil, A. & Perentes, E. 1998. A comparative immunohistochemical study of pancreatic islets in laboratory animals (rats, dogs, mini-pigs, nonhuman primates). *Experimental and Toxicologic Pathology*, 50(3):151-172.
- Wilson, J.E., Martin, J.L., Borroto-Esoda, K., Hopkins, S., Painter, G., Liotta, D.C. & Furman, P.A. 1993. The 5'-triphosphates of the (-) and (+) enantiomers of cis-5-fluoro-1-[2-(hydroxymethyl)-1, 3-oxathiolane-5-yl] cytosine equally inhibit human immunodeficiency virus type 1 reverse transcriptase. *Antimicrobial Agents and Chemotherapy*, 37(8):1720-1722.

- Winston, J.A., Burns, G.C. & Klotman, P.E. 1998. The human immunodeficiency virus (HIV) epidemic and HIV-associated nephropathy. *In Seminars in Nephrology*, 18(4):373-377.
- Wisse, E., Braet, F., Luo, D., De Zanger, R., Jans, D., Crabbe, E. & Vermoesen, A.N. 1996. Structure and function of sinusoidal lining cells in the liver. *Toxicologic Pathology*, 24(1):100-111.
- Wit, F.W., Weverling, G.J., Weel, J., Jurriaans, S. & Lange, J.M. 2002. Incidence of and risk factors for severe hepatotoxicity associated with antiretroviral combination therapy. *The Journal of Infectious Diseases*, 186(1):23-31.
- World Health Organization. 2007. Joint United Nations Programme on HIV/AIDS and World Health Organization. AIDS epidemic update, December 2006.
- Yoldas, A. & Dayan, M.O. 2014. Morphological characteristics of renal artery and kidney in rats. *The Scientific World Journal*, 2014:1-7.
- Yoshikawa, T., Naito, Y., Oyamada, H., Ueda, S., Tanigawa, T., Takemura, T., Sugino, S. & Kondo, M. 1990. Scavenging effects of *Aspalathus linearis* (Rooibos tea) on active oxygen species. In Emerit, I., Packer, L & Auclair, C (eds). *Antioxidants in Therapy and Preventive Medicine* (171-174). New York: Springer US.
- Young, B., Lowe, J.S., Stevens, A. & Heath, J.W. 2006. Wheater's Functional Histology, 5th Ed. Glasgow: Churchill Livingstone.
- Young, S.D., Britcher, S.F., Tran, L.O., Payne, L.S., Lumma, W.C., Lyle, T.A., Huff, J.R., Anderson, P.S., Olsen, D.B. & Carroll, S.S. 1995. L-743, 726 (DMP-266): a novel, highly potent nonnucleoside inhibitor of the human immunodeficiency virus type 1 reverse transcriptase. *Antimicrobial Agents and Chemotherapy*, 39(12):2602-2605.
- Zacharia, C.C. & Whitlatch, H. 2013. Rooibos Herbal Tea Linked to Hepatotoxicity and Severe Hypercholesterolemia. In *Lipids: Therapeutics and Case Reports*. San Francisco: Endocrine Society (SUN-730).
- Zhang, X.P., Zhang, J., Ma, M.L., Cai, Y., Xu, R.J., Xie, Q., Jiang, X.G. & Ye, Q. 2010. Pathological changes at early stage of multiple organ injury in a rat model of severe acute pancreatitis. *Hepatobiliary and Pancreatic Diseases International*, 9(1):83-87.
- Zimmerman, H.J (ed). 1999. *Hepatotoxicity: The Adverse Effects of Drugs and Other Chemicals on The Liver*. Philadelphia: Lippincott Williams & Wilkins.

APPENDICES

Appendix A: Outputs and awards arising from this study

45th Annual Conference of the Anatomical Society of Southern Africa (ASSA), 23-26 April 2017, Langebaan, Western Cape: Pereira, D.L., Imperial, E., Webster, I., Strijdom, H., Widd, I., Chellan, N & Kotzé, S.H. 2017. The phenolic viability of rooibos teas (*Aspalathus linearis*) in research.

Stellenbosch University, Department of Biomedical Sciences Annual Research day 23-November 2016, Tygerberg, Cape Town: Pereira, D.L., Imperial, A., Webster, I., Wiid, I., Chellan, N & Kotzé, S.H. 2016. The viability of the antioxidant properties of rooibos tea under varying storage conditions.

WhiteSci (Whitehead scientific) Best poster presentation 2016: Stellenbosch University, Department of Biomedical Sciences Annual Research day 23 November 2016, Tygerberg, Cape Town: Pereira, D.L., Imperial, A., Webster, I., Wiid, I., Chellan, N & Kotzé, S.H. 2016. The viability of the antioxidant properties of rooibos tea under varying storage conditions.

Appendix B: List of materials**Table 1: List of materials**

Materials	Company
Odimune	<i>Cipla Medpro</i> (Pty) Ltd. Bellville. Western Cape
Sodium Pentobarbitone	Eutha-naze [®] . <i>Bayer</i> (Pty). Ltd. Isando. Gauteng
Standard breeders feed	<i>Nutritionhub</i> (Pty) Ltd, Stellenbosch, South Africa
Tools used for harvesting	
BD red vacationer 1 mL	The Scientific Group (Pty) Ltd. (Milnerton, Western Cape, RSA)
Blue top collection tubes	-
Gloves	-
Plastic Eppendorf tubes 1 mL	-
Scalpel	-
Material for tea preparation	
Aluminium foil	-
Cheese cloth	-
Dried Rooibos leaves	<i>Carmien tea company</i> (Pty) Ltd Brakfontein South Africa
In virtis cryogenic flasks	-
Liquid Nitrogen	-
Protection gloves	Avacare (Pty) Ltd Thailand
Vacuum	Vacutec, Labconco Cat: 7753030
Whatman No. 4 filter paper	-
Whatman No.1 filter paper	-
Material used for histology	
Cover slips (24 x 32 mm)	-
Cover slips (24 x 50 mm)	-
Double frosted glass microscope slides	Kimix, Cat: 7107
Embedding cassettes	SPL Lifesciences (Pty) Ltd Cas: 400600
Low profile microtome blades	Leica microsystems (Pty) Ltd, Germany
Paraffin wax (Embedding wax)	Leica Microsystems (Pty) Ltd Cat: 39602012
Plastic specimen jaws	SPL Lifesciences(Pty) Ltd Cas: 400600
Positively charged microscope slides	Sigma-Aldrich (Pty) Ltd Cat no: S001
Reagents used	
10% Formaldehyde	SigmaAldrich (Pty) Ltd Cat: 47608
5% Paraformaldehyde	Sigma-Aldrich (Pty) Ltd Cat: P6148-1KG
Acid Fuschin	Sigma-Aldrich(Pty) Ltd
AP Enzyme G/2 system AP Rabbit/mouse link (Enhancer)	K5355, <i>Dako</i> , Denmark, Inc
Dako Envision Kit	K5355, <i>Dako</i> , Denmark, Inc
Dako Liquid DAB +Chromogen	K5355, <i>Dako</i> , North America, Inc
DPX mounting media	Associated Chemical Enterprises Batch: 30773
Eosin Yellowish	SAAR218600DC, Merck Chemicals (Pty) Ltd., Gauteng, South Africa
Ethanol 99%	Sigma-Aldrich Cas: 64-17-5
Ferrous sulphate	Sigma-Aldrich Cas: 127-03-55
Glacial Acetic acid	Sigma-Aldrich Cas: 10005706
Hydrogen Peroxide	Merck (Pty) Ltd, Modderfontein, Gauteng
Mayer's Haematoxylin	SAAR282201LC; Merck Chemicals (Pty), Ltd Gauteng
Monoclonal Anti-insulin	K5355, <i>Dako</i> , North America, Inc
Normal Goat Serum	-
Normal Horse Serum	-
Orange G	Sigma-Aldrich Cas: 1936-15-8
Oxalic acid	BDH Chemical Ltd Cat: 10174
Phosphate Buffer solution	Sigma-Aldrich Cas: P5358

Table 1: List of materials continued.

Periodic acid	Sigma-Aldrich Cas: P7875
Permanent red chromogen substrate working solution	K5355, <i>Dako</i> , Denmark, Inc
Phosphotungstic acid	Sigma-Aldrich Cas: P4006
Polyclonal Anti-glucagon	K5355, <i>Dako</i> , North America, Inc
Ponceau de xylydine	Sigma-Aldrich P2395
Potassium permanganate	BDH Chemicals, Cat: 10217
Rabbit/mouse Link	K5355, <i>Dako</i> , Denmark, Inc
Schiff Reagent	Science World Batch: 08-01-127
Silver nitrate	Merch chemicals Pty, Ltd Cat: 576 50 40 DC
Sodium hydroxide	Sigma-Aldrich Cas:S 8045
Strong ammonia (25%)	Merck Chemicals, Pty Ltd Wadeville, Gauteng
Sulfuric acid	Sigma-Aldrich Cas: 339741
Tris Buffer solution	Sigma-Aldrich Cas: T5912
Vector Laboratories ABC Kit	VectorLaboratories Ak-5010
Vector Laboratories Biotinylated	VectorLaboratories Ak-5010
Goat Anti-Rabbit IgG	
Xylene	Sigma-Aldrich Cas: 214736
Equipment used	
Biofuge Pico Centrifuge	(<i>Heraeus</i> . Kendro Laboratory products. Germany
Embedding table	Leica EG 116 Embedder (SMM <i>instruments</i> . Johannesburg
Incubator	Model IH-150; Gallenkamp
Leica Autostainer XL	Leica ST 5010; Serial number 1732/02.2007
Leica RM 2125 RT microtome	Cat no. 045737989, SMM <i>instruments</i> , Gremnay
Lobotec Vacuum	Labcoco TM (<i>Vacutec</i> . Roseveld park. South Africa
Microscope camera	(Nikon Digital Sight DS-Fic. <i>Nikon corporation</i> . Japan)
Nikon Eclipse Ti Automated scanning microscope	(<i>Nikon Instruments Inc</i> . Walt Whitman Road Melville. New York)
Oven	(Model: M53C. serial number 9513249
Processor	Shandon Elliot Duplex Processor <i>OptoLaboratory</i> . Cape Town
Software used	
Leica Qwin professional software	Leica Microsystems. United Kingdom
Nikon NIS Imaging Software v4.40	<i>Nikon Instruments Inc</i> . Copyright 1991-2015
Statistica Version 13.2	Dell. 2014. USA
Zen10 software	Carl Zeiss Microscopy. Oberkochen

Appendix C: Odimune dose calculations (Imperial, 2017).

Active ingredients

Table 2: Active ingredients in one Odimune[®] tablet.

Drug	Active content	Dose given to rats
Efavirenz (EFV)	600 mg	51.0 mg/kg/day
Emtricitabine (FTC)	200 mg	7.4 mg/kg/day
Tenofovir (TDF)	300 mg	28.8 mg/kg/day

Dose calculation for average 70 kg mature human

Let EFV 600 mg= X

Therefore, human dose (X_H) in mg/kg/day= X/70 kg X_H of Efavirenz = 600 mg/70 kg= 8.6 mg/kg/day X_H of Emtricitabine= 200 mg/70 kg= 2.9 mg/kg/day X_H of Tenofovir= 300 mg/70 kg= 4.3 mg/kg/day**Human to rodent conversion**Rodent dose (X_{R1}) = $X_H * 6$

Therefore:

 X_{R1} of Efavirenz = 8.6 * 6= 51 mg/kg/ day X_{R1} of Emtricitabine= 2.9*6= 17.4 mg/kg/day X_{R1} of Tenofovir= 4.3* 6= 25.8 mg/kg/day**Dosage calculation for average rat weighing 250g** X_{R2} of Efavirenz= ($X_{R1} * 0.250$) = 12.9* 0.25= 12.9 X_{R2} of Emtricitabine= 2.9*0.25= 4.35 mg X_{R2} of Tenofovir=25.8 mg* 0.25= 6.45 mg**To determine the weight per tablet per rat**

Weigh the Tablet

Take the human dose (X)/ specific dose of the rat (X_{R2})E.g. for Efavirenz: 600 mg dose/12.9 mg rat dose= 46.51= X_{R3}

Crush tablet with a pestle and mortar until a fine powder is formed

Therefore, the amount of crushed tablet to be dissolved per 1mL of water for Efavirenz= to the weight of the crushed Tablet/ X_{r3} .

Preparation of the drug water mixtures

For a four-day preparation of an entire cage. first determine the average weight of the rats per cage. Therefore. if the average body weight of the animals per cage after crushing is 352 g then the 352 g is first covert to kg therefore = 0.352 kg:

Weight of the tablet after crushing= 1.6 g (1600 mg)

Active ingredients (AI)= 600 mg+200 mg+300 mg=1100 mg

Actual percentage of the AI= 1100/1600= 67.75%

Average weight of the rats in cage= 352 (0.352 kg)

Average weight of rats in cage= 352 g (0.352 kg)

The dose per rat

= EFV: 51.6 mg * 0.352mg =18.163 mg

= EMT: 17.4 mg * 0.352 mg= 9.082 mg

= EFV:600/18.16= (33*68%)/100= y

=FTC: 200/6.125= (33*68%)/100= y

=TDF: 300/9.082= (33*68%)/100= y

Final dose of the tablet per rat: weight of the tablet (X)/Y

EFV= 1600 mg/22.78=70.22 mg

Powder of tablet in 1 mL water= 0.07 g

For a 4-day preparation with 5 rats in a cage= 4*5 = 20 mL water

Therefore. the final dose = 0.070* 20/= 1.40 g/20 mL water.

Appendix D: Blood transaminase methods (NHLS)

0020764957322c501V11.0

ALTL**cobas**[®]

Alanine Aminotransferase acc. to IFCC without pyridoxal phosphate activation

Order information

REF	CONTENT	Analyzer(s) on which cobas c pack(s) can be used
20764957 322	Alanine Aminotransferase acc. to IFCC 500 tests	System-ID 07 6495 7 Roche/Hitachi cobas c 311, cobas c 501/502
10759350 190	Calibrator f.a.s. (12 x 3 mL)	Code 401
10759350 360	Calibrator f.a.s. (12 x 3 mL, for USA)	Code 401
12149435 122	Precinorm U plus (10 x 3 mL)	Code 300
12149435 160	Precinorm U plus (10 x 3 mL, for USA)	Code 300
12149443 122	Precipath U plus (10 x 3 mL)	Code 301
12149443 160	Precipath U plus (10 x 3 mL, for USA)	Code 301
10171743 122	Precinorm U (20 x 5 mL)	Code 300
10171778 122	Precipath U (20 x 5 mL)	Code 301
10171760 122	Precipath U (4 x 5 mL)	Code 301
05117003 190	PreciControl ClinChem Multi 1 (20 x 5 mL)	Code 391
05947626 190	PreciControl ClinChem Multi 1 (4 x 5 mL)	Code 391
05947626 160	PreciControl ClinChem Multi 1 (4 x 5 mL, for USA)	Code 391
05117216 190	PreciControl ClinChem Multi 2 (20 x 5 mL)	Code 392
05947774 190	PreciControl ClinChem Multi 2 (4 x 5 mL)	Code 392
05947774 160	PreciControl ClinChem Multi 2 (4 x 5 mL, for USA)	Code 392
04489357 190	Diluent NaCl 9 % (50 mL)	System-ID 07 6869 3

English

System information

For **cobas c** 311/501 analyzers:**ALTL**: ACN 685For **cobas c** 502 analyzer:**ALTL**: ACN 8685

Intended use

In vitro test for the quantitative determination of alanine aminotransferase (ALT) in human serum and plasma on Roche/Hitachi **cobas c** systems.Summary^{1,2}

The enzyme alanine aminotransferase (ALT) has been widely reported as present in a variety of tissues. The major source of ALT is the liver, which has led to the measurement of ALT activity for the diagnosis of hepatic diseases. Elevated serum ALT is found in hepatitis, cirrhosis, obstructive jaundice, carcinoma of the liver, and chronic alcohol abuse. ALT is only slightly elevated in patients who have an uncomplicated myocardial infarction.

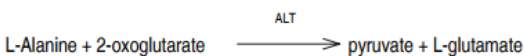
Although both serum aspartate aminotransferase (AST) and ALT become elevated whenever disease processes affect liver cell integrity, ALT is the more liver-specific enzyme. Moreover, elevations of ALT activity persist longer than elevations of AST activity.

In patients with vitamin B₆ deficiency, serum aminotransferase activity may be decreased. The apparent reduction in aminotransferase activity may be related to decreased pyridoxal phosphate, the prosthetic group for aminotransferases, resulting in an increase in the ratio of apoenzyme to holoenzyme.

Test principle

This assay follows the recommendations of the IFCC, but was optimized for performance and stability.^{3,4}

ALT catalyzes the reaction between L-alanine and 2-oxoglutarate. The pyruvate formed is reduced by NADH in a reaction catalyzed by lactate dehydrogenase (LDH) to form L-lactate and NAD⁺.



The rate of the NADH oxidation is directly proportional to the catalytic ALT activity. It is determined by measuring the decrease in absorbance.

Reagents - working solutions

R1 TRIS buffer: 224 mmol/L, pH 7.3 (37 °C); L-alanine: 1120 mmol/L; albumin (bovine): 0.25 %; LDH (microorganisms): ≥ 45 µkat/L; stabilizers; preservative

R2 2-Oxoglutarate: 94 mmol/L; NADH: ≥ 1.7 mmol/L; additives; preservative

R1 is in position B and R2 is in position C.

Precautions and warnings

For in vitro diagnostic use.

Exercise the normal precautions required for handling all laboratory reagents.

Disposal of all waste material should be in accordance with local guidelines. Safety data sheet available for professional user on request.

Reagent handling

Ready for use

Storage and stability

ALTL

Shelf life at 2-8 °C: See expiration date on **cobas c** pack label.

On-board in use and refrigerated on the analyzer: 12 weeks

Diluent NaCl 9 %

Shelf life at 2-8 °C: See expiration date on **cobas c** pack label.

On-board in use and refrigerated on the analyzer: 12 weeks

Specimen collection and preparation

For specimen collection and preparation only use suitable tubes or collection containers.

Only the specimens listed below were tested and found acceptable.

– Serum (free from hemolysis).

– Plasma (free from hemolysis): Li-heparin and K₂-EDTA plasma.

The sample types listed were tested with a selection of sample collection tubes that were commercially available at the time of testing, i.e. not all available tubes of all manufacturers were tested. Sample collection systems from various manufacturers may contain differing materials which could affect the test results in some cases. When processing samples in primary

tubes (sample collection systems), follow the instructions of the tube manufacturer.
Separate the serum or plasma from the clot or cells promptly.
Centrifuge samples containing precipitates before performing the assay.

Stability: 3 days at 15-25 °C^{5,6}
7 days at 2-8 °C^{5,6}
> 7 days at (-60)-(-80) °C⁶

Materials provided

See "Reagents – working solutions" section for reagents.

Materials required (but not provided)

- See "Order information" section
- General laboratory equipment

Assay

For optimum performance of the assay follow the directions given in this document for the analyzer concerned. Refer to the appropriate operator's manual for analyzer-specific assay instructions.

The performance of applications not validated by Roche is not warranted and must be defined by the user.

Application for serum and plasma

cobas c 311 test definition

Assay type	Rate A		
Reaction time / Assay points	10 / 12-31		
Wavelength (sub/main)	700/340 nm		
Reaction direction	Decrease		
Units	U/L (µkat/L)		
Reagent pipetting	Diluent (H ₂ O)		
R1	59 µL	32 µL	
R2	17 µL	20 µL	
Sample volumes	Sample	Sample dilution	
		Sample	Diluent (NaCl)
Normal	9 µL	–	–
Decreased	9 µL	15 µL	135 µL
Increased	9 µL	–	–

cobas c 501 test definition

Assay type	Rate A		
Reaction time / Assay points	10 / 18-46		
Wavelength (sub/main)	700/340 nm		
Reaction direction	Decrease		
Units	U/L (µkat/L)		
Reagent pipetting	Diluent (H ₂ O)		
R1	59 µL	32 µL	
R2	17 µL	20 µL	
Sample volumes	Sample	Sample dilution	
		Sample	Diluent (NaCl)
Normal	9 µL	–	–
Decreased	9 µL	15 µL	135 µL
Increased	9 µL	–	–

cobas c 502 test definition

Assay type	Rate A
Reaction time / Assay points	10 / 18-46

Wavelength (sub/main)	700/340 nm		
Reaction direction	Decrease		
Units	U/L (µkat/L)		
Reagent pipetting	Diluent (H ₂ O)		
R1	59 µL	32 µL	
R2	17 µL	20 µL	
Sample volumes	Sample	Sample dilution	
		Sample	Diluent (NaCl)
Normal	9 µL	–	–
Decreased	9 µL	15 µL	135 µL
Increased	18 µL	–	–

Calibration

Calibrators	S1: H ₂ O S2: C.f.a.s.
Calibration mode	Linear
Calibration frequency	2-point calibration - after reagent lot change - as required following quality control procedures

Traceability: This method has been standardized against the original IFCC formulation, but without Pyp, using calibrated pipettes together with a manual photometer providing absolute values and the substrate-specific absorptivity, ϵ .⁷

Quality control

For quality control, use control materials as listed in the "Order information" section.

In addition, other suitable control material can be used.

The control intervals and limits should be adapted to each laboratory's individual requirements. Values obtained should fall within the defined limits. Each laboratory should establish corrective measures to be taken if values fall outside the defined limits.

Follow the applicable government regulations and local guidelines for quality control.

Calculation

Roche/Hitachi **cobas c** systems automatically calculate the analyte activity of each sample.

Conversion factor: U/L x 0.0167 = µkat/L

Limitations - interference

Criterion: Recovery within $\pm 10\%$ of initial value at an ALT activity of 30 U/L (0.5 µkat/L).

Icterus:⁸ No significant interference up to an I index of 60 for conjugated and unconjugated bilirubin (approximate conjugated and unconjugated bilirubin concentration: 1026 µmol/L or 60 mg/dL).

Hemolysis:⁸ No significant interference up to an H index of 90 (approximate hemoglobin concentration: 56 µmol/L or 90 mg/dL).

Contamination with erythrocytes will elevate results, because the analyte level in erythrocytes is higher than in normal sera. The level of interference may be variable depending on the content of analyte in the lysed erythrocytes.

Lipemia (Intralipid):⁹ No significant interference up to an L index of 150. There is poor correlation between the L index (corresponds to turbidity) and triglycerides concentration.

Lipemic samples may cause > Abs flagging. Choose diluted sample treatment for automatic rerun.

Drugs: No interference was found at therapeutic concentrations using common drug panels.^{9,10} Exceptions: Physiological plasma concentrations of Sulfasalazine and Sulfapyridine may lead to false results.

Calcium dobesilate and Isoniazid can cause artificially low and Furosemide artificially high ALT results at therapeutic concentrations.

Cyanokit (Hydroxocobalamin) may cause interference with results.

In very rare cases, gammopathy, in particular type IgM (Waldenström's macroglobulinemia), may cause unreliable results.¹¹

For diagnostic purposes, the results should always be assessed in conjunction with the patient's medical history, clinical examination and other findings.

ACTION REQUIRED

Special Wash Programming: The use of special wash steps is mandatory when certain test combinations are run together on Roche/Hitachi **cobas c** systems. The latest version of the carry-over evasion list can be found with the NaOHD/SMS/Multiclean/SCCS or the NaOHD/SMS/SmpCln1+2/SCCS Method Sheets. For further instructions refer to the operator's manual. **cobas c** 502 analyzer: All special wash programming necessary for avoiding carry-over is available via the **cobas** link, manual input is not required.

Where required, special wash/carry-over evasion programming must be implemented prior to reporting results with this test.

Limits and ranges

Measuring range

5-700 U/L (0.08-11.7 μ kat/L)

Determine samples having higher activities via the rerun function. Dilution of samples via the rerun function is a 1:10 dilution. Results from samples diluted using the rerun function are automatically multiplied by a factor of 10.

Lower limits of measurement

Lower detection limit of the test

5 U/L (0.08 μ kat/L)

The lower detection limit represents the lowest measurable analyte level that can be distinguished from zero. It is calculated as the value lying 3 standard deviations above that of the lowest standard (standard 1 + 3 SD, repeatability, $n = 21$).

Expected values¹²

Acc. to the optimized standard method (comparable to the IFCC method without pyridoxal phosphate activation¹³):

Males up to 41 U/L (up to 0.68 μ kat/L)

Females up to 33 U/L (up to 0.55 μ kat/L)

Calculated values: A factor of 1.85 is used for the conversion from 25 °C to

37 °C.¹⁴

Each laboratory should investigate the transferability of the expected values to its own patient population and if necessary determine its own reference ranges.

Specific performance data

Representative performance data on the analyzers are given below. Results obtained in individual laboratories may differ.

Precision

Precision was determined using human samples and controls in an internal protocol with repeatability ($n = 21$) and intermediate precision (3 aliquots per run, 1 run per day, 20 days).

The following results were obtained:

Repeatability	Mean	SD	CV
	U/L (μ kat/L)	U/L (μ kat/L)	%
Precinorm U	39.5 (0.660)	0.3 (0.005)	0.6
Precipath U	120 (2.00)	0 (0.00)	0.4
Human serum 1	113 (1.89)	0.5 (0.01)	0.4
Human serum 2	7.2 (0.120)	0.7 (0.012)	9.3
Intermediate precision	Mean	SD	CV
	U/L (μ kat/L)	U/L (μ kat/L)	%
Precinorm U	39.3 (0.656)	0.6 (0.010)	1.4
Precipath U	120 (2.00)	1 (0.02)	1.0
Human serum 3	24.0 (0.401)	0.6 (0.010)	2.6

Human serum 4 98.1 (1.64) 3.2 (0.05) 3.3

Method comparison

ALT values for human serum and plasma samples obtained on a Roche/Hitachi **cobas c** 501 analyzer (y) were compared with those determined using the corresponding reagent on a Roche/Hitachi 917 analyzer (x).

Sample size (n) = 198

Passing/Bablok ¹⁵	Linear regression
$y = 1.000x - 0.292$ U/L	$y = 0.997x - 1.05$ U/L
$\tau = 0.924$	$r = 0.996$

The sample activities were between 4.60 and 383 U/L (0.077 and 6.40 μ kat/L).


References

- Sherwin JE. Liver function. In: Kaplan LA, Pesce AJ, eds. Clinical Chemistry, theory, analysis, and correlation. St. Louis: Mosby 1984;420-438.
- Moss DW, Henderson AR, Kachmar JF. Enzymes. In: Tietz NW, ed. Fundamentals of Clinical Chemistry, 3rd ed. Philadelphia, PA: WB Saunders 1987;346-421.
- Bergmeyer HU, Hørdler M, Rej R. Approved recommendation (1985) on IFCC methods for the measurement of catalytic concentration of enzymes. Part 3. IFCC method for alanine aminotransferase. J Clin Chem Clin Biochem 1986;24:481-495.
- ECCLS. Determination of the catalytic activity concentration in serum of L-alanine aminotransferase (EC 2.6.1.2, ALAT). Klin Chem Mitt 1989;20:204-211.
- Heins M, Heil W, Withold W. Storage of Serum or Whole Blood Samples? Effect of Time and Temperature on 22 Serum Analytes. Eur J Clin Chem Clin Biochem 1995;33:231-238.
- Data on file at Roche Diagnostics.
- Schumann G, Bonora R, Ceriotti F, et al. IFCC Primary Reference Procedures for the Measurement of Catalytic Activity Concentrations of Enzymes at 37 °C – Part 4. Reference Procedure for the Measurement of Catalytic Activity Concentration of Alanine Aminotransferase. Clin Chem Lab Med 2002;40(7):718-724.
- Glick MR, Ryder KW, Jackson SA. Graphical Comparisons of Interferences in Clinical Chemistry Instrumentation. Clin Chem 1986;32:470-475.
- Breuer J. Report on the Symposium "Drug effects in Clinical Chemistry Methods". Eur J Clin Chem Clin Biochem 1996;34:385-386.
- Sonntag O, Scholer A. Drug interference in clinical chemistry: recommendation of drugs and their concentrations to be used in drug interference studies. Ann Clin Biochem 2001;38:376-385.
- Bakker AJ, Mücke M. Gammopathy interference in clinical chemistry assays: mechanisms, detection and prevention. Clin Chem Lab Med 2007;45(9):1240-1243.
- Thefeld W, Hoffmeister H, Busch EW, et al. Referenzwerte für die Bestimmungen der Transaminasen GOT und GPT sowie der alkalischen Phosphatase im Serum mit optimierten Standardmethoden. Dtsch Med Wschr 1974;99(8):343-351.
- Klein G, Lehmann P, Michel E, et al. Vergleich der IFCC-Methoden für ALAT, ASAT und GGT bei 37 °C mit den eingeführten Standardmethoden bei 25 °C und 37 °C. Lab Med 1994;18:403-404.
- Zawta B, Klein G, Bablok W. Temperaturumrechnung in der klinischen Enzymologie? Klin Lab 1994;40:23-32.
- Bablok W, Passing H, Bender R, et al. A general regression procedure for method comparison studies in clinical chemistry, Part III. J Clin Chem Clin Biochem 1988 Nov;26(11):783-790.

A point (period/stop) is always used in this Method Sheet as the decimal separator to mark the border between the integral and the fractional parts of a decimal numeral. Separators for thousands are not used.

Symbols

Roche Diagnostics uses the following symbols and signs in addition to those listed in the ISO 15223-1 standard.

	Contents of kit
	Volume after reconstitution or mixing

FOR US CUSTOMERS ONLY: LIMITED WARRANTY

Roche Diagnostics warrants that this product will meet the specifications stated in the labeling when used in accordance with such labeling and will be free from defects in material and workmanship until the expiration date printed on the label. THIS LIMITED WARRANTY IS IN LIEU OF ANY OTHER WARRANTY, EXPRESS OR IMPLIED, INCLUDING ANY IMPLIED WARRANTY OF MERCHANTABILITY OR FITNESS FOR PARTICULAR PURPOSE. IN NO EVENT SHALL ROCHE DIAGNOSTICS BE LIABLE FOR INCIDENTAL, INDIRECT, SPECIAL OR CONSEQUENTIAL DAMAGES.

COBAS, COBAS C, PRECINORM, PRECIPATH and PRECICONTROL are trademarks of Roche.

All other product names and trademarks are the property of their respective owners.

Significant additions or changes are indicated by a change bar in the margin.

© 2014, Roche Diagnostics



Roche Diagnostics GmbH, Sandhofer Strasse 116, D-68305 Mannheim
www.roche.com

Distribution in USA by:
Roche Diagnostics, Indianapolis, IN
US Customer Technical Support 1-800-428-2336



ASTL**cobas**[®]

Aspartate Aminotransferase acc. to IFCC without pyridoxal phosphate activation

Order information

REF	CONTENT	Analyzer(s) on which cobas c pack(s) can be used
20764949 322	Aspartate Aminotransferase acc. to IFCC 500 tests	System-ID 07 6494 9 Roche/Hitachi cobas c 311 , cobas c 501/502
10759350 190	Calibrator f.a.s. (12 x 3 mL)	Code 401
10759350 360	Calibrator f.a.s. (12 x 3 mL, for USA)	Code 401
12149435 122	Precinorm U plus (10 x 3 mL)	Code 300
12149435 160	Precinorm U plus (10 x 3 mL, for USA)	Code 300
12149443 122	Precipath U plus (10 x 3 mL)	Code 301
12149443 160	Precipath U plus (10 x 3 mL, for USA)	Code 301
10171743 122	Precinorm U (20 x 5 mL)	Code 300
10171778 122	Precipath U (20 x 5 mL)	Code 301
10171760 122	Precipath U (4 x 5 mL)	Code 301
05117003 190	PreciControl ClinChem Multi 1 (20 x 5 mL)	Code 391
05947626 190	PreciControl ClinChem Multi 1 (4 x 5 mL)	Code 391
05947626 160	PreciControl ClinChem Multi 1 (4 x 5 mL, for USA)	Code 391
05117216 190	PreciControl ClinChem Multi 2 (20 x 5 mL)	Code 392
05947774 190	PreciControl ClinChem Multi 2 (4 x 5 mL)	Code 392
05947774 160	PreciControl ClinChem Multi 2 (4 x 5 mL, for USA)	Code 392
04489357 190	Diluent NaCl 9 % (50 mL)	System-ID 07 6869 3

English

System information

For **cobas c 311/501** analyzers:

ASTL: ACN 687

SASTL: ACN 587 (STAT, reaction time: 7)

For **cobas c 502** analyzer:

ASTL: ACN 8687

SASTL: ACN 8587 (STAT, reaction time: 7)

Intended use

In vitro test for the quantitative determination of aspartate aminotransferase (AST) in human serum and plasma on Roche/Hitachi **cobas c** systems.Summary^{1,2}

The enzyme aspartate aminotransferase (AST) is widely distributed in tissue, principally hepatic, cardiac, muscle, and kidney. Elevated serum levels are found in diseases involving these tissues. Hepatobiliary diseases, such as cirrhosis, metastatic carcinoma, and viral hepatitis also increase serum AST levels. Following myocardial infarction, serum AST is elevated and reaches a peak 2 days after onset.

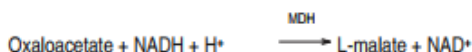
In patients undergoing renal dialysis or those with vitamin B₆ deficiency, serum AST may be decreased. The apparent reduction in AST may be related to decreased pyridoxal phosphate, the prosthetic group for AST, resulting in an increase in the ratio of apoenzyme to holoenzyme.

2 isoenzymes of AST have been detected, cytoplasmic and mitochondrial. Only the cytoplasmic isoenzyme occurs in normal serum, while the mitochondrial, together with the cytoplasmic isoenzyme, has been detected in the serum of patients with coronary and hepatobiliary disease.

Test principle

This assay follows the recommendations of the IFCC, but was optimized for performance and stability.^{3,4}

AST in the sample catalyzes the transfer of an amino group between L-aspartate and 2-oxoglutarate to form oxaloacetate and L-glutamate. The oxaloacetate then reacts with NADH, in the presence of malate dehydrogenase (MDH), to form NAD⁺.



The rate of the NADH oxidation is directly proportional to the catalytic AST activity. It is determined by measuring the decrease in absorbance.

Reagents - working solutions

- R1** TRIS buffer: 264 mmol/L, pH 7.8 (37 °C); L-aspartate: 792 mmol/L; MDH (microorganism): ≥ 24 μkat/L; LDH (microorganisms): ≥ 48 μkat/L; albumin (bovine): 0.25 %; preservative
- R2** NADH: ≥ 1.7 mmol/L; 2-oxoglutarate: 94 mmol/L; preservative

Precautions and warnings

For in vitro diagnostic use.

Exercise the normal precautions required for handling all laboratory reagents.

Disposal of all waste material should be in accordance with local guidelines. Safety data sheet available for professional user on request.

Reagent handling

Ready for use

Storage and stability

ASTL

Shelf life at 2-8 °C: See expiration date on **cobas c** pack label.

On-board in use and refrigerated on the analyzer: 12 weeks

Diluent NaCl 9 %

Shelf life at 2-8 °C: See expiration date on **cobas c** pack label.

On-board in use and refrigerated on the analyzer: 12 weeks

Specimen collection and preparation

For specimen collection and preparation only use suitable tubes or collection containers.

Only the specimens listed below were tested and found acceptable.

Serum.

Plasma: Li-heparin and K₂-EDTA plasma

The sample types listed were tested with a selection of sample collection tubes that were commercially available at the time of testing, i.e. not all available tubes of all manufacturers were tested. Sample collection systems from various manufacturers may contain differing materials which could affect the test results in some cases. When processing samples in primary tubes (sample collection systems), follow the instructions of the tube manufacturer.

Centrifuge samples containing precipitates before performing the assay.

Stability: 24 hours at 15-25 °C⁵
7 days at 2-8 °C⁶

Materials provided

See "Reagents – working solutions" section for reagents.

Materials required (but not provided)

See "Order information" section

General laboratory equipment

Assay

For optimum performance of the assay follow the directions given in this document for the analyzer concerned. Refer to the appropriate operator's manual for analyzer-specific assay instructions.

The performance of applications not validated by Roche is not warranted and must be defined by the user.

Application for serum and plasma

cobas c 311 test definition

Assay type	Rate A		
Reaction time / Assay points	10 / 12-31 (STAT 7 / 12-31)		
Wavelength (sub/main)	700/340 nm		
Reaction direction	Decrease		
Units	U/L (µkat/L)		
Reagent pipetting	Diluent (H ₂ O)		
R1	40 µL	51 µL	
R2	17 µL	20 µL	
Sample volumes	Sample	Sample dilution	
		Sample	Diluent (NaCl)
Normal	9 µL	–	–
Decreased	9 µL	15 µL	135 µL
Increased	9 µL	–	–

cobas c 501 test definition

Assay type	Rate A		
Reaction time / Assay points	10 / 18-46 (STAT 7 / 18-46)		
Wavelength (sub/main)	700/340 nm		
Reaction direction	Decrease		
Units	U/L (µkat/L)		
Reagent pipetting	Diluent (H ₂ O)		
R1	40 µL	51 µL	
R2	17 µL	20 µL	
Sample volumes	Sample	Sample dilution	
		Sample	Diluent (NaCl)

Normal	9 µL	–	–
Decreased	9 µL	15 µL	135 µL
Increased	9 µL	–	–

cobas c 502 test definition

Assay type	Rate A		
Reaction time / Assay points	10 / 18-46 (STAT 7 / 18-46)		
Wavelength (sub/main)	700/340 nm		
Reaction direction	Decrease		
Units	U/L (µkat/L)		
Reagent pipetting	Diluent (H ₂ O)		
R1	40 µL	51 µL	
R2	17 µL	20 µL	
Sample volumes	Sample	Sample dilution	
		Sample	Diluent (NaCl)
Normal	9 µL	–	–
Decreased	9 µL	15 µL	135 µL
Increased	18 µL	–	–
Calibration			
Calibrators	S1: H ₂ O S2: C.f.a.s.		

Calibration mode	Linear
Calibration frequency	2-point calibration • after reagent lot change • as required following quality control procedures

Traceability: This method has been standardized against the original IFCC formulation using calibrated pipettes together with a manual photometer providing absolute values and the substrate-specific absorptivity, ϵ .⁷

Quality control

For quality control, use control materials as listed in the "Order information" section.

In addition, other suitable control material can be used.

The control intervals and limits should be adapted to each laboratory's individual requirements. Values obtained should fall within the defined limits. Each laboratory should establish corrective measures to be taken if values fall outside the defined limits.

Follow the applicable government regulations and local guidelines for quality control.

Calculation

Roche/Hitachi **cobas c** systems automatically calculate the analyte activity of each sample.

Conversion factor: U/L x 0.0167 = µkat/L

Limitations - interference

Criterion: Recovery within ± 10 % of initial value at an AST activity of 30 U/L (0.50 µkat/L).

Icterus:⁸ No significant interference up to an I index of 60 for conjugated and unconjugated bilirubin (approximate conjugated and unconjugated bilirubin concentration: 1026 µmol/L or 60 mg/dL).

Hemolysis:⁸ No significant interference up to an H index of 40 (approximate hemoglobin concentration: 25.6 µmol/L or 40 mg/dL).

Contamination with erythrocytes will elevate results, because the analyte level in erythrocytes is higher than in normal sera. The level of interference

may be variable depending on the content of analyte in the lysed erythrocytes.

Lipemia (Intralipid):⁸ No significant interference up to an L index of 150. There is poor correlation between the L index (corresponds to turbidity) and triglycerides concentration.

Lipemic specimens may cause > Abs flagging. Choose diluted sample treatment for automatic rerun.

Drugs: No interference was found at therapeutic concentrations using common drug panels.^{9,10}

Exceptions: Isoniazid can cause artificially low and Furosemide artificially high AST results at therapeutic concentrations.

Cyanokit (Hydroxocobalamin) may cause interference with results.

Physiological plasma concentrations of Sulfasalazine and Sulfapyridine may lead to false results.

In very rare cases, gammopathy, in particular type IgM (Waldenström's macroglobulinemia), may cause unreliable results.¹¹

For diagnostic purposes, the results should always be assessed in conjunction with the patient's medical history, clinical examination and other findings.

ACTION REQUIRED

Special Wash Programming: The use of special wash steps is mandatory when certain test combinations are run together on Roche/Hitachi **cobas c** systems. The latest version of the carry-over evasion list can be found with the NaOHD/SMS/Multiclean/SCCS or the NaOHD/SMS/SmpCln1+2/SCCS Method Sheets. For further instructions refer to the operator's manual. **cobas c** 502 analyzer: All special wash programming necessary for avoiding carry-over is available via the **cobas** link, manual input is not required.

Where required, special wash/carry-over evasion programming must be implemented prior to reporting results with this test.

Limits and ranges

Measuring range

5-700 U/L (0.08-11.7 μ kat/L)

Determine samples having higher activities via the rerun function. Dilution of samples via the rerun function is a 1:10 dilution. Results from samples diluted using the rerun function are automatically multiplied by a factor of 10.

Lower limits of measurement

Lower detection limit of the test

5 U/L (0.08 μ kat/L)

The lower detection limit represents the lowest measurable analyte level that can be distinguished from 0. It is calculated as the value lying 3 standard deviations above that of the lowest standard (standard 1 + 3 SD, repeatability, n = 21).

Expected values¹²

Acc. to the optimized standard method (comparable to the IFCC method without pyridoxal phosphate activation¹³):

Males: up to 40 U/L (up to 0.67 μ kat/L)

Females: up to 32 U/L (up to 0.53 μ kat/L)

Calculated values: A factor of 2.13 is used for the conversion from 25 °C to 37 °C.¹⁴

Each laboratory should investigate the transferability of the expected values to its own patient population and if necessary determine its own reference ranges.

Specific performance data

Representative performance data on the analyzers are given below. Results obtained in individual laboratories may differ.

Precision

Precision was determined using human samples and controls in an internal protocol with repeatability (n = 21) and intermediate precision (3 aliquots per run, 1 run per day, 20 days).

The following results were obtained:

Repeatability	Mean	SD	CV
	U/L (μ kat/L)	U/L (μ kat/L)	%
Precinorm U	36.6 (0.611)	0.3 (0.005)	0.8
Precipath U	128 (2.14)	1 (0.02)	0.4
Human serum 1	126 (2.10)	1 (0.02)	0.4
Human serum 2	12.0 (0.200)	0.4 (0.007)	3.1
Intermediate precision	Mean	SD	CV
	U/L (μ kat/L)	U/L (μ kat/L)	%
Precinorm U	36.7 (0.613)	0.5 (0.008)	1.3
Precipath U	130 (2.17)	1 (0.02)	0.8
Human serum 3	30.0 (0.501)	0.7 (0.012)	2.3
Human serum 4	121 (2.02)	2 (0.03)	1.9

Method comparison

AST values for human serum and plasma samples obtained on a Roche/Hitachi **cobas c** 501 analyzer (y) were compared with those determined using the corresponding reagent on a Roche/Hitachi 917 analyzer (x).

Sample size (n) = 192

Passing/Bablok ¹⁵	Linear regression
$y = 1.000x - 0.149 \text{ U/L}$	$y = 0.991x + 1.22 \text{ U/L}$
$r = 0.970$	$r = 0.999$

The sample activities were between 30.4 and 674 U/L (0.508 and 11.3 μ kat/L).

References

- Nagy B. Muscle disease. In: Kaplan LA, Pesce AJ, eds. Clinical Chemistry, theory, analysis, and correlation. St. Louis: Mosby 1984;514.
- Moss DW, Henderson AR, Kachmar JF. Enzymes. In: Tietz NW, ed. Fundamentals of Clinical Chemistry, 3rd ed. Philadelphia, PA: WB Saunders 1987;346-421.
- Bergmeyer HU, Hørdler M, Rej R. Approved recommendation (1985) on IFCC methods for the measurement of catalytic concentration of enzymes. Part 2. IFCC Method for aspartate aminotransferase. J Clin Chem Clin Biochem 1986;24:497-510.
- ECCLS. Determination of the catalytic activity concentration in serum of L-aspartate aminotransferase (EC 2.6.1.1,ASAT). Klin Chem Mitt 1989;20:198-204.
- Tietz NW, ed. Clinical Guide to Laboratory Tests, 3rd ed. Philadelphia PA: WB Saunders Company 1995;76-77.
- Use of Anticoagulants in Diagnostic Laboratory Investigations. WHO Publication WHO/DIL/LAB/99.1 Rev.2.
- Schumann G, Bonora R, Ceriotti F, et al. IFCC Primary Reference Procedures for the Measurement of Catalytic Activity Concentrations of Enzymes at 37 °C – Part 5. Reference Procedure for the Measurement of Catalytic Activity Concentrations of Aspartate Aminotransferase. Clin Chem Lab Med 2002;40(7):725-733.
- Glick MR, Ryder KW, Jackson SA. Graphical Comparisons of Interferences in Clinical Chemistry Instrumentation. Clin Chem 1986;32:470-475.

- 9 Breuer J. Report on the Symposium "Drug effects in Clinical Chemistry Methods". Eur J Clin Chem Clin Biochem 1996;34:385-386.
- 10 Sonntag O, Scholer A. Drug interference in clinical chemistry: recommendation of drugs and their concentrations to be used in drug interference studies. Ann Clin Biochem 2001;38:376-385.
- 11 Bakker AJ, Mücke M. Gammopathy interference in clinical chemistry assays: mechanisms, detection and prevention. Clin Chem Lab Med 2007;45(9):1240-1243.
- 12 Thefeld W, Hoffmeister H, Busch EW, et al. Referenzwerte für die Bestimmungen der Transaminasen GOT und GPT sowie der alkalischen Phosphatase im Serum mit optimierten Standardmethoden. Dtsch Med Wschr 1974;99(8):343-351.
- 13 Klein G, Lehmann P, Michel E, et al. Vergleich der IFCC-Methoden für ALAT, ASAT und GGT bei 37 °C mit den eingeführten Standardmethoden bei 25 °C und 37 °C. Lab Med 1994;18:403-404.
- 14 Zawta B, Klein G, Bablok W. Temperaturumrechnung in der klinischen Enzymologie? Klin Lab 1994;40:23-32.
- 15 Bablok W, Passing H, Bender R, et al. A general regression procedure for method transformation. Application of linear regression procedures for method comparison studies in clinical chemistry, Part III. J Clin Chem Clin Biochem 1988 Nov;26(11):783-790.

A point (period/stop) is always used in this Method Sheet as the decimal separator to mark the border between the integral and the fractional parts of a decimal numeral. Separators for thousands are not used.

Symbols

Roche Diagnostics uses the following symbols and signs in addition to those listed in the ISO 15223-1 standard.

CONTENT	Contents of kit
→	Volume after reconstitution or mixing

FOR US CUSTOMERS ONLY: LIMITED WARRANTY

Roche Diagnostics warrants that this product will meet the specifications stated in the labeling when used in accordance with such labeling and will be free from defects in material and workmanship until the expiration date printed on the label. THIS LIMITED WARRANTY IS IN LIEU OF ANY OTHER WARRANTY, EXPRESS OR IMPLIED, INCLUDING ANY IMPLIED WARRANTY OF MERCHANTABILITY OR FITNESS FOR PARTICULAR PURPOSE. IN NO EVENT SHALL ROCHE DIAGNOSTICS BE LIABLE FOR INCIDENTAL, INDIRECT, SPECIAL OR CONSEQUENTIAL DAMAGES.

COBAS, COBAS C, PRECINORM, PRECIPATH and PRECICONTROL are trademarks of Roche.

All other product names and trademarks are the property of their respective owners.

Significant additions or changes are indicated by a change bar in the margin.

©2013, Roche Diagnostics



Roche Diagnostics GmbH, Sandhofer Strasse 116, D-68305 Mannheim
www.roche.com

Distribution in USA by:
Roche Diagnostics, Indianapolis, IN
US Customer Technical Support 1-800-428-2336



Appendix E: Tissue processing**Protocol:**

1. Fix tissue in 5% paraformaldehyde for 48 hours.
2. Add tissue to labelled cassettes with without litt.
3. Process tissue in the tissue processor (Table 3).
4. Once complete embed with paraffin wax and block.

Table 3: Tissue processing steps

Order	Solution	Time	Purpose
1	5% Paraformaldehyde	12-24 h	Fixation
2	70% Ethanol	2.0 h	Dehydration
3	95% Ethanol	1.5 h	Dehydration
4	95% Ethanol	1.5 h	Dehydration
5	100% Ethanol	1.5 h	Dehydration
6	100% Ethanol	1.5 h	Dehydration
7	100% Ethanol	1.5 h	Dehydration
8	100% Xylene	1.5 h	Clearing
9	100% Xylene	1 h	Clearing
10	Paraffin (60 °C)	2 h	Processing
11	Paraffin (60 °C)	2 h	Processing

Appendix F: Haematoxylin and eosin automatic staining protocol**Protocol:**

1. Place deparaffinized slides into a plastic tissue rack.
2. Place rack in the auto-stainer.
3. Follow the programmed procedure listed in Table 4.

Table 4: Haematoxylin and eosin staining protocol.

Staining step	Reagents	Time	Repetition
1	Xylene	10 min	2
2	99% Ethanol	5 min	2
3	96% Ethanol	2 min	1
4	70% Ethanol	2 min	1
5	Distilled water	5 sec	1
6	Haematoxylin	8 min	1
7	Running water	5 min	1
8	Ethanol (1% acidic alcohol)	30 sec	1
9	Running water	1 min	1
10	0.2% Ammonia	45 sec	1
11	Running water	5 min	2
12	96% Ethanol	10 dips	1
13	Eosin	45 sec	1
14	96% Ethanol	5 min	2
15	Xylene	5 min	2

Appendix G: Immunolabelling for anti-glucagon and anti-insulin

As per the protocol from The Medical Research Council of South Africa (Diabetes Discovery Platform): **SOP No: ICC\B7-V01.**

Table 5: Results of immunolabelling

Cell	Label
α -cells	Brown
β -cells	Red/pink

Table 6: Reagents and quantities of immunolabelling kits.

Reagents	Quantity
DAKO Polyclonal Anti-glucagon (rabbit) 1:100	1 μ l anti-glucagon + 99 μ l 0.1M PBS = 100 μ l/slide
Vector Laboratories Biotinylated Goat Anti-Rabbit IgG	11.25 μ l made up to 2.5 mL 0.05 M TBS pH 7.2
Vector Laboratories Vectastain ABC Kit	5 mL distilled water + 1 drop A and 1 drop B
DAKO Liquid DAB+ Chromogen	1 mL substrate buffer + 1 drop DAB chromogen=100 μ L/slide/10x
Sigma-Aldrich Monoclonal Anti-Insulin (mouse) 1:1 000	5 μ L 1:50 anti-insulin + 95 μ L 0.1 M PBS = 100 μ L/slide
DAKO Envision Kit	
Rabbit/Mouse Link	100 μ L/slide
AP Enzyme (ENHANCER)	100 μ L/slide
Permanent Red Chromogen Substrate Working Solution	10 μ L permanent red chromogen + 1 000 μ L permanent red substrate buffer = 100 μ L/slide (10 slides)

Table 7: Immunolabelling protocol.

Step	Description	Time
1	Dewax sections through xylene and alcohol	-
2	Rinse slides in staining jar in distilled water	-
3	Block for endogenous peroxidase with 3% hydrogen peroxide (H ₂ O ₂)	5 min
4	Rinse slides with 0.05 M TBS pH 7.2	5 min
5	Dry around the section	
6	Add 1:20 dilution of normal goat serum (NGS) to slides in a moisture chamber at room temperature (18 °C-20 °C)	20 min
7	Blot excess serum	-
8	Add 100 µL anti-glucagon primary antibody 1:100 to sections in moisture chamber and incubate at room temperature (18 °C-20 °C)	30 min
9	Jet wash with 0.05 M TBS pH 7.2 and rinse in staining jar in 0.05 M TBS pH 7.2	5 min
9.1	Make up Biotinylated Anti-Rabbit igg and Vectastain)	-
10	Dry around sections and add Biotinylated Anti-Rabbit IgG 1:200 to slides in moisture chamber at room temperature (18 °C-20°C)	30 min
11	Jet wash with 0.05 M TBS pH 7.2 and rinse in staining jar in 0.05M TBS pH 7.2	10 min
12	Dry around sections and add Vectastain to slides in moisture chamber at room temperature (18 °C-20 °C)	1 h
13	Jet wash slides with 0.05 M TBS pH 7.2 and rinse in 0.05M TBS pH 7.2 in staining jar.	10 min
14	Dry around sections and add Liquid DAB + Chromogen solution to slides on a rack over the sink	5 min
15	Jet wash slides with distilled water and rinse with distilled water in a staining jar	5 min
16	Rinse slides in 0.05 M TBS pH 7.2 in staining jar	5 min
17	Dry around section and add normal horse serum (NHS) 1:20 to slides in a moisture chamber minutes at room temperature (18 °C-20 °C).	20 min
18	Blot excess serum	-
19	Add 100 µL anti-insulin 1:10 000 to sections in moisture chamber and incubate 4 °C	Overnight
20	Remove slides from the refrigerator and allow slides to reach room temperature	-
21	Jet wash with 0.05 M TBS pH 7.2 and rinse in staining jar in 0.05 M TBS pH 7.2	5 min
22	Dry around sections and add 100 µL Rabbit/Mouse (LINK) to slides in moisture chamber room temperature (18 °C-20 °C)	30 min
23	Jet wash with 0.05 M TBS pH 7.2 and rinse in staining jar in 0.05 M TBS pH 7.2	10 min
24	Dry around sections and add 100 µL AP Enzyme (ENHANCER) to slides in moisture chamber room temperature (18 °C-20 °C)	30 min
25	Jet wash slides with 0.05 M TBS pH 7.2 and rinse in 0.05 M TBS pH 7.2 in staining jar.	10 min
26	Dry around sections and add Substrate Working Solution to slides on a rack at room temperature (18 °C-20 °C). Check progress under microscope	3-5 min
27	Jet wash slides with distilled water and rinse in distilled water in staining jar	5 min
28	Counterstain with haematoxylin	2-4 min
29	Rinse well in tap water	-
30	Leave to “blue” in tap water	30 min
31	Dry completely on paper towel (section facing upwards)	-
32	Mount slides in DPX	-

Appendix H: Gordan and Sweet staining protocol**Table 8: Results of Gordan and Sweet's silver impregnation.**

Structure	Stain
Reticulin fibres	Black
Nuclei	Red

Table 9: Gordan and Sweet's staining solutions.

Stock solutions	Quantity
Acidified Potassium permanganate XE	
0.5% Potassium permanganate	95 mL
3% Sulphuric acid	5 mL
Silver solution	
To 5 mL of 10% aqueous silver nitrate add strong ammonia drop by drop until the precipitate is just dissolved. Add 5 mL of 3% sodium hydroxide. Then add strong ammonia drop by drop until the resulting precipitate is almost completely dissolved. Make up to 50 mL using distilled water then pour into a clean coplin jar. NOTE: If too much ammonia is added there is a great loss of sensitivity	
2% aqueous oxalic acid	
Oxalic acid (analytical)	2 g
Distilled water	100 mL
Light green solution 0.1%	
Light green	0.1 g
Acetic acid water 0.2%	100 mL
4% aqueous iron alum	
Iron alum (Ferric ammonium sulphate)	4 g
10% formalin	
Formaldehyde 40 g/L	10 mL
Distilled water	90 mL
Sodium thiosulphate (HYPO)	
Sodium thiosulphate	2 g
Distilled water	100 mL

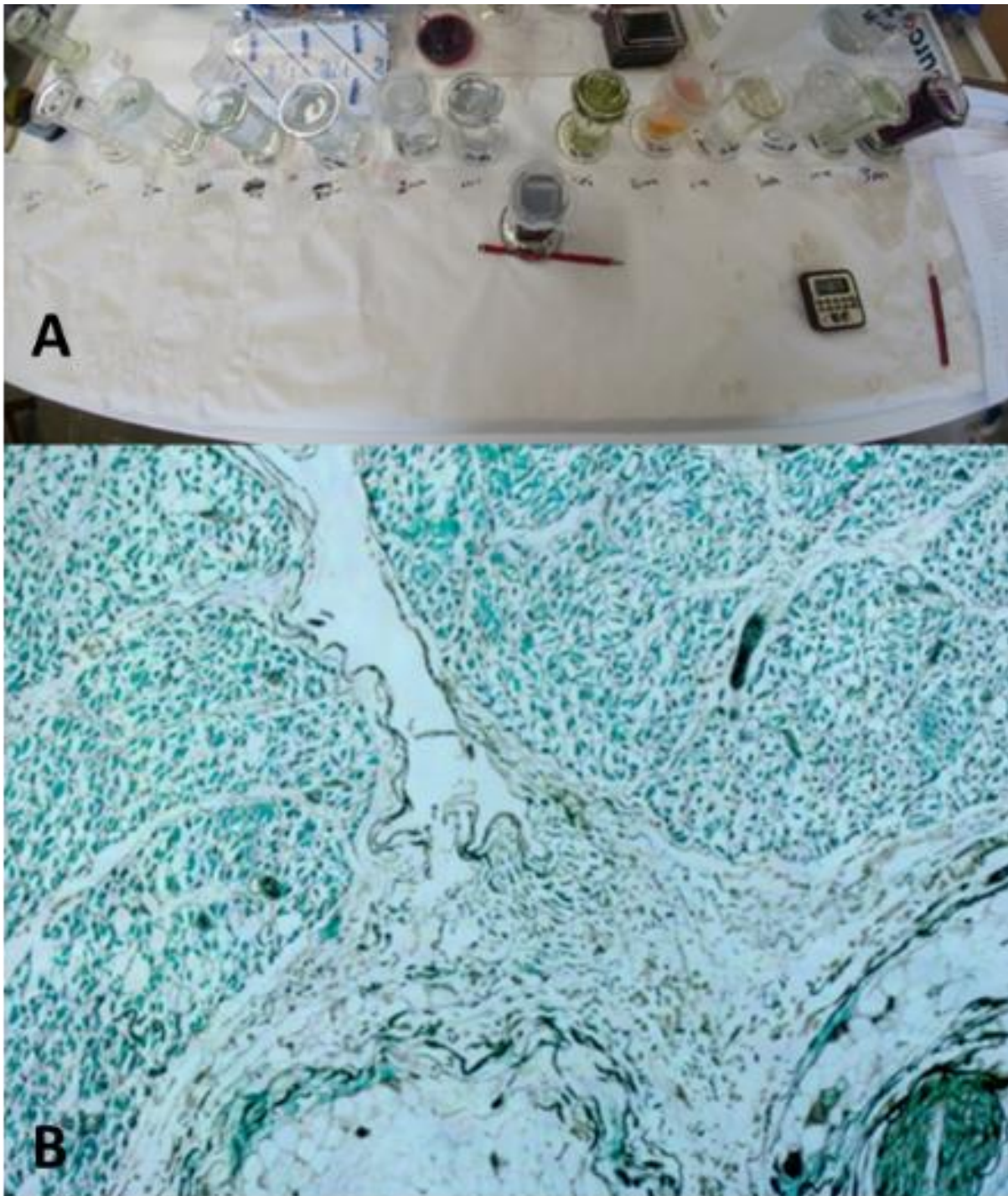


Figure 1: Bench work of the reticulin stain and photomicrograph of positive skin control.

Appendix I: Periodic acid schiff staining protocol

Table 10: Period acid Schiff stain results.

Structure	Stain
Glycogen, mucin and some basement membranes	Red/purple
Fungi	Red/purple
Background	Blue

Table 11: Periodic acid Schiff staining solutions.

Stock solution	Quantity
0.5% Periodic acid solution	
Periodic acid	0.5 g
Distilled water	100 mL
Mayer's Haematoxylin	Used as counterstain

Test for Schiff Reagent.

Pour 10 mL of 37% formalin into a watch glass. Using a pasteurized plastic pipette add a few drops of Schiff reagent to be tested. Usable Schiff will rapidly turn a red-purple colour. A deteriorating Schiff reagent will give a delayed reaction and the colour produced will be a deep blue-purple.

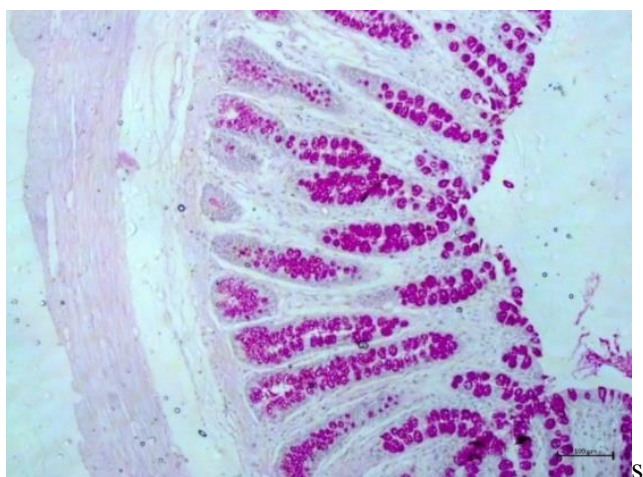


Figure 2: Periodic acid Schiff positive control.

Table 12: Staining procedure for periodic acid Schiff.

Step	Procedure
1	Deparaffinize and hydrate to water
2	Oxidize in 0.5% periodic acid solution for 5 min
3	Rinse in distilled water
4	Place in Schiff reagent for 15 min (sections become a light pink colour in this step)
5	Wash in luke warm water for 5 min (sections turn a dark pink colour in this step)
6	Wash in running tap water for 5 min
7	Dehydrate and mount using DPX mounting medium

Appendix J: Masson's trichrome staining protocol**Table 13: Results of Masons trichrome stain.**

Structure	Stain
Nuclei	Black
Cytoplasm	Red
Mucin	Green
Erythrocytes	Yellow/Orange

Table 14: Masson's Trichrome staining solutions.

Stock solutions	Quantity
Haematoxylin	Counterstain
Acetic acid water	
Glacial acetic acid	2 mL
Distilled water	100 mL
Masson Fuchson Ponceau-Orange G: Stock solution	
Ponceau de xylidine (Ponceau 2R)	2 g
Acid Fuchson	1 g
Orange G	2 g
Acetic Acid water 0.2%	300 mL
Masson Fuchson Ponceau-Orange G: Working solution	
No. 3 (MFPOG)	0.1 g
Acetic acid water 0.2%	100 mL
Light green solution 0.1%	
Light green	0.1g
Acetic acid water 0.2%	100 mL
5% Phosphotungstic acid	
Phosphotungstic acid	5 g
Distilled water	100 mL

Table 15: Masson's trichrome staining procedure

Step	Procedure
1	Deparaffinize sections as usual, wash in tap water, place in Distilled water
2	Stain in Haematoxylin for 5 min. Place in tap water for 3 min until dark blue
3	Rinse in distilled water
4	Stain the sections in filtered working solution of Fuschin ponceau-orange G for 20 min
5	Rinse in acetic acid water
6	Mordant in 5% Phosphotungstic acid solution for 5 min
7	Rinse in acetic acid water for 1 min
8	Stain in light green solution for 20 mi
9	Treat with acetic acid water for 5 min
10	Dehydrate as usual
11	Mount in DPX

Appendix K: Randomisation techniques for the kidney

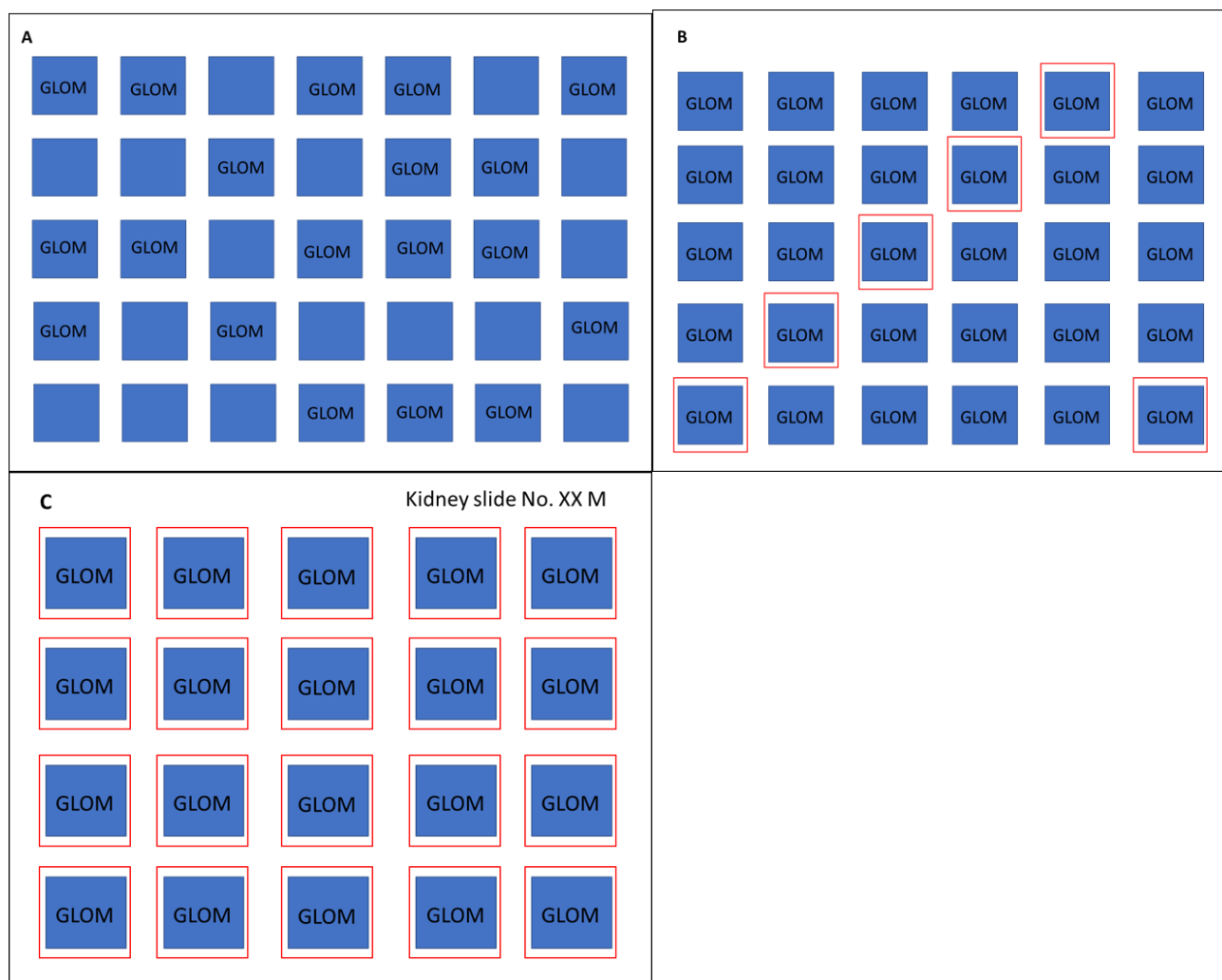


Figure 3: Randomisation of the kidney images to be measured. A) Images in a folder for the specific slide were captured and added to a Microsoft computer folder. B) All images containing one or more glomerular corpuscle (GLOM) were selected and placed in a secondary file “B”. C) From file “B” every 5th image was selected and placed in a third file “C”. D) File “C” was labelled with the slide number and a letter M indicating that it was the measurement file.

Appendix L: Freeze drying techniques

Table 16: Freeze drying procedures.

Step	Procedure
1	Make up 2% tea solution using 20 g tea leaves to 100 mL water
2	Filter the tea using the Whatman No.1 and No.4 filter paper
3	Follow the experimental procedure of storage
4	Place tea in virtis cryogenic flasks
5	Place tea in liquid nitrogen constantly turning to “shell “the tea
6	Once frozen add tea to the vacuum until completely powdered (3-4 days)
7	Collect tea and place in blue top labelled collection jars wrapped in aluminium foil
8	Place freeze dried material in a dark dry cupboard until analysis



Figure 4: Tea preparation for freeze drying. A) Tea is placed in virtis cryogenic flask. B) Tea is placed in liquid nitrogen for shelling. C) Tea is added to the vacuum for freeze drying.



Figure 5: Final tea product in powdered form.

Appendix M: Supplementary data

Body weight

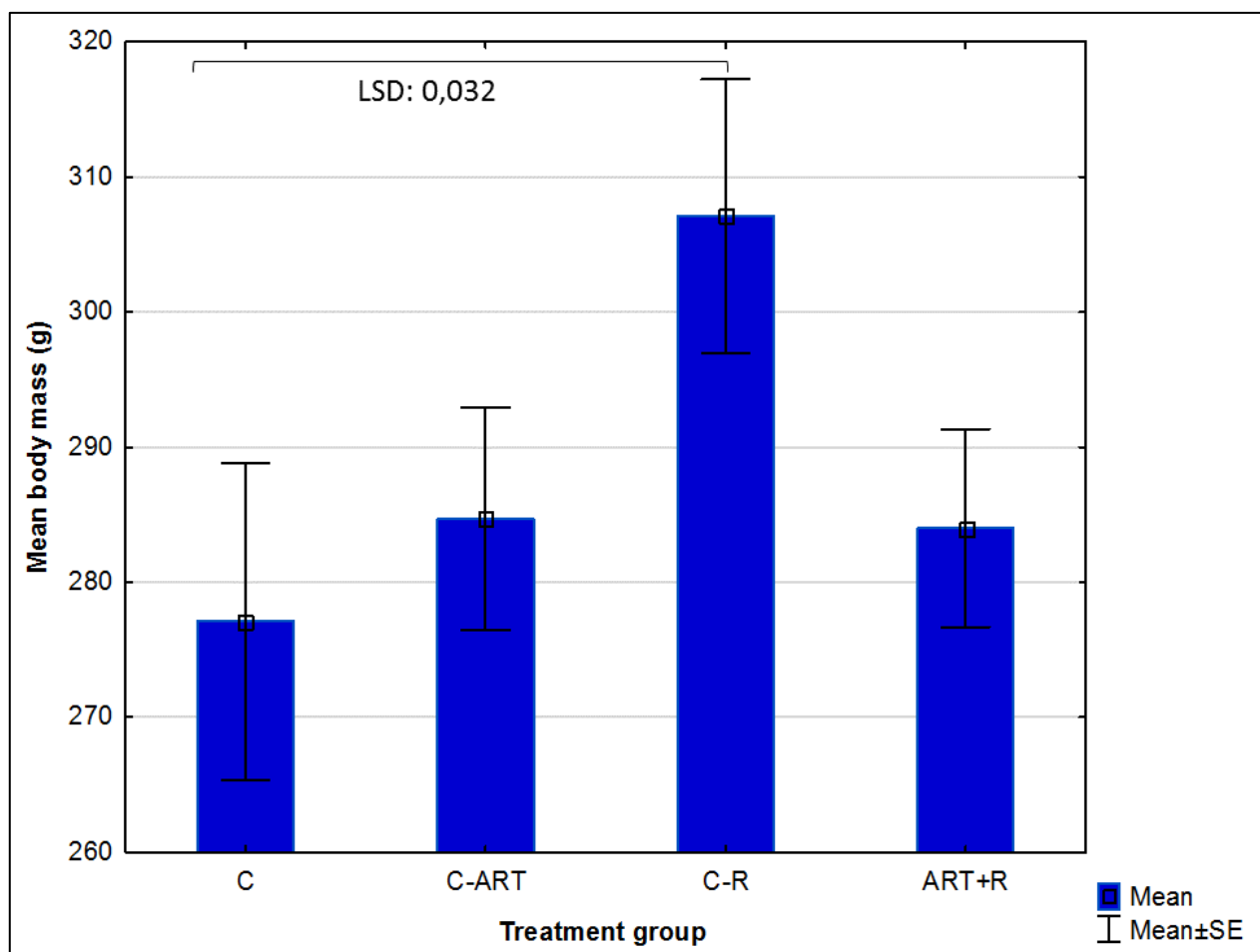


Figure 6: Body mass and Post hoc values of the various treatment groups. Control (C); Control antiretroviral therapy (C-ART); Control rooibos (C-R), Experimental (ART+R).

Table 17: Post hoc tests for body weight.

Body weight				
	C	C-ART	C-R	ART+R
C	-	0.575514	0.032027	0.611053
C-ART	0.575514	-	0.104484	0.958778
C-R	0.032027	0.104484	-	0.094463
ART+R	0.611053	0.958778	0.094463	-

Red values indicate trends between groups. Control (C); Control antiretroviral therapy (C-ART); Control rooibos (C-R), Experimental (ART+R).

Supplementary data of the pancreas

Table 18: Pancreas tissue, islet and α - and β -cell areas.

	Control	Control ART	Control rooibos	Experimental	ANOVA
Total tissue area	56769450.20 ±15418089.17	42010002.95± 13680705.74	48832091.96± 22742602.63	1824331.12± 14726164.83	P= 0.18
Total islet area	531643.48± 196382.79	42010002.95± 13680705.74	390043.82± 242175.09	392958.05± 216995.24	P= 0.21
Mean total tissue area	284625.55± 35291.64	296050.94± 63474.00	269161.83± 31287.63	291683.93± 66141.82	P= 0.67
Mean islet area	6687.41± 1814.76	8490.46± 1913.10	7045.13± 1849.34	7642.43± 3833.00	P= 0.41
Total α-cell area	58386.29± 21707.81	38968.23± 18220.07	45311.38± 26933.84	38654.43± 21894.71	P= 0.19
Total β-cell area	325057.13± 114828.43	200088.85± 98123.16	218006.68± 130203.86	250194.25± 122158.03	P= 0.10
Mean α-cell area	750.19± 277.73	1004.76± 359.70	853.38± 187.04	781.28± 513.30	P= 0.40
Mean β-cell area	4066.03± 1049.48	5134.54± 1202.88	4046.94± 1176.65	5124.45± 2996.43	P= 0.33
Mean islet to mean tissue area	0.410983± 0.256026	0.311348± 0.206240	0.332261± 0.188032	0.395518± 0.188435	P= 0.67
Percentage β-cells	61.19120± 4.157628	60.62224± 4.705751	57.22070± 3.761853	65.51155± 7.315311	P= 0.01
Percentage α-cells	11.01506± 2.248966	11.73030± 2.967841	12.78256± 4.051737	9.82752± 1.681862	P= 0.15

Red values indicate significant difference $p < 0.05$. Control (C); Control antiretroviral therapy (C-ART); Control rooibos (C-R), Experimental (ART+R).

Table 19: Post hoc tests for the pancreas.

Pancreas section areas				
	C	C-ART	C-R	ART+R
C	-	0.060387	0.304043	0.057376
C-ART	0.060387	-	0.376108	0.980676
C-R	0.304043	0.376108	-	0.363400
ART+R	0.057376	0.980676	0.363400	-
Mean pancreas section areas				
C	-	0.623167	0.506621	0.761223
C-ART	0.623167	-	0.251105	0.850812
C-R	0.506621	0.251105	-	0.335088
ART+R	0.761223	0.850812	0.335088	-
Total number of islets				
C	-	0.006118	0.101526	0.217657
C-ART	0.006118	-	0.225811	0.105997
C-R	0.101526	0.225811	-	0.672849
ART+R	0.217657	0.105997	0.672849	-
Total α -cell area				
C	-	0.060506	0.200213	0.056658
C-ART	0.060506	-	0.530703	0.975190
C-R	0.200213	0.530703	-	0.510690
ART+R	0.056658	0.975190	0.510690	-
Total β -cell area				
C	-	0.022216	0.047994	0.160876
C-ART	0.022216	-	0.733855	0.344362
C-R	0.047994	0.733855	-	0.542075
ART+R	0.160876	0.344362	0.542075	-
Total islet area				
C	-	0.044541	0.138281	0.146331
C-ART	0.044541	-	0.575037	0.554243
C-R	0.138281	0.575037	-	0.975284
ART+R	0.146331	0.554243	0.975284	-
Mean islet area				
C	-	0.117878	0.520199	0.845949
C-ART	0.117878	-	0.347108	0.168184
C-R	0.520199	0.347108	-	0.652761
ART+R	0.845949	0.168184	0.652761	-
Mean β -cell area				
C	-	0.191930	0.981178	0.196059
C-ART	0.191930	-	0.184298	0.990055
C-R	0.981178	0.184298	-	0.188301
ART+R	0.196059	0.990055	0.188301	-

Table 19: Post hoc tests for the pancreas continued.

Mean α-cell area				
C	-	0.117878	0.520199	0.845949
C-ART	0.117878	-	0.347108	0.168184
C-R	0.520199	0.347108	-	0.652761
ART+R	0.845949	0.168184	0.652761	-
Percentage of α-cells				
C	-	0.581730	0.178032	0.362181
C-ART	0.581730	-	0.418846	0.147884
C-R	0.178032	0.418846	-	0.027565
ART+R	0.362181	0.147884	0.027565	-
Percentage of β-cells				
C	-	0.807178	0.094789	0.070059
C-ART	0.807178	-	0.150259	0.041610
C-R	0.094789	0.150259	-	0.000998
ART+R	0.070059	0.041610	0.000998	-
Mean number of islets per section area				
C	-	0.299208	0.410761	0.871045
C-ART	0.299208	-	0.826270	0.379460
C-R	0.410761	0.826270	-	0.507922
ART+R	0.871045	0.379460	0.507922	-

Red values indicate trends between group. Control (C); Control antiretroviral therapy (C-ART); Control rooibos (C-R), Experimental (ART+R).

Supplementary data of the liver

Table 20: Descriptive statistics and standard deviations (\pm) of serum analysis.

	C	C-ART	C-R	ART+R	ANOVA
ALT	62.40 \pm 36.44	54.40 \pm 30.55	60.30 \pm 30.29	56.40 \pm 68.11	P= 0.98
AST	181.50 \pm 107.14	160.80 \pm 75.50	170.80 \pm 109.94	143.50 \pm 141.08	P= 0.89
AST: ALT	2.92 \pm 0.60	3.02 \pm 0.70	2.94 \pm 1.10	2.78 \pm 0.59	P= 0.92
Haemoglobin	50.90 \pm 27.91	98.00 \pm 69.80	49.60 \pm 25.60	52.60 \pm 24.1	P= 0.04
Lipaemia	12.00 \pm 12.70	8.25 \pm 2.38	9.40 \pm 4.27	12.70 \pm 13.83	P= 0.63

Red values indicate significant difference $p < 0.05$. Control (C); Control antiretroviral therapy (C-ART); Control rooibos (C-R), Experimental (ART+R).

Table 21: Post hoc tests of serum tests.

Serum ALT				
	C	C-ART	C-R	ART+R
C	-	0.844722	0.767083	0.915994
C-ART	0.844722	-	0.919980	0.763257
C-R	0.767083	0.919980	-	0.688118
ART+R	0.915994	0.763257	0.688118	-
Serum AST				
C	-	0.585310	0.841299	0.830360
C-ART	0.585310	-	0.729187	0.448435
C-R	0.841299	0.729187	-	0.678802
ART+R	0.830360	0.448435	0.678802	-
Serum lipaemia				
C	-	0.385565	0.774485	0.493292
C-ART	0.385565	-	0.271596	0.853194
C-R	0.774485	0.271596	-	0.352964
ART+R	0.493292	0.853194	0.352964	-
Serum AST: ALT				
C	-	0.644110	0.821639	0.963499
C-ART	0.644110	-	0.492777	0.677130
C-R	0.821639	0.492777	-	0.786282
ART+R	0.963499	0.677130	0.786282	-
Serum haemoglobin				
C	-	0.865161	0.013612	0.941331
C-ART	0.865161	-	0.019997	0.923331
C-R	0.013612	0.019997	-	0.016105
ART+R	0.941331	0.923331	0.016105	-

Red values indicate trends between groups. Control (C); Control antiretroviral therapy (C-ART); Control rooibos (C-R), Experimental (ART+R).

Supplementary data of the kidney

Table 22: Descriptive statistics and standard deviations (\pm) of kidney measurements.

	C	C-ART	C-R	ART+R	
Corpuscle area	7483.33 \pm 502.72	7662.31 \pm 1275.82	8147.81 \pm 1067.56	6954.41 \pm 1249.32	P= 0.11
Corpuscle perimeter	316.82 \pm 10.85	319.84 \pm 26.93	329.51 \pm 21.69	304.37 \pm 26.84	P= 0.12
Corpuscle diameter	96.48 \pm 3.24	97.59 \pm 8.07	100.55 \pm 6.48	93.37 \pm 9.04	P= 0.17
Glomerular area	4975.91 \pm 336.15	4915.14 \pm 741.04	5384.6 \pm 855.79	4741.51 \pm 866.02	P= 0.26
Glomerular perimeter	297.52 \pm 15.10	313.26 \pm 36.84	315.68 \pm 32.46	283.40 \pm 37.67	P= 0.10
Glomerular diameter	78.28 \pm 2.96	77.69 \pm 5.90	81.30 \pm 6.17	76.64 \pm 7.87	P= 0.36
Renal space area	2507.42 \pm 284.83	2747.18 \pm 637.98	2763.14 \pm 680.75	2212.90 \pm 473.95	P= 0.10
Renal space width	18.20 \pm 1.89	19.90 \pm 3.49	19.25 \pm 4.51	16.73 \pm 2.56	P= 0.16

Control (C); Control antiretroviral therapy (C-ART); Control rooibos (C-R), Experimental (ART+R).

Table 23: Post hoc tests of glomerular corpuscle and glomerulus.

Corpuscle area				
	C	C-ART	C-R	ART+R
C	-	0.710612	0.173544	0.276418
C-ART	0.710612	-	0.317148	0.147798
C-R	0.173544	0.317148	-	0.017379
ART+R	0.276418	0.147798	0.017379	-
Corpuscle perimeter				
C	-	0.766384	0.216340	0.224647
C-ART	0.766384	-	0.343928	0.133560
C-R	0.216340	0.343928	-	0.017365
ART+R	0.224647	0.133560	0.017365	-
Corpuscle diameter				
C	-	0.727530	0.205028	0.331016
C-ART	0.727530	-	0.353695	0.189767
C-R	0.205028	0.353695	-	0.028890
ART+R	0.331016	0.189767	0.028890	-
Glomerular area				
C	-	0.853797	0.219981	0.478707
C-ART	0.853797	-	0.160231	0.599203
C-R	0.219981	0.160231	-	0.057272
ART+R	0.478707	0.599203	0.057272	-
Glomerular perimeter				
C	-	0.276488	0.210514	0.328190
C-ART	0.276488	-	0.866050	0.043153
C-R	0.210514	0.866050	-	0.029554
ART+R	0.328190	0.043153	0.029554	-
Glomerular diameter				
C	-	0.826950	0.266965	0.544781
C-ART	0.826950	-	0.186152	0.697969
C-R	0.266965	0.186152	-	0.090589
ART+R	0.544781	0.697969	0.090589	-
Renal space area				
C	-	0.329425	0.298692	0.232478
C-ART	0.329425	-	0.947897	0.034071
C-R	0.298692	0.947897	-	0.029365
ART+R	0.232478	0.034071	0.029365	-
Renal space width				
C	-	0.329425	0.298692	0.232478
C-ART	0.329425	-	0.947897	0.034071
C-R	0.298692	0.947897	-	0.029365
ART+R	0.232478	0.034071	0.029365	-

Red values indicate trends between groups. Control (C); Control antiretroviral therapy (C-ART); Control rooibos (C-R), Experimental (ART+R).

Table 24: Post hoc tests of the proximal convoluted tubules.

Outer surface area				
	C	C-ART	C-R	ART+R
C	-	0.792179	0.316467	0.620982
C-ART	0.792179	-	0.457873	0.449723
C-R	0.316467	0.457873	-	0.138596
ART+R	0.620982	0.449723	0.138596	-
Outer surface perimeter				
C	-	0.753112	0.271227	0.694184
C-ART	0.753112	-	0.428704	0.480256
C-R	0.271227	0.428704	-	0.138820
ART+R	0.694184	0.480256	0.138820	-
Outer surface diameter				
C	-	0.816939	0.370979	0.815334
C-ART	0.816939	-	0.505383	0.642286
C-R	0.370979	0.505383	-	0.261309
ART+R	0.815334	0.642286	0.261309	-
Luminal surface area				
C	-	0.942646	0.072681	0.268109
C-ART	0.942646	-	0.084091	0.239026
C-R	0.072681	0.084091	-	0.005222
ART+R	0.268109	0.239026	0.005222	-
Luminal perimeter				
C	-	0.941045	0.115218	0.338141
C-ART	0.941045	-	0.132374	0.302879
C-R	0.115218	0.132374	-	0.013938
ART+R	0.338141	0.302879	0.013938	-
Luminal diameter				
C	-	0.971471	0.084018	0.317194
C-ART	0.971471	-	0.090226	0.300560
C-R	0.084018	0.090226	-	0.008347
ART+R	0.317194	0.300560	0.008347	-
PCT wall area				
C	-	0.733730	0.850852	0.950892
C-ART	0.733730	-	0.878917	0.780472
C-R	0.850852	0.878917	-	0.899356
ART+R	0.950892	0.780472	0.899356	-
PCT wall diameter				
C	-	0.746867	0.257475	0.272601
C-ART	0.746867	-	0.148670	0.435345
C-R	0.257475	0.148670	-	0.029645
ART+R	0.272601	0.435345	0.029645	-

Control (C); Control antiretroviral therapy (C-ART); Control rooibos (C-R), Experimental (ART+R).

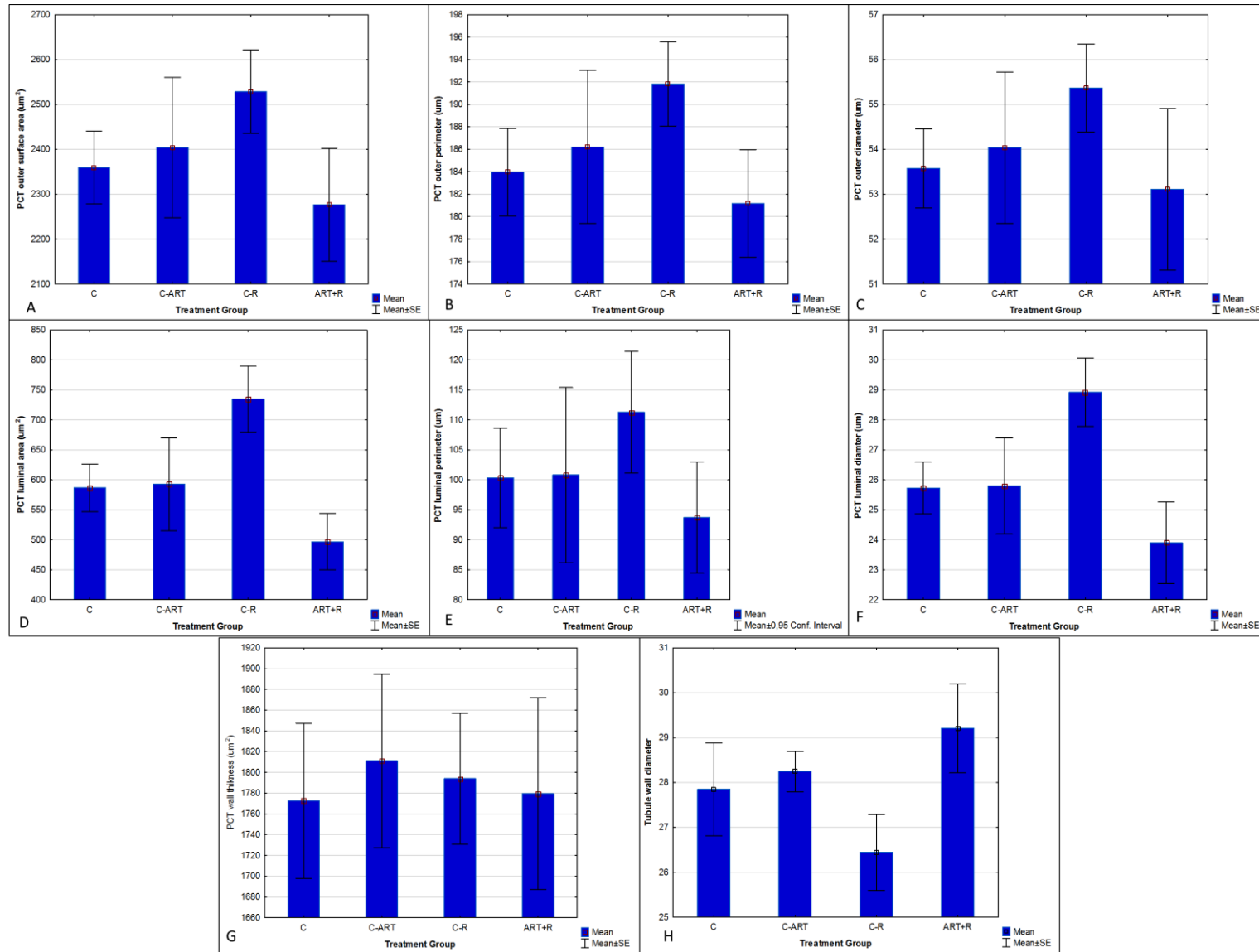


Figure 7: Bar graphs showing the size of the PCTs. Control (C); Control antiretroviral therapy (C-ART); Control rooibos (C-R), Experimental (ART+R).

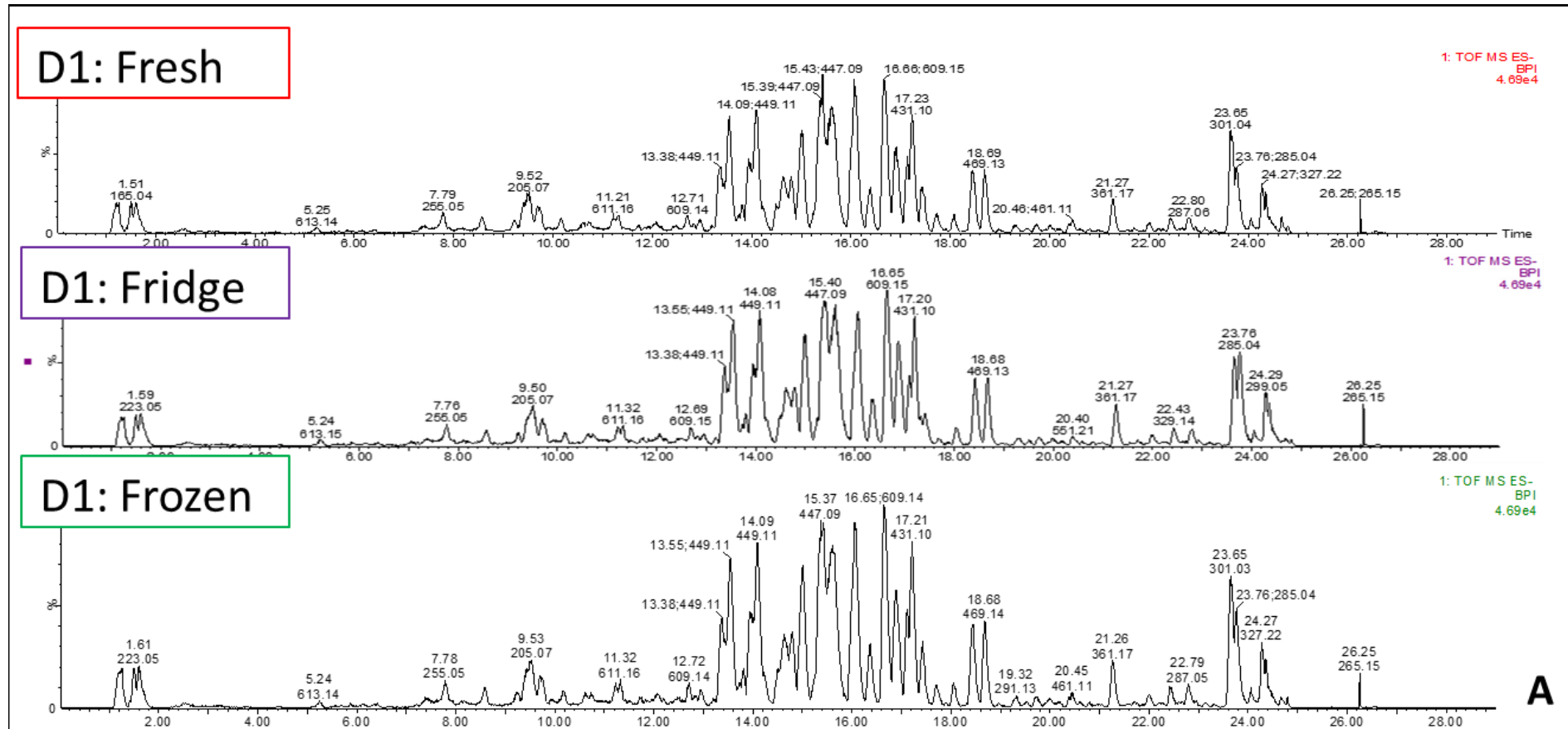


Figure 8: Single roibos chromatograms of Day 1 samples, with retention times and molecular weights of the compounds. Day 1 (D1).

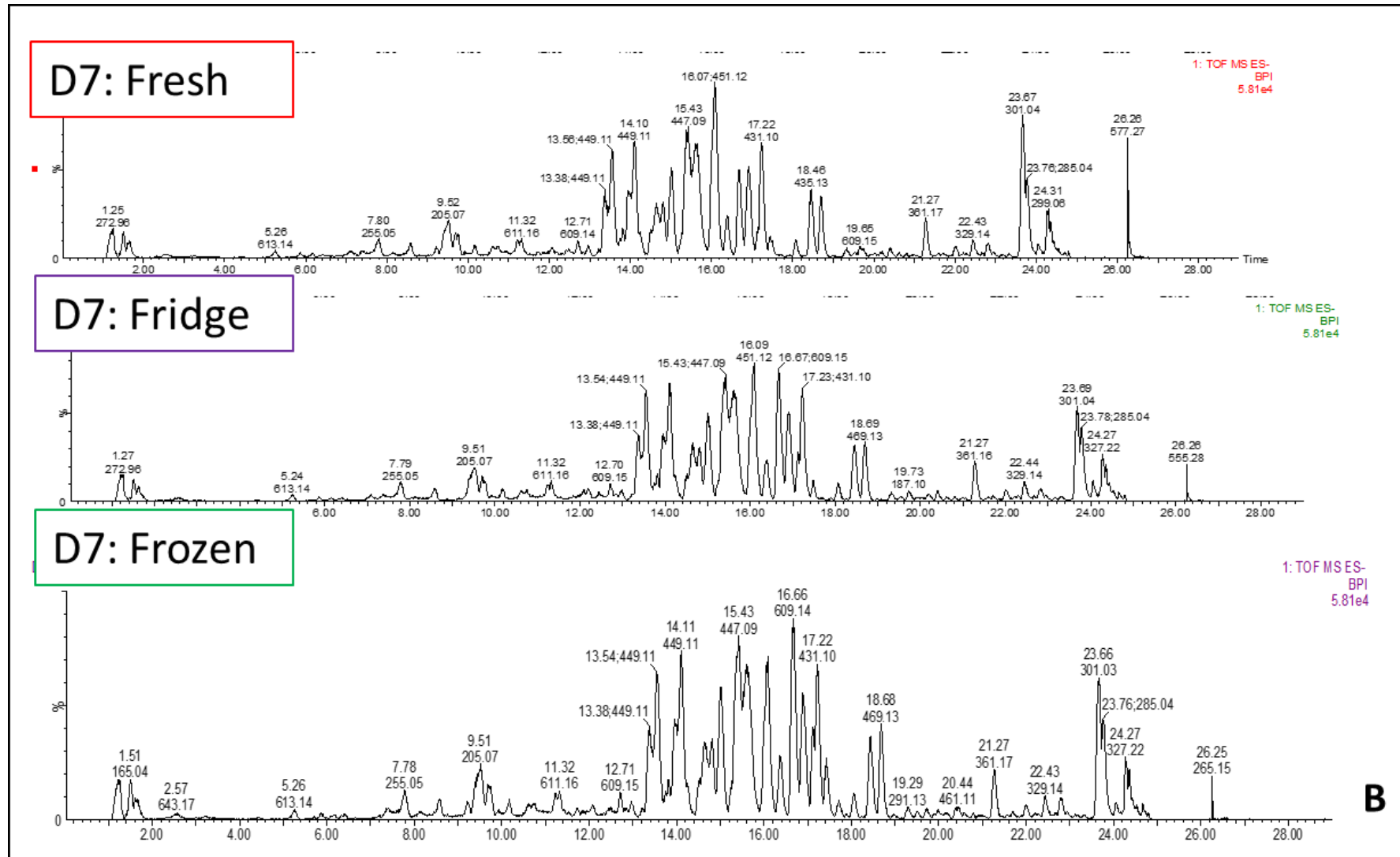


Figure 9: Single rooibos chromatograms of Day 7 samples, with retention times and molecular weights of the compounds. Day 7 (D7).

Table 25: Pathology overview: Pancreas.

	Animal number	Granular changes	Vacuolation	Lymph infiltration	Description
Control	C1	0	0	0	normal
	C2	0	0	0	normal
	C3	0	0	0	normal
	C4	0	0	0	normal
	C5	0	0	0	normal
	C6	0	0	0	normal
	C7	0	0	0	normal
	C8	0	0	0	normal
	C9	0	0	0	normal
	C10	0	0	0	normal
Control ART	C-ART1	0	0	0	normal
	C-ART2	0	0	0	normal
	C-ART3	0	0	0	normal
	C-ART4	0	0	0	normal, lymph node shows mild activity
	C-ART5	0	0	0	normal, lymph node with active centre
	C-ART6	0	0	0	normal
	C-ART7	0	0	0	normal
	C-ART8	0	0	0	normal, mild activity at the lymph node
	C-ART9	0	0	0	normal
	C-ART10	0	0	0	normal, mild lymph activity at the lymph node
Control rooibos	C-R1	0	0	0	normal
	C-R2	0	0	0	normal
	C-R3	0	0	0	normal
	C-R4	0	0	0	normal, lymph node with active centre
	C-R5	0	0	0	normal
	C-R6	0	0	0	normal, lymph node with active centre
	C-R7	0	0	0	normal, lymph node with active centre
	C-R8	0	0	0	normal

Table 25: Pathology overview: Pancreas continued.

	C-R9	0	0	0	normal
	C-R10	0	0	0	normal
Experimental	ART+R1	0	0	0	normal
	ART+R2	0	0	0	normal, lymph node with active centre
	ART+R3	0	0	0	normal, lymph node with active centre
	ART+R4	0	0	0	normal, lymph node with active centre
	ART+R5	0	0	0	normal
	ART+R6	0	0	0	normal
	ART+R7	0	0	0	normal
	ART+R8	0	0	0	normal
	ART+R9	0	0	0	normal
	ART+R10	0	0	0	normal, lymph node shows mild activity

Control (C); Control antiretroviral therapy (C-ART); Control rooibos (C-R), Experimental (ART+R).

Table 26: Pathology overview: Liver.

	Animal number	Granular cytoplasm	Vacuolation	Lymph infiltration	Description
Control	C1	1	1	0	Slight vacuolisation present diffuse, granular cytoplasm observed, minimal disruption of reticulin towards capsule
	C2	0	0	0	Normal
	C3	0	0	1	Very slight lymph infiltration otherwise normal only localised at one portal tract
	C4	0	0	0	Normal
	C5	1	1	1	Vacuolisation around central veins, granular appearance mostly diffuse, lymph infiltration
	C6	0	0	0	Normal
	C7	1	0	0	Slight granular appearance of the cytoplasm mostly diffuse
	C8	0	1	0	Slight vacuolation present diffuse, slight disruption of RT at vacuolated areas and towards capsule
	C9	0	1	0	Slight vacuolisation evident at the central veins
	C10	0	1	0	Vacuolation around portal tracts and central vein, RT disruption in vacuolated areas and towards capsule
Control ART	C-ART1	1	1	1	Granular cytoplasm, vacuolisation around central veins, inflammatory cells diffuse RT, disruption around vacuolated areas
	C-ART2	0	1	1	Slight inflammatory foci present, slight vacuolisation is observed, RT disruption to wards capsule
	C-ART3	1	1	0	Slight vacuolisation and granular appearance of the cytoplasm around central veins, RT disruption towards capsule and around vacuolated areas
	C-ART4	1	1	0	vacuolisation and granular cytoplasmic appearances around portal areas and central veins, Disruption
	C-ART5	1	1	0	Granular cytoplasm slight vacuolation present
	C-ART6	0	1	1	Slight vacuolisation seen around the portal regions, slight lymphocyte infiltration slight disruption of RT and vacuolated areas
	C-ART7	0	0	0	Normal
	C-ART8	0	0	0	Normal
	C-ART9	0	1	0	Slight vacuolation mostly diffuse, RT disrupted at vacuolated areas and at the capsule
	C-ART10	1	1	0	Vacuolisation and, slight granular cytoplasm is visible. Liver looks slightly hyperaemic
Con	C-R1	0	0	0	Normal
	C-R2	0	0	0	Normal

Table 26: Pathology overview: Liver continued.

	C-R3	1	1	0	Slight vacuolisation mostly diffuse granular cytoplasm observed, RT slight disruption in vacuolated areas
	C-R4	0	1	0	Slight granular cytoplasm
	C-R5	1	1	0	Slight vacuolisation, granular cytoplasm mostly diffuse, RT slight disruption in vacuolated areas
	C-R6	0	1	0	Slight vacuolisation present RT slight disruption in vacuolated areas
	C-R7	1	0	0	Granulated cytoplasm with slight vacuolisation diffuse
	C-R8	1	0	0	Granular cytoplasm mostly diffuse
	C-R9	1	0	0	Slight vacuolisation around the central veins, RT slight disruption in vacuolated areas and towards the capsule
	C-R10	1	1	0	Slight vacuolisation around portal areas and central vein, slight granular cytoplasm, RT slight disruption in vacuolated areas
Experimental	ART+R 1	0	0	0	Normal, see slight bridging confirm with MT. No bridging found on trichrome, RT slight disruption in vacuolated areas and around portal areas
	ART+R 2	1	0	0	Slight granular appearance of the cytoplasm mostly diffuse
	ART+R 3	0	1	0	Slight vacuolisation, RT slight disruption in vacuolated areas
	ART+R 4	0	1	0	Slight vacuolisation, RT slight disruption in vacuolated areas
	ART+R 5	1	1	0	Slight vacuolisation around portal areas and granulated cytoplasm, RT slight disruption in vacuolated areas
	ART+R 6	0	1	0	Slight vacuolisation around portal regions, RT slight disruption in vacuolated areas
	ART+R 7	0	0	0	Normal
	ART+R 8	1	1	0	Slight vacuolisation around portal areas and granulated cytoplasm, RT slight disruption in vacuolated areas
	ART+R 9	0	1	0	Slight vacuolisation around portal regions, slight granular appearance mostly diffuse, RT slight disruption in vacuolated areas and towards the capsule could be artefactual
	ART+R 10	1	1	0	Slight vacuolisation around portal areas and granulated cytoplasm. RT slight disruption in vacuolated areas

Reticulin fibres (RT); Masson's Trichrome (MT). Control (C); Control antiretroviral therapy (C-ART); Control rooibos (C-R), Experimental (ART+R).

Table 27: Pathology overview: Kidney.

	Animal number	Granular cytoplasm	Vacuolation	Lymph infiltration	Description
Control	C1	0	0	0	Normal, slight congestion slight autolysis
	C2	0	0	0	Normal, random vacuolation
	C3	0	0	0	Protein casts present
	C4	0	0	0	Vacuolation is present but negligible and some proteinaceous material
	C5	0	0	0	Normal
	C6	0	0	0	Proteinaceous material present, random vacuolation
	C7	0	0	0	Normal
	C8	0	0	0	Normal
	C9	0	0	0	Slight basophilic (artefactual), slight congestion
	C10	0	0	0	Slight basophilic (artefactual), slight congestion
Control ART	C-ART1	0	0	0	Random vacuolation (could be due to autolysis)
	C-ART2	0	0	0	Random vacuolation
	C-ART3	0	0	0	Protein casts, slight congestion
	C-ART4	0	0	0	Protein casts present, with what appears to be vacuolation (autolysis)
	C-ART5	0	0	0	Mild autolysis
	C-ART6	0	0	0	Slight protein casts
	C-ART7	0	0	0	Random vacuolation (artefactual)
	C-ART8	0	0	0	Looks slight basophilic (artefactual), slight congestion
	C-ART9	0	0	0	Looks slightly congested
	C-ART10	0	0	0	Normal, slightly congestion, random vacuolation
Control rooibos	C-R1	0	0	0	Normal
	C-R2	0	0	0	Normal
	C-R3	0	0	0	Normal
	C-R4	0	0	0	Proteinaceous material/ casts present
	C-R5	0	0	0	Proteinaceous material present, vacuolation present but negligible
	C-R6	0	0	0	Proteinaceous material was found
	C-R7	0	0	0	Proteinaceous material was found
	C-R8	0	0	0	Protein casts present, random slight vacuolation

Table 27: Pathology overview: Kidney continued.

	C-R9	0	0	0	Slight artefactual, random vacuolation in DCT
	C-R10	0	0	0	Looks slightly congested, random vacuolation
Experimental	ART+R1	0	0	0	Normal
	ART+R2	0	0	0	Normal
	ART+R3	0	0	0	Normal
	ART+R4	0	0	0	Proteinaceous material was present, red blood cells look slightly engorged
	ART+R5	0	0	0	Mild autolysis
	ART+R6	0	0	0	Engorged red blood cell, autolysis could be misinterpreted as hydropic change
	ART+R7	0	0	0	Protein casts present, random vacuolation in medullary region
	ART+R8	0	0	0	Normal
	ART+R9	0	0	0	Protein casts
	ART+R10	0	0	0	Some protein casts

Control (C); Control antiretroviral therapy (C-ART); Control rooibos (C-R), Experimental (ART+R).